HAW HAMBURG

Project

Identifying Wave Drag for the Generic Drag Polar Equation – Unveiling Polars of 16 Passenger Aircraft

Author: Marlis Krull

Supervisor: Prof. Dr.-Ing. Dieter Scholz, MSME
Submitted: 2025-03-07

Faculty of Engineering and Computer Science
Department of Automotive and Aeronautical Engineering

DOI:
https://doi.org/xxxxxxxx

URN:
https://nbn-resolving.org/urn:nbn:de:gbv:18302-aero2025-03-07.011
Associated URLs:
https://nbn-resolving.org/html/urn:nbn:de:gbv:18302-aero2025-03-07.011

Any further request may be directed to:
Prof. Dr.-Ing. Dieter Scholz, MSME
E-Mail see: http://www.ProfScholz.de

This work is part of:
Digital Library - Projects & Theses - Prof. Dr. Scholz
http://library.ProfScholz.de

Published by
Aircraft Design and Systems Group (AERO)
Department of Automotive and Aeronautical Engineering
Hamburg University of Applied Science

This report is deposited and archived:
- Deutsche Nationalbibliothek (https://www.dnb.de)
- Repository of Leibniz University Hannover (https://www.repo.uni-hannover.de)
- Internet Archive (https://archive.org)
  Item: https://archive.org/details/TextKrullMaster.pdf

This report has associated data published in Harvard Dataverse:
https://doi.org/10.7910/DVN/2UBNIE

Abstract

Purpose – This work systematically derives the best form of a generic drag polar equation together with the optimum numerical values of its parameters to unveil the drag coefficient of 16 passenger aircraft as a function of lift coefficient and Mach number. The parameters are selected such that they can be estimated also for other aircraft mainly from their geometry.
Methodology – Drag polars in graphical form from Obert (2009) are the starting point. Numerical values of the drag coefficient are obtained with the WebPlotDigitizer. In the generic equation, zero lift drag is assumed constant, the term representing induced drag is taken from Niţă (2012). For the wave drag term, seven functions of Mach number are investigated. The difference between Mach number and critical Mach number to the power of 4 is the classic approach based on Lock (1951). Two more general power functions, tan, tanh, sinh, and an exponential function are looked at. Parameters are optimized by minimizing the Root Mean Squared Percentage Error (RMSPE). Optimization is done with the Solver in Excel using the Generalized Reduced Gradient (GRG2) code supplied by Frontline Systems.
Findings – Based on all 16 investigated aircraft, a generic drag polar using the hyperbolic tangent (tanh) to express wave drag is best with mean RMSPE of only 0.68%. The second best is the most general power function with mean RMSPE of 0.75%. Its special case, the often quoted but unflexible function from Lock comes out last here with a mean RMSPE of 0.95%. Nevertheless, all seven functions can be used to represent wave drag. The zero lift drag coefficient is identified between 0.013 (B777) and 0.020 (A320). The Mach dependence of the drag coefficient comes not only from wave drag, but also from induced drag and its Mach dependence beyond 0.3 Mach. Calculated parameters are plausible and come close to reference values from literature.
Research Limitations – Aerodynamic data is generally confidential. Therefore, public drag data is limited. The extension of the method to other aircraft yields a drag estimate.
Practical Implications – The generic equation can be used in preliminary aircraft design as well as in calculations in aircraft performance and flight operations.
Originality – This project formulates a generic drag polar equation with a choice of new wave drag terms some based on a historic precursor. The new approach with a hyperbolic tangent function is recommended.

HAW HAMBURG

DEPARTMENT OF AUTOMOTIVE AND AERONAUTICAL ENGINEERING

Identifying Wave Drag for the Generic Drag Polar Equation – Unveiling Polars of 16 Passenger Aircraft

Task for a Project

Background

The drag polar of an aircraft shows its aerodynamic behavior. Drag consists of zero lift drag, wave drag (due to shock waves) and induced drag (due to lift). The drag coefficient is expressed primarily as a function of the lift coefficient. The result is plotted or expressed in the well-known equation, $C_D = C_{D,0} + C_{D,W} + C_L^2/(\pi Ae)$. The next important parameter is the Mach number. All three drag components depend on Mach number. The drag coefficient is plotted versus lift coefficient with Mach number as a parameter. Alternatively, drag coefficient is plotted versus Mach number with lift coefficient as a parameter. For the drag polar equation, the graphical representation does not matter. Mach number influences induced drag when compressibility becomes noticeable (beyond compressibility Mach number, typically beyond 0.3). Wave drag starts beyond the critical Mach number, M_{crit} (where shock waves start to form). Per definition, the wave drag coefficient is 0,0020 (20 drag counts) at drag divergence Mach number, M_{DD}. Desired is a difference $\Delta M = M_{DD} - M_{crit}$ as large as possible. Passenger jet aircraft are usually designed such that they cruise at M_{DD} and hence with 20 drag counts of wave drag. This gives a good design compromise. The generic drag polar equation must have a convenient structure (made up of different terms, functions, and parameters) to describe all this and more. The history of aerodynamics shows many pragmatic approaches to such an equation. Also, the Aircraft Design and Systems Group (AERO) has contributed to the discussion, but work has not come to an end so far. Aerodynamic data of (passenger jet) aircraft is needed to determine a practical generic drag polar equation. First, an optimum form of the equation must be determined together with the numerical values of the parameters that achieve a representation of available real-world aircraft data with sufficient accuracy. The next task is to answer the question: How are the parameters in the generic drag polar equation related to the geometry of the aircraft? With these relationships established, a generic drag polar equation can be written also for new aircraft in preliminary design based on their geometry.

Task

Task of this project is to study the drag polar of 16 passenger jet aircraft presented in Obert (2009) in graphical form. Obert plots drag coefficient versus Mach number with lift coefficient as a parameter. Propose a suitable form for a generic drag polar equation. Find the numerical values of the parameters in the generic equation representing the 16 aircraft. Focus on wave drag but include older findings on induced drag in your equation. The subtasks are:

- Perform a literature review on the topic so that you can link your results to the history of aerodynamics in the field.
- Scan and digitize Obert's diagrams. This can be done e.g. with the WebPlotDigitizer used also in Chapter 2.5 of this project.
- Examine existing approaches (here and here) and new mathematical approaches for the wave drag term in the generic drag polar equation. Propose a function best suitable for the task.
- Based on the selected form of the generic drag polar equation, unveil the polars of the 16 passenger jet aircraft by providing parameters and plots for visualization.
- Propose how parameters in the generic equation can be linked to the geometry of the aircraft. In this way it should be possible to estimate the drag coefficient for new aircraft in preliminary design.

The report has to be written in English based on German or international standards on report writing.

Drag polars are given in Chapter 24 of:
OBERT, Ed, 2009. *Aerodynamic Design of Transport Aircraft*. Delft, The Netherlands: IOS Press.

- DC 10 / MD 11 (Fig. 24.26),
- B 707 (Fig. 24.49),
- B 727 (Fig. 24.53),
- B 737-200/-300/-800 (Fig. 24.72),
- B 747-100 (Fig. 24.78),
- B 757 (Fig. 24.90),
- B 767 (Fig. 24.96),
- B 777 (Fig. 24.99),
- A 300-B2 (Fig. 24.107),
- A 320 and B 737-800 (Fig. 24.123),
- A 340-200 (Fig. 24.131),
- Fokker 28 (Fig. 24.142),
- Fokker 100 (Fig. 24.143).

Table of Contents

List of Figures

List of Tables

List of Symbols

a	parameter
A	aspect ratio
b	parameter / span
c	parameter / chord
C_D	drag coefficient
C_{fe}	equivalent skin-friction coefficient
C_L	lift coefficient
d	parameter / width
D	drag
e	parameter / Oswald efficiency factor / Euler's number
E	glide Ratio
f	parameter
k	correction factor
K	factor
K_A	airfoil technology factor
L	lift
M	Mach number
P	parameter
Q	parameter
S	area
y	variable

Greek Symbols

λ	taper ratio
π	pi
φ	sweep angle

Indices

0	zero lift / freestream
^	estimated by regression
25	25% of chord
c	compressible
CC	crest critical
comp	compressible
crit	critical
D	drag
DD	drag divergence
e	Oswald factor
E	glide ratio
F	fuselage
geo	geometrical
i	induced / lower limit
L	lift
M	Mach number
max	maximum
min	minimum
n	upper limit
ref	reference
root	at root
t	parameter
theo	theoretical
tip	at tip
u	parameter
v	parameter
w	wave Drag / parameter
W	wing
wet	wetted

List of Abbreviations

AIAA	American Institute of Aeronautics and Astronautics
AERO	Aircraft Design and Systems Group
AGARD	Advisory Group for Aerospace Research and Development
ASCE	American Society of Civil Engineers
cts	Counts
DGLR	German Society for Aeronautics and Astronautics
MCMC	Markov Chain Monte Carlo
MSE	Mean Squared Error
NATO	North Atlantic Treaty Organization
RMSE	Root Mean Squared Error
RMSPE	Root Mean Squared Percentage Error
SSE	Sum of Squared Errors

Definitions

Critical Mach number
"The lowest (subsonic) free-stream Mach number for which the maximum value of the local velocity becomes sonic" (Bertin 2009) is the critical Mach number.

Drag divergence Mach number
"The Mach number at which the abrupt drag rise starts is called the drag divergence Mach number" (Shevell 1989)

Induced drag
The induced drag is the "drag due to the trailing vortex system" (Bertin 2009).

Transonic
"Mixed subsonic/supersonic flow fields are termed transonic flows" (Bertin 2009).

Wave drag
Wave drag is the "drag arising from the formation of shock waves" (AGARD 1980).

1 Introduction

1.1 Motivation

An aircraft's drag is an essential part of the aerodynamics. Also, add-on subjects like the calculation of costs depend on the knowledge of an aircraft's drag. Several approaches exist to define an equation for the drag containing all components of the drag. In this, especially the wave drag is difficult to describe. The reason for this is the complexity of the wave drag and its dependence on several aerodynamic and aircraft parameters. The most common approach defining the wave drag exists since the 1950s. This approach is based on Lock (1951) and provides a simple and quick, but rough estimation. Now, with the existence of multiple drag polars of real aircraft in Obert (2009) this and further mathematical approaches can be analyzed in practice.

1.2 Title Terminology

Identifying
To *identify* means to "recognize someone or something and say or prove who or what that person or thing is" (Cambridge University Press 2025d).

Wave Drag
The term *drag* is defined as "the component of the total aerodynamic force in the direction of the undisturbed relative airflow. In powered flight, contributions to this component arising from thrust are excluded" (AGARD 1980). *Wave drag* describes the "drag arising from the formation of shock waves" (AGARD 1980).

Generic
A *generic* something is "shared by, typical of, or relating to a whole group of similar things, rather than to any particular thing" (Cambridge University Press 2025c).

Drag Polar
"The drag curve or *drag polar* is the relationship between the drag on an aircraft and other variables, such as lift, the coefficient of lift, angle-of-attack or speed. It may be described by an equation or displayed as a graph" (Wikipedia 2025a).

Equation
An *equation* is "a mathematical statement in which you show that two amounts are equal using mathematical symbols" (Cambridge University Press 2025b).

Unveiling
Unveiling means “to show or introduce something new or make it known publicly for the first time” (Cambridge University Press 2025f).

Polars
Here, *polar* refers to a drag polar, which is the “standard presentation format for aerodynamic data used in performance calculations” (Raymer 1992).

16
Obert gives the graphs of the drag polar for the following *16* aircraft: DC-10-30, MD-11, B707-120, B727-200, B737-200, B737-300, B737-800, B747-100, B757-200, B767-300, B777-200, A300-B2, A320-200, A340-200, F28-Mk4000, F100.

Passenger
A *passenger* is “a person who is travelling in a vehicle, or on a train or plane, but is not driving it, flying it, or working on it” (Cambridge University Press & Assessment 2025e).

Aircraft
An *aircraft* is “any vehicle, with or without an engine, that can fly, such as a plane or helicopter” (Cambridge University Press & Assessment 2025a). Here the work is limited to subsonic aircraft.

1.3 Objectives

The main objective of this project is to generate equations for the drag and especially the wave drag that fit real drag data of selected subsonic aircraft. Based on this, a second objective is to create a general estimation of the wave drag for any aircraft.

The project aims to study the drag polar of 16 passenger jet aircraft, focusing mainly on the wave drag. The key objectives include conducting a literature review on aerodynamic history, digitizing drag polar data from Obert (2009), and exploring existing and new mathematical approaches for wave drag. A generic drag polar equation will be proposed, incorporating wave and induced drag, with parameters calculated and visualized for each aircraft. Additionally, the project will explore how the parameters relate to aircraft geometry, enabling the estimation of drag coefficients for new aircraft in preliminary design.

1.4 Previous Research

This work is based on the drag polars for 16 aircraft presented in Obert (2009) in the form of drag coefficient over Mach number with lift coefficient as the parameter.

The fundamentals of aerodynamic drag of this work are mainly based on Raymer (1992), Shevell (1989), Niţă (2012a)) and Scholz (2015).

Mathematical approaches defining the wave drag essential for this work are made by Segiovia Garcia (2013), Gudmundsson (2014), Lock (1951), Scholz (2015) and Scholz (2017).

1.5 Structure of the Work

The structure of this work is as follows:

Chapter 2 presents the state of the art.

Chapter 3 states fundamentals of aerodynamic drag and metrics for evaluation regression models.

Chapter 4 covers the extraction of data by re-engineering from selected diagrams which present the drag polar of real aircraft.

Chapter 5 examines different mathematical approaches defining the wave drag.

Chapter 6 states the generic equation, gives information on the implementation and compares the outcome.

Chapter 7 provides parameters and plots for visualization of the best regression.

Chapter 8 gives a general guideline of how to estimate the wave drag for any aircraft.

Appendix A refers to Chapter 4 and verifies the additional conditions for the remaining regressions.

Appendix B presents the parameters for the remaining regressions of Chapter 6.

The associated Excel spreadsheets are available at: https://doi.org/10.7910/DVN/2UBNIE.

2 State of the Art

A literature review is done to gain information on the recent papers and check if the intention of this work is innovative. The following papers present current investigations in the field.

Filippone (2008) presents the historical approach with Lock's fourth power law (3.21) and the Korn equation (3.29).

Poll (2024) presents a model to estimate the wave drag and the effects of compressibility. The method presented is not user-friendly. This study intends to enhance accuracy in fuel burn estimation as the effects of the wave drag are crucial for fuel efficiency.

Wislicenus (2022) discusses the role of wave drag in estimating the performance of transport-category aircraft. A model is arrived at "after tedious algebraic reductions". The derivation is not given. Parameters a to e are defined. They are used to calculate parameters A to K. They are used to calculate the wave drag coefficient from a long polynomial of aircraft speed. Numerical results are not given.

Sun (2019) discusses drag polars in Chapter 7 of his dissertation. Interesting is the approach to evaluate climbing flights of aircraft taking off from Amsterdam Schiphol airport. Data is collected using the Mode-S receiver at the TU Delft. In addition, ground speed is obtained from ADS-B. Markov Chain Monte Carlo (MCMC) simulation is used to derive the drag polar for the 20 most used common aircraft. The approach is interesting but cannot be used for aircraft in preliminary design.

Scholz (2005) investigates the empirical investigation of parameters and equations related to the Mach number, relative thickness, sweep and lift coefficient. This paper presents a neat outline of different approaches estimating the drag divergence Mach number.

Gudmundsson (2022) provides guidance on designing an aircraft by discussing the thrust, stability and control of an aircraft. This work presents a new mathematical approach for the wave drag as described in Subchapter 3.2.4.

Barton (2023) presents a methodology for designing hydrogen aircraft that minimize persistent contrails. This paper uses Lock's forth power law to define the influence of compressible drag.

Poole (2017) focuses on the optimization of transonic airfoils. This paper proposes a range optimization approach to mitigate performance degradation at off-design conditions. In this the work discusses compressible drag in the context of transonic flows around airfoils. Aircraft drag polars are not given.

Some of the current papers on the topic work with wave drag calculated from Lock's fourth power law from 1951. Other papers derive complicated new equations for wave drag without showing numerical results. Further it is stated that the knowledge of details on the compressible drag is essential but limited available. This work is therefore necessary and attempts to fill that gap with a new approach.

3 Fundamentals

This chapter covers the fundamentals of aerodynamic drag, drag polars and the calculation of the drag coefficient. Furthermore, this chapter presents metrics to evaluate regression models.

3.1 Drag Polars

A drag polar represents the aerodynamic of an aircraft. Plotting the lift coefficient over the drag coefficient yields the so called drag polar by Otto Lilienthal. Figure 3.1 shows a drag polar for a single Mach number. In case of an uncambered wing the zero lift drag coefficient C_{D0} equals the minimum drag coefficient $C_{D,Min}$. (Raymer 1992)

Taking a step back, a drag polar with the Mach number as a general parameter presents further details on aerodynamics as illustrated in Figure 3.2. This form of presentation shows that the three parameters, lift coefficient, drag coefficient and Mach number, depend on each other. The same data set can also be presented in a different form with the drag coefficient over the Mach number with the lift coefficient as the parameter like in Figure 3.3. This form of presentation reveals a nearly constant drag coefficient at low Mach numbers and a sharp rise at transonic Mach numbers. (Shevell 1989)

A drag polar can also be described by an equation. The definition of a drag polar equation and its components are described in Subchapter 3.2.

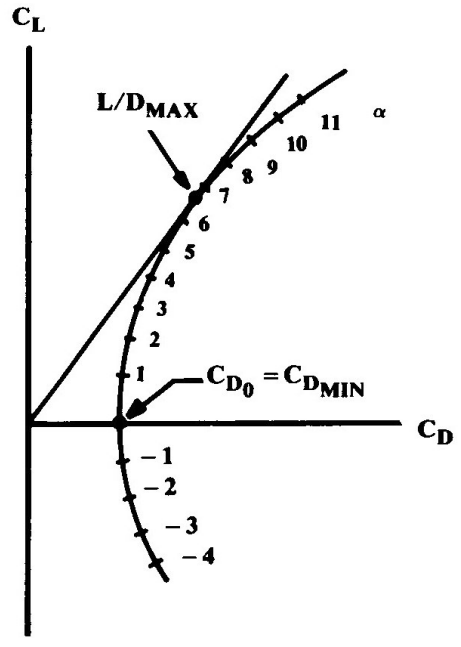

Figure 3.1 Drag polar uncambered and cambered (adapted from Raymer (1992))

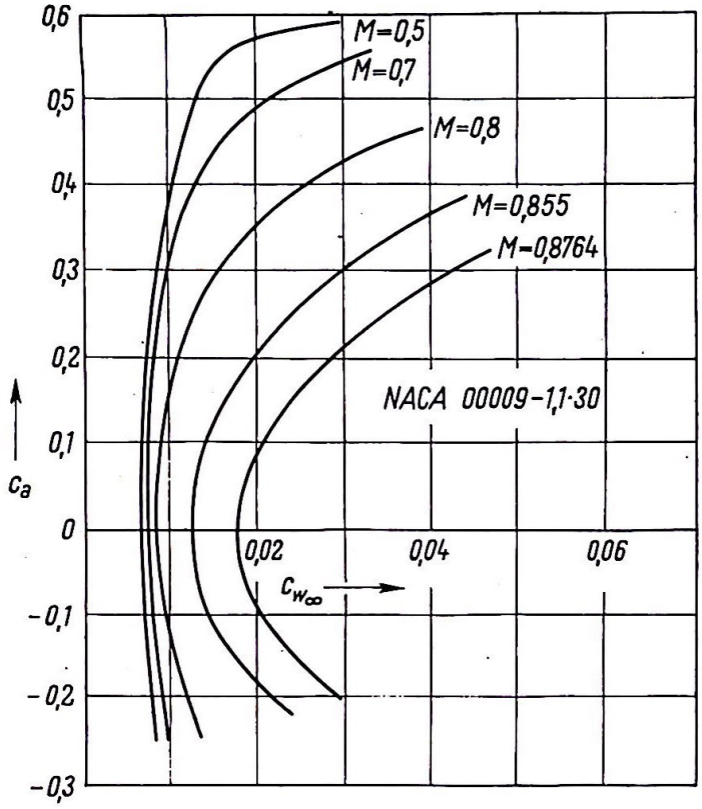

Figure 3.2 Lift coefficient versus drag coefficient (Dubs 1975) with C_a=C_L and C_w=C_D

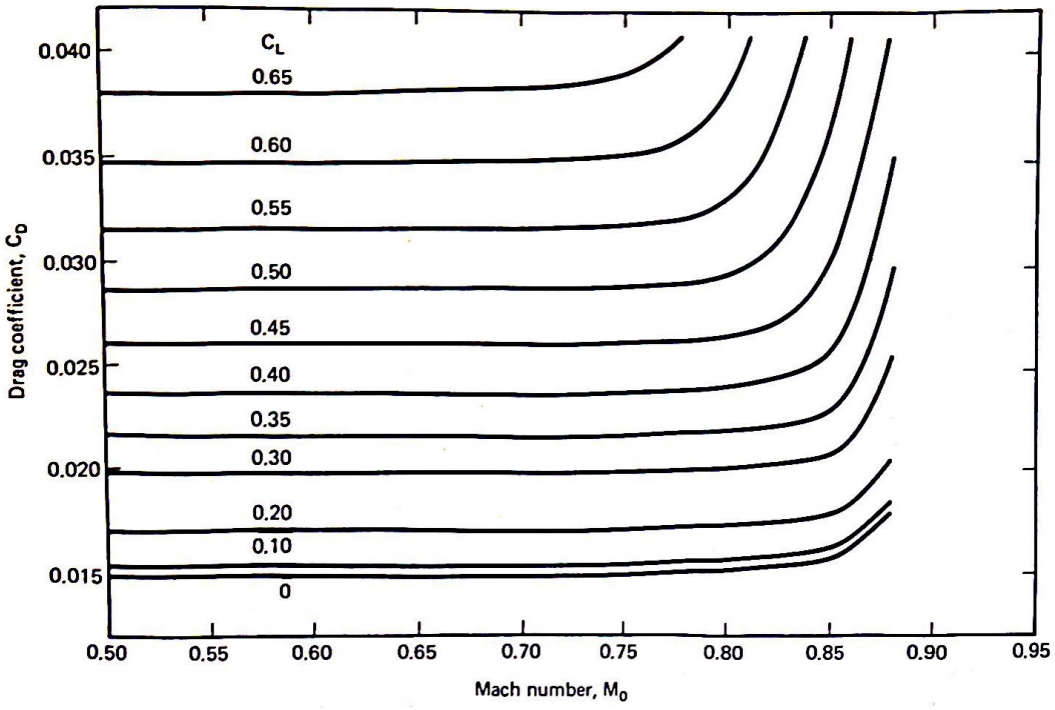

Figure 3.3 Drag coefficient versus Mach number (Shevell 1989)

3.2 Aerodynamic Drag and its Components

Aerodynamic drag can be subdivided into many components. Figure 3.4 shows this exemplarily by dividing the drag into parasite and induced drag due to shear or pressure forces. (Raymer 1992)

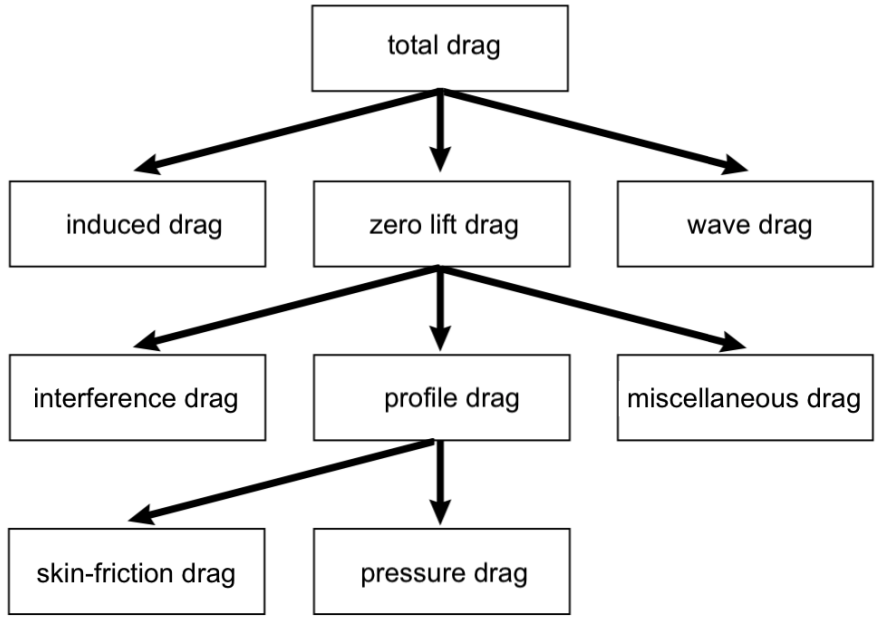

Figure 3.4 Drag terminology matrix (adapted from Scholz (2015))

Drag is spoken of as so many counts (cts) of drag with 1 cts = 0.0001. In a transonic region a common approach is to divide the drag into a component of zero lift, a component due to lift and a component due to compressibility. In other words, summing up the zero lift, induced and wave drag coefficient yields the total drag coefficient as defined in (3.1). Whether a drag polar is depicted with the lift coefficient versus drag coefficient as in Figure 3.2 or with the drag coefficient versus Mach number as in Figure 3.3 doesn't change Equation (3.1). (Shevell 1989)

$$C_D = C_{D0} + C_{Di} + C_{Dw} \tag{3.1}$$

3.2.1 Zero Lift Drag Coefficient

The zero lift drag coefficient C_{D0} is the drag coefficient when the lift is zero. Based on Scholz (2017) the zero lift drag coefficient can be calculated by

$$C_{D0} = \frac{\pi A e}{4 E_{max}^2} \quad . \tag{3.2}$$

In (3.2) E_{max} is the maximum glide ratio. Graphically it can be estimated as depicted in Figure **3.1**. Mathematically it is calculated by

$$E_{max} = k_E \sqrt{\frac{A}{S_{wet}/S_W}} \tag{3.3}$$

with

$$k_E = \frac{1}{2} \sqrt{\frac{\pi e}{C_{fe}}} \quad . \tag{3.4}$$

Table 3.1 and Figure 3.5 indicate values for the wetted area S_{wet} and the equivalent skin-friction drag coefficient C_{fe} for a general estimation. Further information on the wetted area S_{wet} and the equivalent skin-friction drag coefficient C_{fe} as well as other mathematical approaches to calculate the zero lift drag coefficient C_{D0} are discussed in Scholz (2015). Scholz (2015) also presents that the skin-friction coefficient and therefore the zero lift drag coefficient depends on the Mach number. But as this influence is neglectable small, the zero lift drag coefficient is typically set constant. The calculation of the Oswald efficiency factor e in (3.2) and (3.4) is described in Subchapter 3.2.3.

Table 3.1 The equivalent skin-friction drag coefficient on the basis of general experience (adapted from Scholz (2015) based on Roskam 1997)

aircraft type	C_{fe} - subsonic
jets	0.003 … 0.004
twins	0.004 … 0.007
singles	0.005 … 0.007

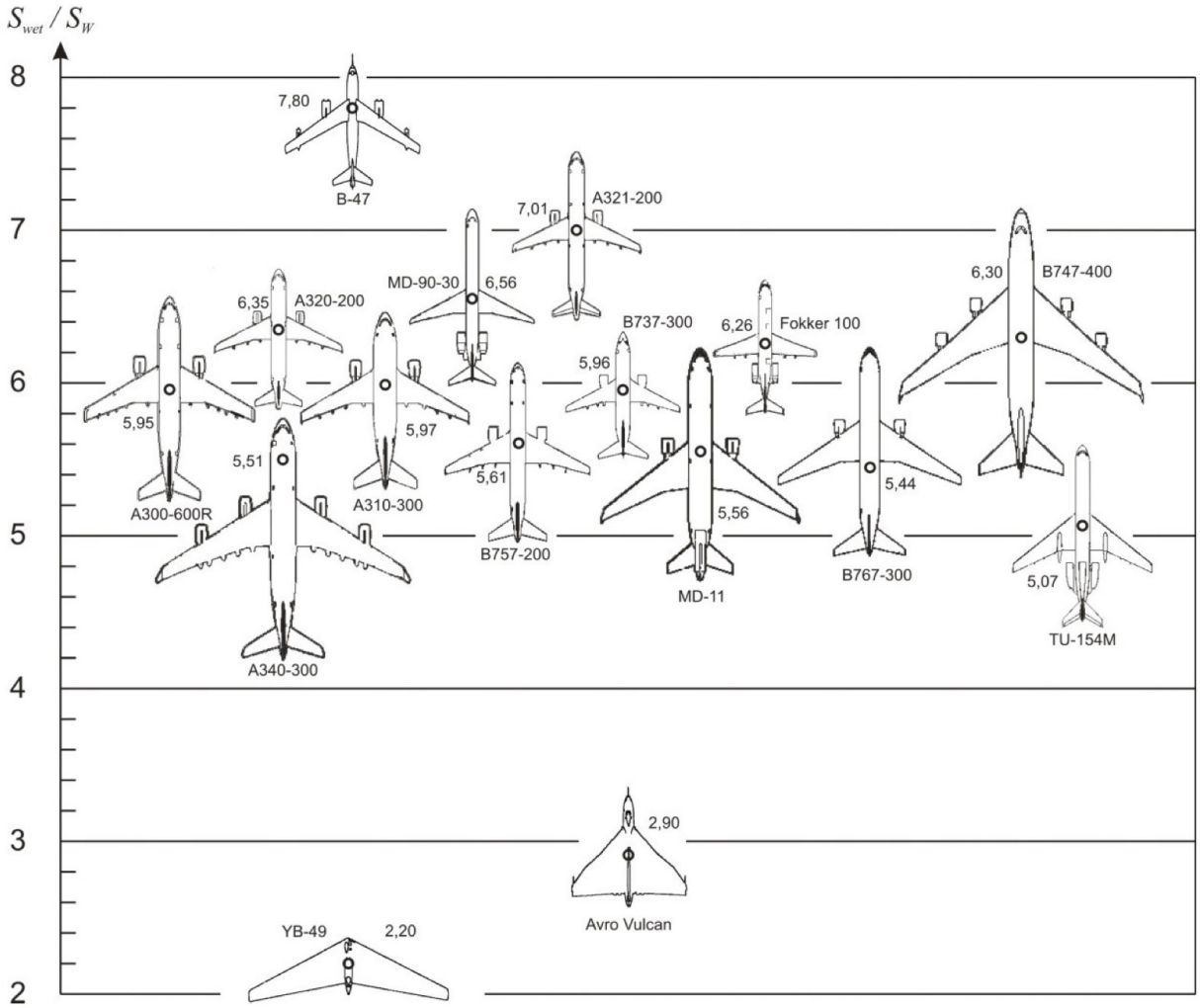

Figure 3.5 Aircraft plan forms and their relative wetted area S_{wet} / S_W (Scholz 2017)

3.2.2 Induced Drag Coefficient

The induced drag coefficient represents the drag due to lift. As defined in (3.5) it is dependent on the lift coefficient, the aspect ratio and the Oswald efficiency factor (Bertin 2009). The calculation of the Oswald efficiency factor e is described in Subchapter 3.2.3. Because the Oswald efficiency factor depends on the Mach number, the induced drag does, too.

$$C_{Di} = \frac{C_L^2}{\pi A e} \tag{3.5}$$

3.2.3 Oswald Efficiency Factor

The Oswald efficiency factor e corrects the aspect ratio for the calculation of drag coefficients. This chapter presents two methods based on Niţă (2012a and 2012b) to estimate the Oswald efficiency factor e.

The first method calculates the Oswald efficiency factor e without input of the zero lift drag coefficient and is therefore used for preliminary sizing. Here the Oswald efficiency factor e is the product of a theoretical Oswald efficiency factor e_{theo} and correction factors.

$$e = e_{theo} \cdot k_{e,F} \cdot k_{e,D0} \cdot k_{e,M} \tag{3.6}$$

The theoretical Oswald factor represents the inviscid drag due to lift only and is estimated by

$$e_{theo} = \frac{1}{1 + f(\lambda) \cdot A} \quad . \tag{3.7}$$

At this, f(λ) is a function of taper ratio depicted in Figure 3.6. Hoerner (1965) expresses the additional induced drag of tapered wings with this function. For unswept wings this function can be approximated by

$$f(\lambda) = 0.0524\lambda^4 - 0.15\lambda^3 + 0.1659\lambda^2 - 0.0706\lambda + 0.0119 \quad . \tag{3.8}$$

The definition of the taper ratio is

$$\lambda = \frac{c_{tip}}{c_{root}} \quad . \tag{3.9}$$

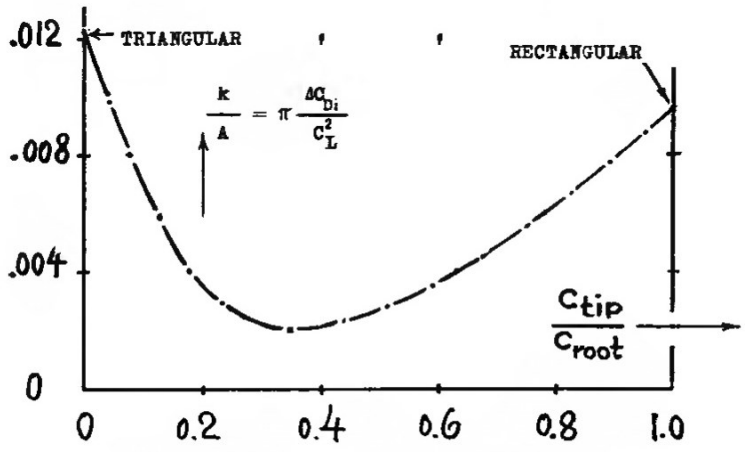

Figure 3.6 Function of taper ratio representing additional induced drag (Hoerner 1965)

In case of a swept wing the definition of the theoretical Oswald efficiency factor changes to

$$e_{theo} = \frac{1}{1 + f(\lambda - \Delta\lambda) \cdot A} \quad . \tag{3.10}$$

With

$$\Delta\lambda = -0.357 + 0.45e^{-0.0375\varphi_{25}} \tag{3.11}$$

the function of taper ratio becomes

$$\begin{gathered} f(\lambda - \Delta\lambda) = 0.0524(\lambda - \Delta\lambda)^4 - 0.15(\lambda - \Delta\lambda)^3 + 0.1659(\lambda - \Delta\lambda)^2 + \ldots \\ \ldots - 0.0706(\lambda - \Delta\lambda) + 0.0119 \quad . \end{gathered} \tag{3.12}$$

In (3.11) the sweep angle is inserted in degrees. Moreover, the correction factors are necessary to calculate the Oswald efficiency factor in (3.6). The correction factor $k_{e,F}$ stands for losses due to the fuselage and is therefore dependent on the ratio of fuselage width over wing span. This correction factor can either be taken from Table 3.2 or for greater detail calculated by

$$k_{e,F} = 1 - 2\left(\frac{d_F}{b}\right)^2 \quad . \tag{3.13}$$

Table 3.2 presents, dependent on the type of aircraft, also values for the correction factor $k_{e,D0}$ to consider the viscous drag due to lift.

Table 3.2 Correction factors for the Oswald efficiency factor (based on Niţă 2012b)

Aircraft category	All	Jet	Business Jet	Turboprop	General Aviation
d_F / b	0.114	0.116	0.120	0.102	0.119
$k_{e,F}$	0.974	0.973	0.971	0.979	0.971
$k_{e,D0}$	-	0.873	0.864	0.804	0.804

The correction factor $k_{e,M}$ represents compressibility effects on induced drag. It is therefore dependent on the Mach number as defined as

$$k_{e,M} = 1 + a_e\left(\frac{M}{M_{comp}} - 1\right)^{b_e} \tag{3.14}$$

with

$$a_e < 0 \text{ and usually } M_{comp} = 0.3 \quad .$$

Generic values for the parameters are a_e=-0.00152 and b_e=10.82. The correction factor $k_{e,M}$ is the only Mach number dependent part of the Oswald efficiency factor e. The other three terms only depend on the geometry of the aircraft. They can therefore be combined to a geometrical Oswald efficiency factor e_{geo} as (3.15) shows. The Oswald efficiency factor e is then shortened to (3.16).

$$e_{geo} = e_{theo} \cdot k_{e,F} \cdot k_{e,D0} \tag{3.15}$$

$$e = e_{geo} \cdot k_{e,M} \tag{3.16}$$

The second method to estimate the Oswald efficiency factor e uses the zero lift drag coefficient C_{D0} as an input parameter and is therefore used when C_{D0} is calculated from handbook methods as given in Scholz (2015, Chapter 13). In this method the Oswald efficiency factor e is defined by

$$e = \frac{k_{e,M}}{Q + P\pi A} \tag{3.17}$$

with

$$Q = \frac{1}{e_{theo} k_{e,F}} \tag{3.18}$$

and

$$P = KC_{D0} \quad . \tag{3.19}$$

In similarity to method 1, the theoretical Oswald efficiency factor is needed as well as the correction factors $k_{e,M}$ and $k_{e,F}$. The definition of these parameters is the same as in the first method. Additionally, a factor K with a generic value of K=0.38 is used. This method can be further extended to include the effect of twist. This is described in Niţă (2012b).

3.2.4 Wave Drag Coefficient

Wave drag, also called compressible drag or drag rise, occurs at high subsonic and transonic speeds. The wave drag is characterized by a rapid rise in drag as depicted in Figure 3.7 due to the formation of shock waves. (Raymer 1992)

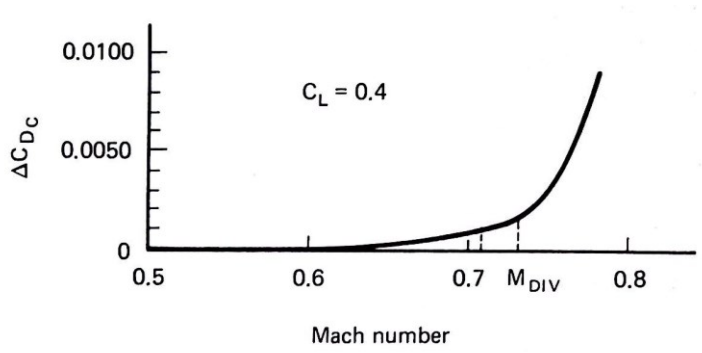

Figure 3.7 Typical wave drag variation with Mach number (adapted from Shevell (1989)) with $C_{Dc}=C_{Dw}$ and $M_{DIV}=M_{DD}$

As the critical Mach number M_{crit} is defined as the Mach number at which the local Mach number on the airfoil first reaches $M=1$, shock waves and therefore the wave drag appears first at $M=M_{crit}$. The steep rise of wave drag defines the drag divergence Mach number M_{DD} as depicted in Figure 3.7. As the fuel consumption and moreover the costs of a flight increase with increasing drag, the drag divergence Mach number is a main design parameter for aircraft. (Shevell 1989)

Equation (3.20) states the correlation of the critical Mach number and the drag divergence Mach number. Raymer (1992) states the delta in Mach number to be about $\Delta M = 0.08$ whereas Scholz (2017) states the delta in Mach number to be about $\Delta M = 0.14 \ldots 0.20$ based on analysed aircraft data. Further information on the drag divergence Mach number is presented in Subchapter 3.2.5.

$$M_{crit} = M_{DD} - \Delta M \tag{3.20}$$

Several mathematical approaches exist to describe the wave drag. The most common one is

$$C_{Dw} = 20(M - M_{crit})^4 \quad . \tag{3.21}$$

This equation originates from Lock (1951) and was spread by Mason (2019). See also Malone (1995).

Scholz (2015) presents a similar approach as stated in (3.22) using variable parameters.

$$C_{Dw} = a\left(\frac{M}{M_{crit}} - 1\right)^b \tag{3.22}$$

Another common reference on the wave drag is displayed in Figure 3.8. Shevell (1989) states that the correlation between the ratio of the wave drag to the cosine to the third power of the sweep angle and the ratio of the freestream Mach number to the crest critical Mach number is

as Figure 3.8 shows. Based on this, Segiovia Garcia (2013) presents an equation for the wave drag as stated in (3.23).

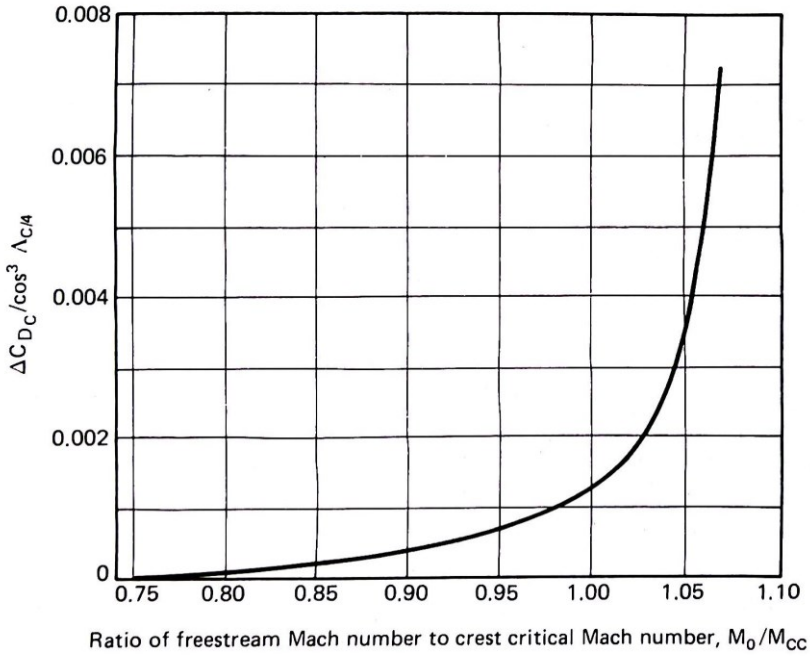

Figure 3.8 Incremental drag coefficient due to compressibility (Shevell 1989) with C_{DC}=C_{DW} and $\Lambda = \varphi$

$$C_{Dw} = A \tan\left(B \frac{M}{M_{crit}} - B\right) \tag{3.23}$$

Furthermore, Gudmundsson (2022) presents the most recent approach to estimate the wave drag. This approach is based on the hyperbolic tangent as Figure 3.9 shows.

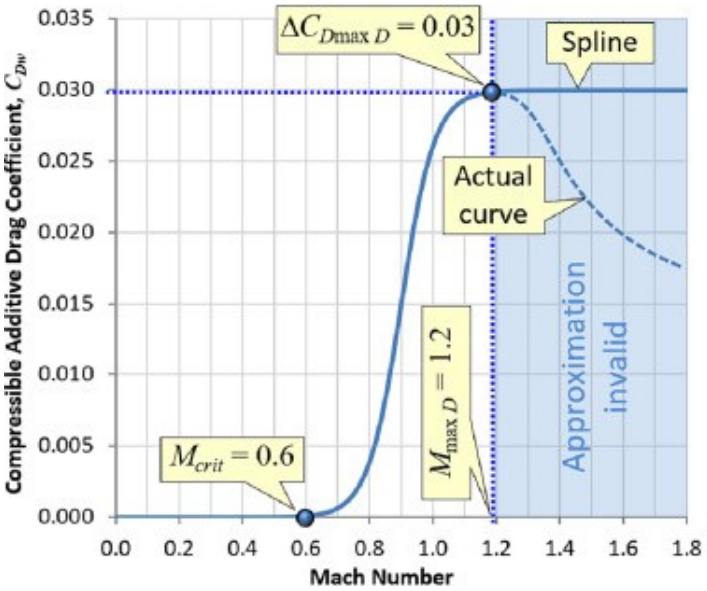

Figure 3.9 Wave drag approximation (Gudmundsson 2022)

He defines the wave drag as

$$C_{Dw} = \frac{\Delta C_{D,maxD}}{2}(1 + \tanh(AM_\infty - B)) \tag{3.24}$$

with

$$A = f(C_{D,maxD}, M_{maxD}, M_{crit}) \tag{3.25}$$

and

$$B = f\left(C_{D,maxD}, M_{crit}\right) \ . \tag{3.26}$$

3.2.5 Drag Divergence Mach Number

The drag divergence Mach number M_{DD} is defined by a steep rise of wave drag as depicted in Figure 3.7 (Shevell 1989).

According to Raymer (1992), two common definitions exist for the drag divergence Mach number. The first definition is called the "Boeing definition". It is depicted in Figure 3.10 and in Equation (3.27). In this definition the drag divergence Mach number is the Mach number at which the wave drag first reaches 20 counts. The second definition called the "Douglas definition" defines the drag divergence Mach number as the Mach number at which the rate of change in drag with Mach number first reached 0.10. Equation (3.28) describes this definition.

$$c_{Dw}(M = M_{DD}) = 0.002 = 20 \text{ cts} \tag{3.27}$$

$$\frac{dc_D}{dM}(M = M_{DD}) = 0.1 \tag{3.28}$$

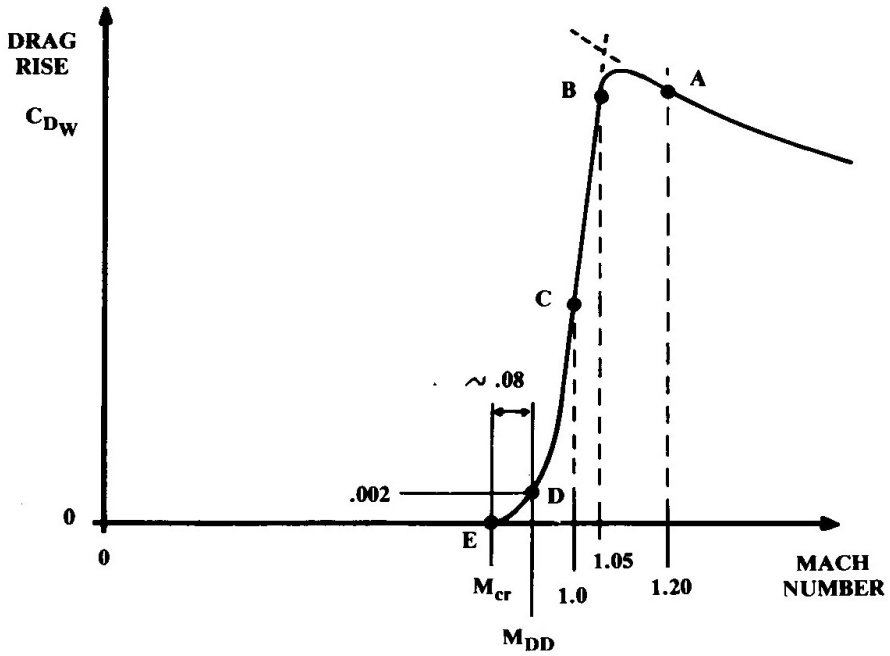

Figure 3.10 Transonic drag rise estimation (Raymer 1992) with M_{cr}=M_{crit}

Equation (3.20) states the correlation between the critical Mach number and the drag divergence Mach number. In the same manner as the critical Mach number changes with a change in lift coefficient and wing sweep, so changes the drag divergence Mach number, too, as illustrated in Figure 3.11. The correlation between the drag divergence Mach number and the lift coefficient is depicted in Figure 3.12.

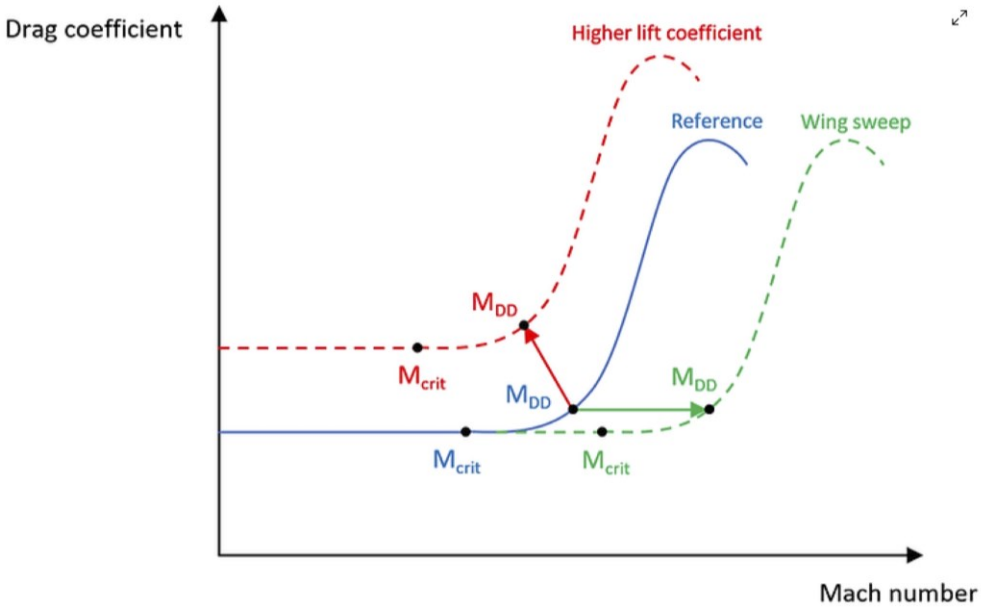

Figure 3.11 Change of characteristic Mach numbers with lift coefficient and sweep (Horn 2022)

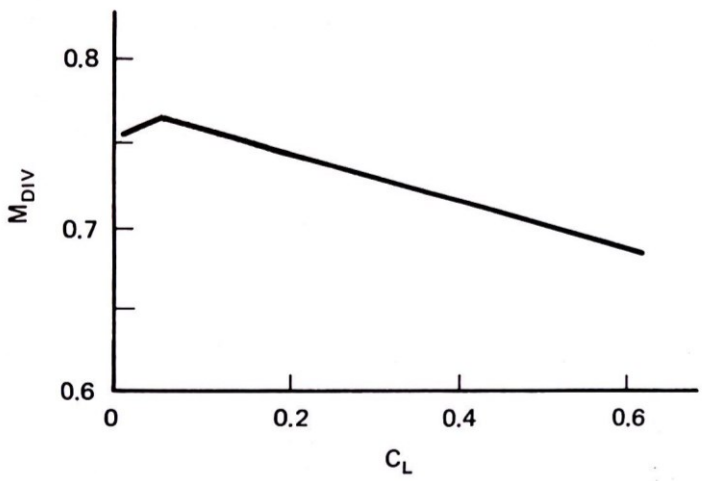

Figure 3.12 Drag divergence Mach number versus lift coefficient (Shevell 1989) with $M_{DIV}=M_{DD}$

Several approaches exist to calculate the drag divergence Mach number. A common approach is the Korn equation spread by Mason (2019). See also Malone (1995). It is defined as

$$M_{DD} = \frac{K_A}{\cos\varphi_{25}} - \frac{\frac{t}{c}}{\cos^2\varphi_{25}} - \frac{C_L}{10\cos^3\varphi_{25}} \tag{3.29}$$

based on an aircraft's geometry, the lift coefficient and an airfoil technology factor K_A which is approximately K_A=0.80…0.90 (Scholz 2005). Scholz (2005) presents a neat outline of different approaches. In their work a nonlinear regression yields the best solution. The equation is stated as

$$\frac{t}{c} = k_t \cdot M_{DD}^t \cdot \cos\varphi_{25}{}^u \cdot C_L^v \cdot k_M^w \tag{3.30}$$

with t/c being the relative thickness of the wing. k_t, t, u, v and w are parameters. Optimized values of these parameters are (Scholz 2005): k_t=0.127, t=-0.204, u=0.573, v=0.065 and w=0.556.

The parameter k_M depends on the generation of the airfoil as stated in Table 3.3. Rearranging (3.30) to M_{DD} yields

$$\begin{aligned} M_{DD} &= \sqrt[t]{\frac{\frac{t}{c}}{k_t \cdot \cos\varphi_{25}{}^u \cdot C_L^v \cdot k_M^w}} = k_t^{-\frac{1}{t}} \cdot \frac{t}{c}^{\frac{1}{t}} \cdot \cos\varphi_{25}{}^{-\frac{u}{t}} \cdot C_L^{-\frac{v}{t}} \cdot k_M^{-\frac{w}{t}} \\ M_{DD} &= k_t^{4.902} \cdot \frac{t}{c}^{-4.902} \cdot \cos\varphi_{25}{}^{2.809} \cdot C_L^{0.319} \cdot k_M^{2.725} \quad . \end{aligned} \tag{3.31}$$

Table 3.3 Parameter k_M used for Equation (3.30) (Scholz 2005)

parameter	value
k_M for conventional	0.921
k_M for peaky	0.928
k_M for older supercritical	1.017
k_M for modern supercritical	0.932

3.3 Statistical Metrics

This subchapter states metrics used for the evaluation of regression models and is based on Sagi (2024) unless stated otherwise. In a regression the difference between an estimated value $\hat{y}_i$ and an actual value y_i is of interest. This difference is also called error. The smaller the difference the better the regression. Squaring the difference cancels out the algebraic-sign and sanctions greater differences more than smaller ones.

The sum of squared estimate of errors (SSE) is also called the residual sum of squares (RSS). It is the sum of the squared difference of the estimated and the actual value for all data points. Dividing the SSE by the number of data points yields the mean squared error (MSE). This is akin to the variance. The lower the score of SSE or MSE, the better the regression model. (Wikipedia 2023 and Wikipedia 2025b)

$$SSE = \sum_{i=1}^{n} (y_i - \hat{y}_i)^2 \tag{3.32}$$

$$MSE = \frac{1}{n} \sum_{i=1}^{n} (y_i - \hat{y}_i)^2 \tag{3.33}$$

The root mean squared error (RSME) is the standard deviation of a dataset. An advantage of this metric is the simple interpretation as the RSME is in the same unit as the original data. Taking the root of the MSE yields the RSME. It measures the concentration of the data around the regression line. A lower score of RSME means a better regression model.

$$RMSE = \sqrt{\frac{1}{n} \sum_{i=1}^{n} (y_i - \hat{y}_i)^2} \tag{3.34}$$

SSE, MSE and RSME are in the unit of the original data. To gain a unitless metric, the difference of the estimated and actual values has to be divided by the actual value. This metric

is called root mean squared percentage error (RMSPE). Its prediction error is smaller than from RMSE and can be used to compare results unitless. Still, the lowest score yields the best regression model.

$$RMSPE = \sqrt{\frac{1}{n}\sum_{i=1}^{n}\left(\frac{y_i - \hat{y}_i}{y_i}\right)^2} \tag{3.35}$$

4 Digitalization of the Diagrams

This chapter explains how the diagrams are digitalized. Obert (2009) gives the drag polar for 16 aircraft in the form of drag coefficient over Mach number with the lift coefficient as a parameter. The diagrams in Obert (2009) differ in quality and present one to three aircraft each for three to six lift coefficients. Here, Figure 4.1 and Figure 4.2 show this exemplarily. The drag coefficient is mostly given in counts.

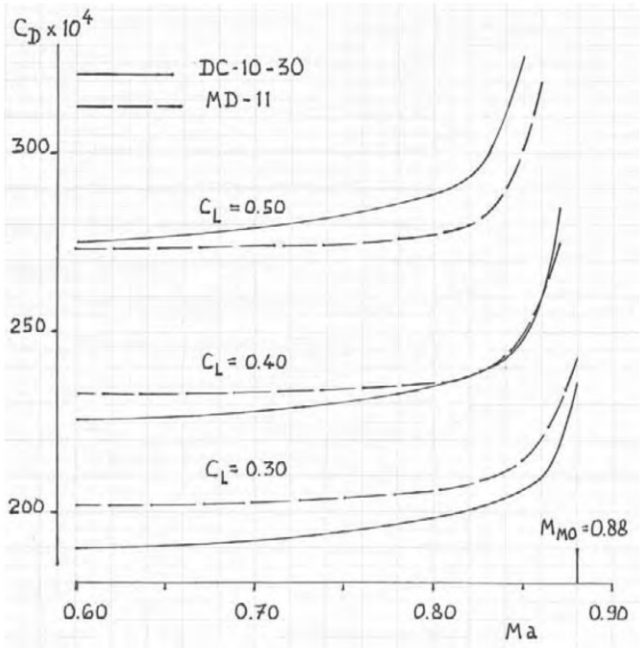

Figure 4.1 Drag polars of the DC-10-30 and MD-11 (Fig. 24.26 in Obert (2009))

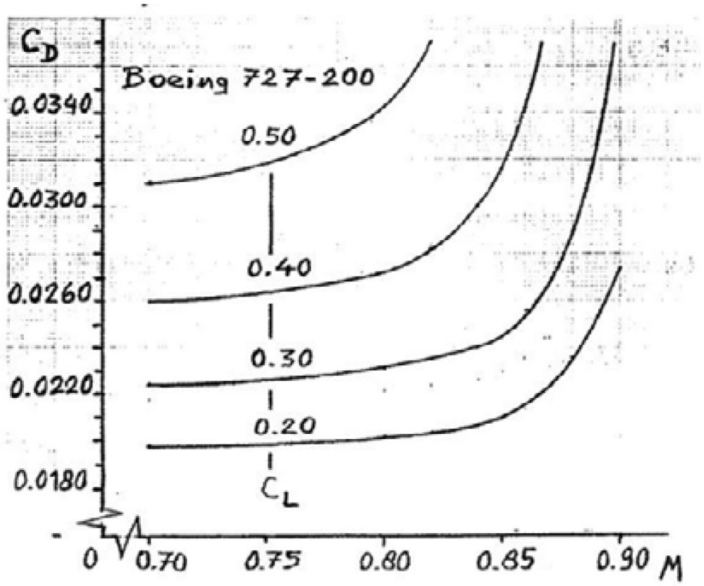

Figure 4.2 Drag polars of the B727-200 (Fig. 24.53 in Obert (2009))

The WebPlotDigitizer is used to digitalize the diagrams. This tool has already been used by Bensel (2018) after testing several programs. The two main advantages of the WebPlotDigitizer are that it's fully open source and easy to handle. As of March 2025, the tool is available at Rohatgi (2024). The first step in digitalizing a diagram is to upload it as a picture format and to calibrate the axes as shown in Figure 4.3. The four reference points can be manually adjusted by using the arrow keys, so that a precise calibration is possible.

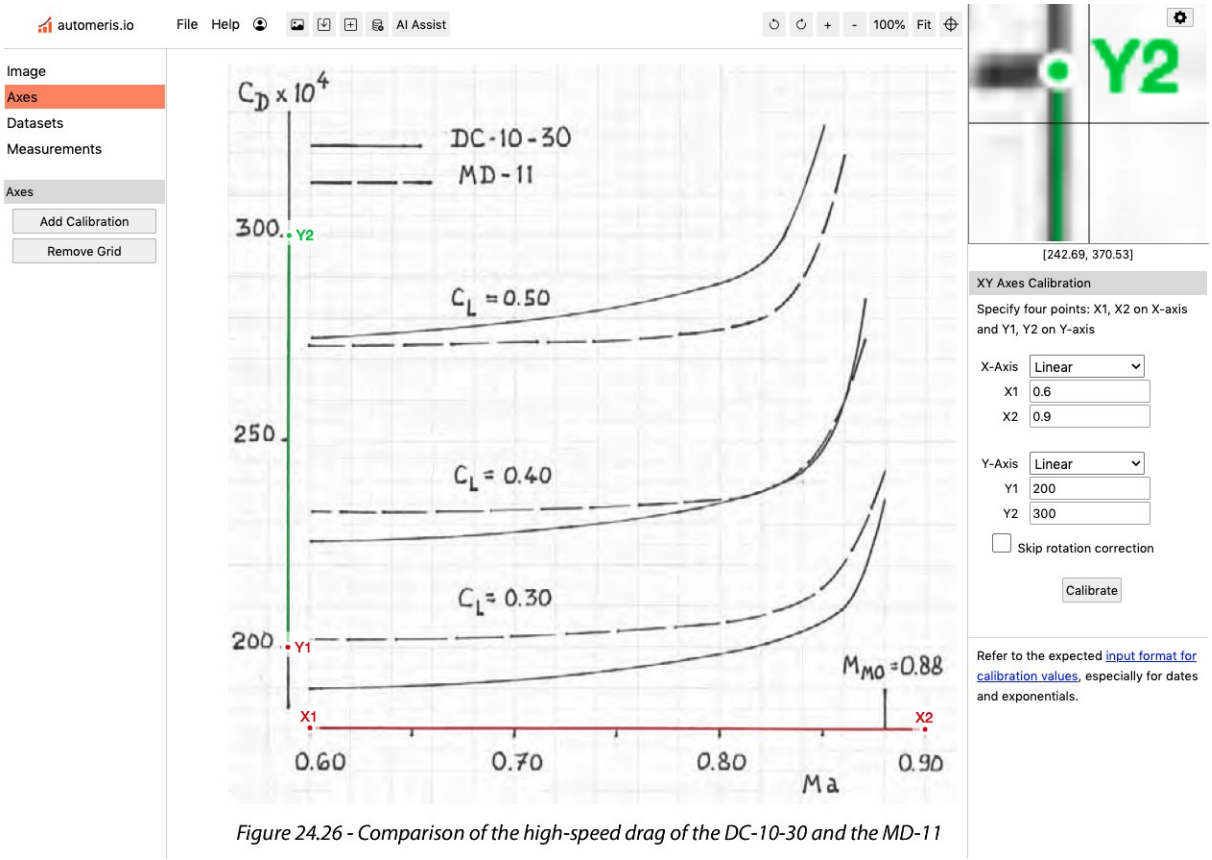

Figure 4.3 Calibration of the axes with the WebPlotDigitizer

After this, the main part of the digitalization takes place. A single line of the drag polar is roughly marked with a pen as shown in Figure 4.4. The menu on the right-hand side is used to select the color of the line and to change the settings of a run. It is possible to edit the distance between two data points and the level of color filtering. The better the quality of the diagram is the lower score of color filtering is necessary to generate evenly spread data points. After a run, several data points are generated as Figure 4.5 shows. Most of these data points are precisely on the line, but a few data points especially in areas of overlapping lines are off the line, so that every data point needs to be checked. Data points can be adjusted, deleted or created as necessary. The zoom area at the top right helps at this. Figure 4.6 shows the same line after inspection. Then, this process is repeated for every line in every diagram. The final layout of all data points for DC-10-30 and MD-11 is presented in Figure 4.7. Further information is available at the "Help" section in the upper left corner.

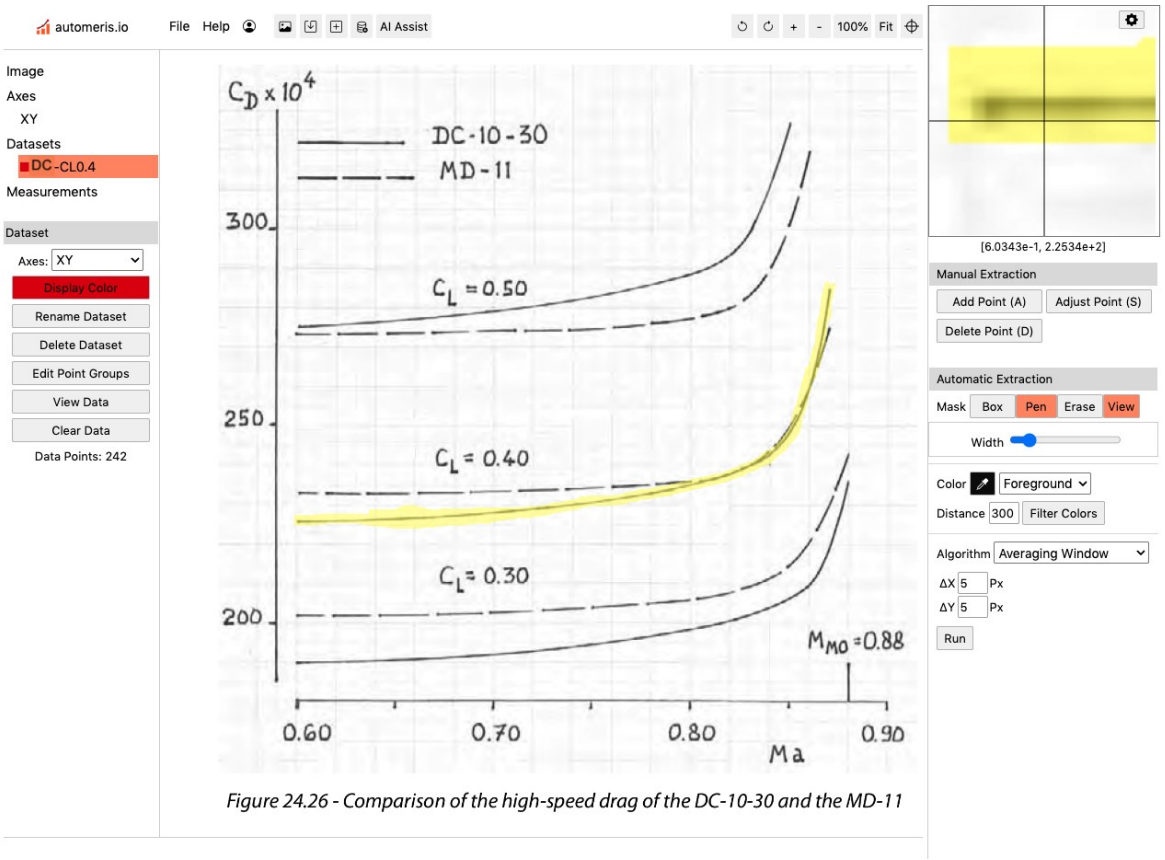

Figure 24.26 - Comparison of the high-speed drag of the DC-10-30 and the MD-11

Figure 4.4 Preparations for a run

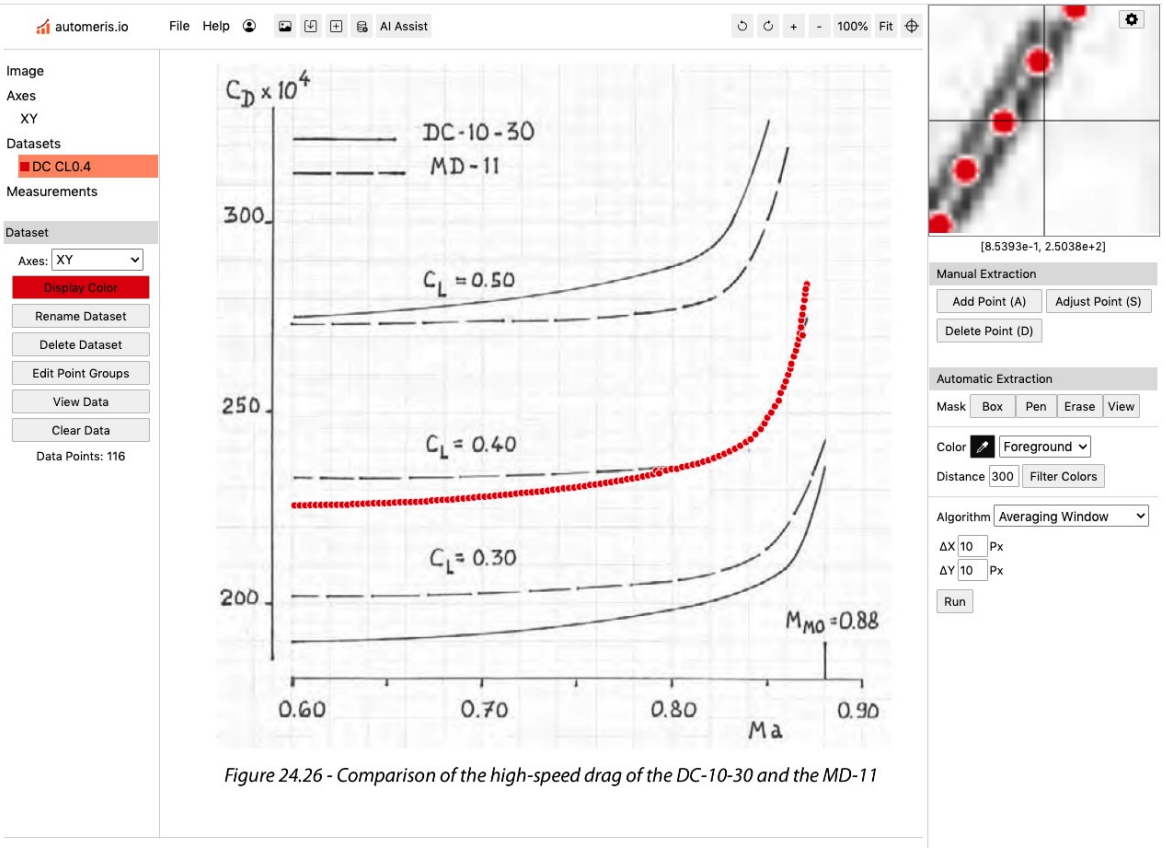

Figure 24.26 - Comparison of the high-speed drag of the DC-10-30 and the MD-11

Figure 4.5 Error-prone data points after a single run

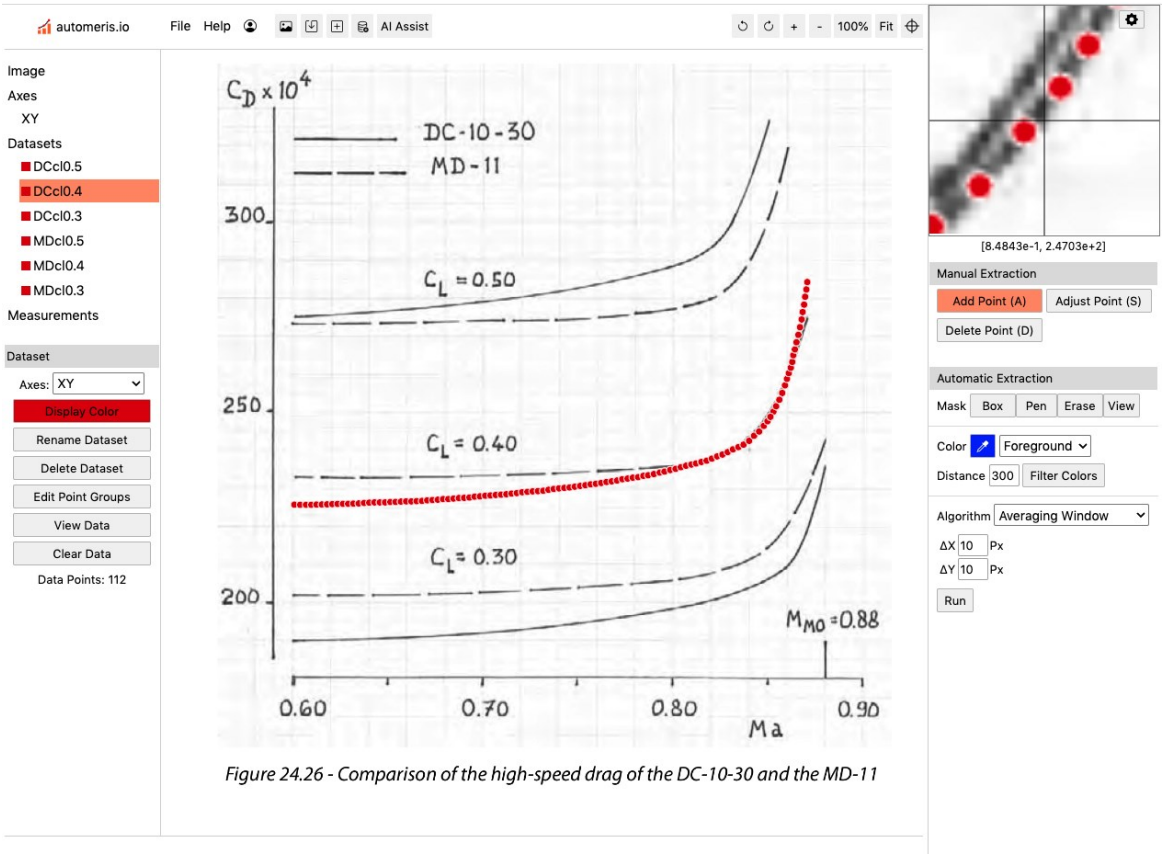

Figure 24.26 - Comparison of the high-speed drag of the DC-10-30 and the MD-11

Figure 4.6 Edited and revised data points of a single run

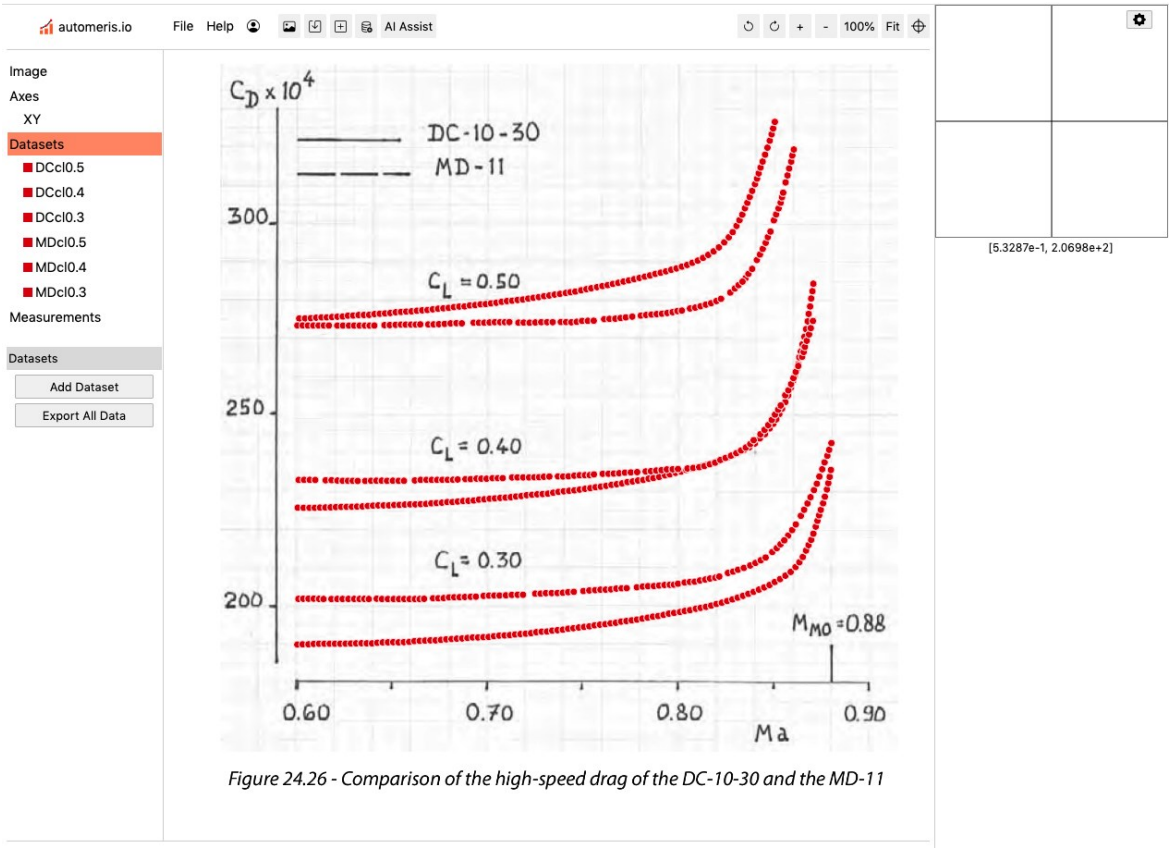

Figure 24.26 - Comparison of the high-speed drag of the DC-10-30 and the MD-11

Figure 4.7 Checked data points for all lift coefficients

Finally, the data points can be exported as a file with comma-separated values. Here, this data is rearranged and edited in Excel for further work. Based on these data points the new diagrams of the DC-10-30, MD-11 and B727-200 are depicted in Figure 4.8, Figure 4.9 and Figure 4.10.

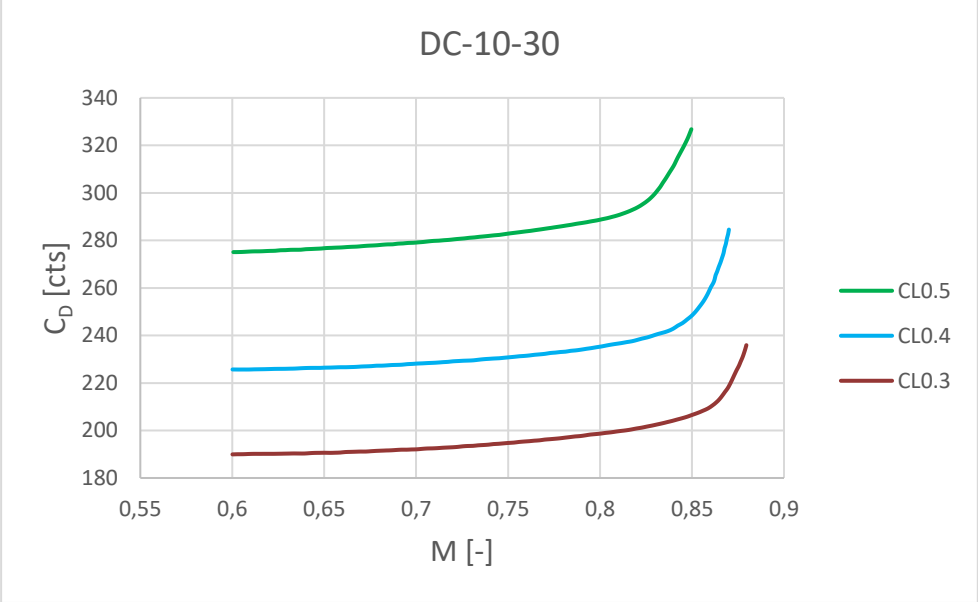

Figure 4.8 Drag polar of the DC-10-30

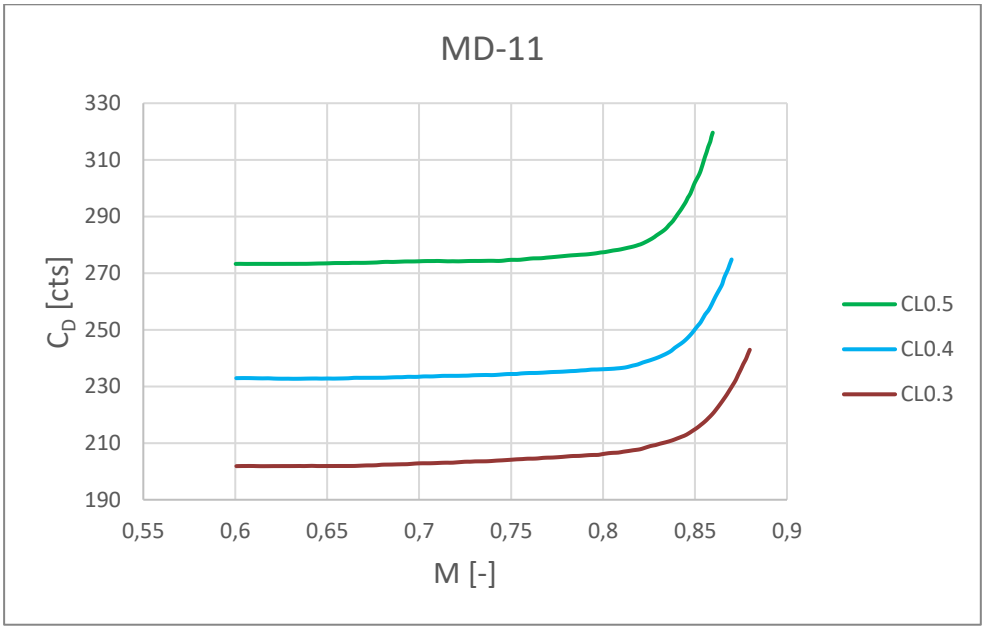

Figure 4.9 Drag polar of the MD-11

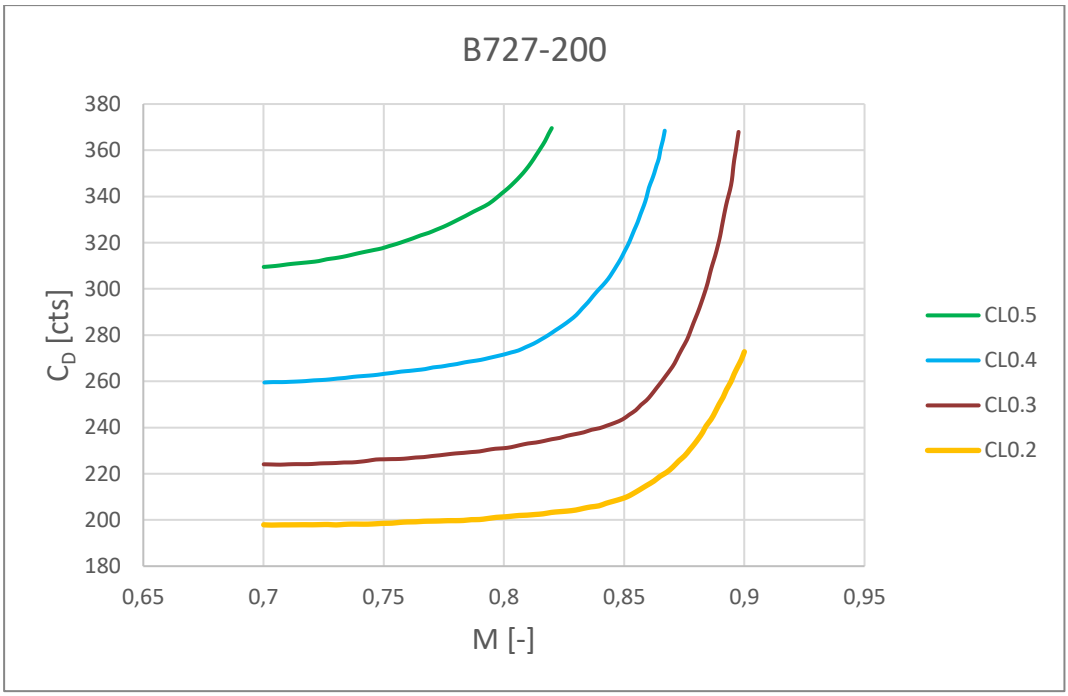

Figure 4.10 Drag polar of the B727-200

5 Examination of Existing and New Equations for the Wave Drag

The history of aerodynamics already presents some approaches for the wave drag as stated in Subchapter 3.2.4. In this chapter these approaches are analyzed as well as new mathematical approaches.

5.1 First Outline of Mathematical Approaches

As described in Subchapter 3.2.4, a widely common approach for the wave drag originates on Lock (1951) and is spread by Mason (2019). See also Malone (1995). This approach is partially based on aerodynamics and is stated in (3.21) and (3.29). An advantage of this approach is its simpleness. Its lack of parameters enables a quick estimation in general.

$$C_{Dw} = 20(M - M_{crit})^4 \tag{3.21}$$

The downside of no parameters is, that an adjustment on varying aircraft aerodynamics due to geometrical factors is not possible. For that reason, Equation (3.21) is additionally generalized to Equation (5.1), keeping the power of four. With a=20 and b=M_{crit}, Equation (5.1) turns into (3.21).

$$C_{Dw} = a\left(b\frac{M}{M_{crit}} - b\right)^4 \tag{5.1}$$

Thinking this through to the end, Equation (5.2) presents the fully generalized mathematical approach of (3.21). With a=20, b=M_{crit} and c=4, Equation (5.2) turns into (3.21). The more parameters there are, the more complex is the regression and the more time is needed. But on the other hand, the more parameters there are, the better is the accurate adaption to original data.

$$C_{Dw} = a\left(b\frac{M}{M_{crit}} - b\right)^c \tag{5.2}$$

Another existing approach is (5.3). This approach is based on Shevell (1989) and Segiovia Garcia (2013) as described in Subchapter 3.2.4.

$$C_{Dw} = a\tan\left(b\frac{M}{M_{crit}} - c\right) \tag{5.3}$$

The function of tangent is a periodic function, which could be obstructive in terms of a regression. Therefore, the tangent is additionally replaced by the hyperbolic sine because the hyperbolic sine has similar characteristics as the tangents without the periodicity. Keeping the same structure of the mathematical approach yields Equation (5.4).

$$C_{Dw} = a \sinh\left(b \frac{M}{M_{crit}} - c\right) \tag{5.4}$$

As stated in Subchapter 3.2.4, Gudmundsson (2022) recognizes the hyperbolic tangent to fit the structure of the wave drag curve. As the wave drag curve is zero for $M<M_{crit}$ the tangent hyperbolics is shifted by one, so that the tangent hyperbolics is also zero for $M \to -\infty$. Keeping the structure of the other mathematical approaches yields Equation (5.5).

$$C_{Dw} = a \left(1 + \tanh\left(b \frac{M}{M_{crit}} - c\right)\right) \tag{5.5}$$

In general, hyperbolic functions are based on exponential function with the Euler's number *e* as its base. Considering this, a direct formulation of the wave drag as an exponential function is possible as well. Keeping the structure of the other mathematical approaches yields Equation (5.6).

$$C_{Dw} = a e^{b \frac{M}{M_{crit}} - c} \tag{5.6}$$

5.2 Additional Conditions

Per definition the wave drag occurs at $M \geq M_{crit}$, so that the first appearance at $M=M_{crit}$ needs to be further looked at. On the assumption that nature doesn't make jumps the point of transition at $M=M_{crit}$ has to be without a jump in drag. As a consequence, the initial value of the wave drag at the critical Mach number is zero as denoted in (5.7.). Equation (5.7) is further called the first condition.

$$C_{Dw}(M = M_{crit}) \stackrel{!}{=} 0 \tag{5.7}$$

In like manner, the drag polar is assumed to be without a kink at the point of transition. Consequently, the initial rise of the wave drag at the critical Mach number is zero as denoted in (5.8). Equation (5.8) is further called the second condition.

$$\frac{d}{dM} C_{Dw}(M = M_{crit}) \stackrel{!}{=} 0 \tag{5.8}$$

The conditions (5.7) and (5.8) are examined for the mathematical approaches made in Subchapter 5.1. Exemplary, this is presented with Equation (5.2) here. As Equation (5.2) is the general form of (5.1) and (3.21), all three approaches fulfill the conditions, if (5.2) fulfills it. Equation (5.9) shows the first condition and Equation (5.10) shows the second condition for the approach made in (5.2). Both conditions are fulfilled, independent of the parameters. This is another main advantage of these mathematical approaches.

$$C_{Dw}(M = M_{crit}) \stackrel{!}{=} 0 = a\left(b\frac{M_{crit}}{M_{crit}} - b\right)^{c} = a \cdot (0)^{c} = 0 \tag{5.9}$$

$$\frac{d}{dM}C_{Dw}(M = M_{crit}) \stackrel{!}{=} 0 = a\frac{bc}{M_{crit}}\left(b\frac{M_{crit}}{M_{crit}} - b\right)^{c-1} = a\frac{bc}{M_{crit}} \cdot (0)^{c-1} = 0 \tag{5.10}$$

For reasons of clarity and comprehensibility the validation of these two conditions for the other mathematical approaches is done in Appendix A. It yields that a correction term is necessary to fulfill the conditions exactly. In practice, this correction factor is approximately zero, so that this term can be neglected if the values of the parameters are checked on plausibility. Furthermore, the first condition is fulfilled for (5.3) and (5.4), if the parameter b equals c. Consequently, this result is implemented in the mathematical approach for further work. Subchapter 5.3 displays the final mathematical approaches of the wave drag. A summary of findings of this chapter is displayed in Table 5.1. Based on these findings the "Raise to Power" approach is expected to yield the best regression.

Table 5.1 Overview of characteristics of mathematical approaches

Equation	Name	Number of Parameters	Condition 1 fulfilled	Condition 2 fulfilled	Notes
(3.21)	Lock	0	yes	yes	simple; quick estimation
(5.1)	Lock general	2	yes	yes	adaption possible to aircraft
(5.2)	Raise to Power	3	yes	yes	individual adaption to aircraft; more time necessary for regression
(3.23)	tangent	2	yes	roughly	individual adaption to aircraft; parameters to be checked for validation of condition 2
(5.11)	hyperbolic sine	2	yes	roughly	individual adaption to aircraft; parameters to be checked for validation of condition 2
(5.5)	hyperbolic tangent (+1)	3	roughly	roughly	individual adaption to aircraft; more time necessary for regression; parameters to be checked for validation of conditions
(5.6)	exponential	3	roughly	roughly	individual adaption to aircraft; more time necessary for regression; parameters to be checked for validation of conditions

5.3 Final Outline of Mathematical Approaches

After inserting the additional conditions, the seven mathematical approaches used in the further work are

$$C_{Dw} = 20(M - M_{crit})^4 \quad , \tag{3.21}$$

$$C_{Dw} = a\left(b\frac{M}{M_{crit}} - b\right)^4 \quad , \tag{5.1}$$

$$C_{Dw} = a\left(b\frac{M}{M_{crit}} - b\right)^c \quad , \tag{5.2}$$

$$C_{Dw} = a\tan\left(b\frac{M}{M_{crit}} - b\right) \quad , \tag{3.23}$$

$$C_{Dw} = a\sinh\left(b\frac{M}{M_{crit}} - b\right) \quad , \tag{5.11}$$

$$C_{Dw} = a\left(1 + \tanh\left(b\frac{M}{M_{crit}} - c\right)\right) \tag{5.5}$$

and

$$C_{Dw} = ae^{b\frac{M}{M_{crit}} - c} \quad . \tag{5.6}$$

Figure 5.1 shows these different mathematical approaches for suitable values of the parameters (in counts). These values of the parameters originate on the resulting mean and median parameters of all 16 aircraft as describes in Subchapter 6.4. Here, Figure 5.1 is embedded to give an idea of how the graphs of the mathematical approaches look. The wave drag is only considered for $M \geq M_{crit}$. In Figure 5.1 the critical Mach number is set to M_{crit}=0.6. Further, Figure 5.1 displays the difficulty of the tangent and the hyperbolic sine approach to fulfill the second condition.

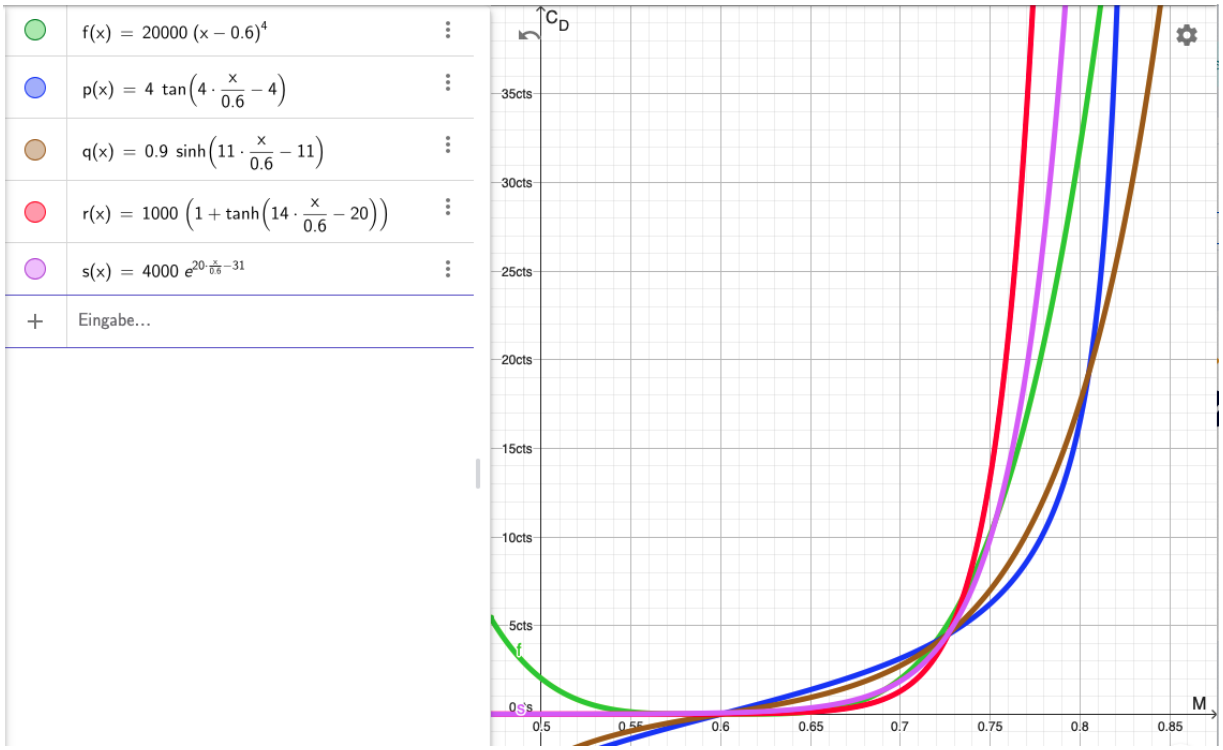

Figure 5.1 Mathematical approaches for the wave drag

6 Implementation

This chapter describes the implementation of the mathematical approaches for the wave drag as described in Chapter 5 on real drag data. This drag data of 16 aircraft is extracted from Obert (2009) as described in Chapter 4. The regression is done in Excel using of the Excel Solver.

6.1 Structure of the Generic Drag Polar

The general equation describing the drag coefficient is (3.1). The induced drag coefficient C_{Di} is generally defined in (3.5) with the Oswald efficiency factor e. The Oswald efficiency factor itself consists of the geometrical aspect and Mach number dependent part as stated in (3.16). The Mach number dependent correction factor is stated by Niţă (2012a and 2012b) as displayed in (3.14). The parameter a_e is negative. These equations and further information on the fundamentals are described in Subchapter 3.2.

$$C_D = C_{D0} + C_{Di} + C_{Dw} \tag{3.1}$$

$$C_{Di} = \frac{C_L^2}{\pi A e} \tag{3.5}$$

$$e = e_{geo} \cdot k_{e,M} \tag{3.16}$$

$$k_{e,M} = 1 + a_e \left(\frac{M}{M_{comp}} - 1 \right)^{b_e} \tag{3.14}$$

In this work the zero lift drag coefficient C_{D0} is kept constant. The wave drag coefficient is replaced by each mathematical approach of Chapter 5 for $M \geq M_{crit}$. These mathematical approaches have zero to three free parameters noted as a, b and c. The induced drag of the generic equation is based on (3.5). To be independent of aircraft parameters in the regression and to keep it as simple as possible, the geometrical constants of (3.5) and (3.16) are combined in a parameter d as stated in (6.1). In (3.14) the parameters a_e and b_e are variable as well. For reasons of clarity, they are further called e and f with e=-a_e and f=b_e. Additionally, this yields the advantage of having only positive parameters, which saves time in the regression. Equation (6.2) presents the structure of the induced drag coefficient used for the regression.

$$C_{Di} = \frac{C_L^2 \cdot d}{k_{e,M}} \tag{6.1}$$

$$C_{Di} = \frac{C_L^2 \cdot d}{-e\left(\frac{M}{M_{comp}} - 1\right)^f + 1} \tag{6.2}$$

Summing up, the equation used for the regression is stated in (6.3). For example, with the mathematical approach of the hyperbolic tangent for wave drag, the equation used for the regression looks like (6.4).

$$C_D = C_{D0} + \frac{C_L^2 \cdot d}{-e\left(\frac{M}{M_{comp}} - 1\right)^f + 1} + C_{Dw} \tag{6.3}$$

$$C_D = C_{D0} + \frac{C_L^2 \cdot d}{-e\left(\frac{M}{M_{comp}} - 1\right)^f + 1} + a\left(1 + \tanh\left(b\frac{M}{M_{crit}} - c\right)\right) \tag{6.4}$$

In this work M_{comp} is set to M_{comp}=0.3. The critical Mach number is calculated by (3.20). In this, the drag divergence Mach number is calculated based on the Boeing definition with the data of the original aircraft. As the critical Mach number changes with changing lift coefficient, the drag divergence Mach number and the critical Mach number are calculated separately for every lift coefficient. The ΔM is computed by the Excel Solver for every lift coefficient.

$$M_{crit} = M_{DD} - \Delta M \tag{3.20}$$

In total, the parameters being optimized by the Excel Solver are: C_{D0}, *a, b, c, d, e* and *f* per aircraft and ΔM for every lift coefficient per aircraft. Figure 6.1 shows exemplarily, that 10 parameters are optimized for the B767-300.

The wave drag exists only at $M \geq M_{crit}$ as already mentioned. In Excel this is realised through an "IF"-function. If the Mach number of the regression in smaller than the critical Mach number of the regression, than the drag coefficient is calculated by (6.5). Else the drag coefficient is calculated by (6.3). For the hyperbolic tangent and the exponential approach this separation is not necessary as their functional value tends to zero for lower Mach number.

$$C_D = C_{D0} + \frac{C_L^2 \cdot d}{-e\left(\frac{M}{M_{comp}} - 1\right)^f + 1} \tag{6.5}$$

	Parameter	
	a	293.130154
	b	21.01007
	c	29.2502573
	d	466.593854
	cd0	133.101402
	e	0.001376
	f	8.7923412
0.3	deltaM	0.18412775
0.4	deltaM	0.17613884
0.5	deltaM	0.16813701

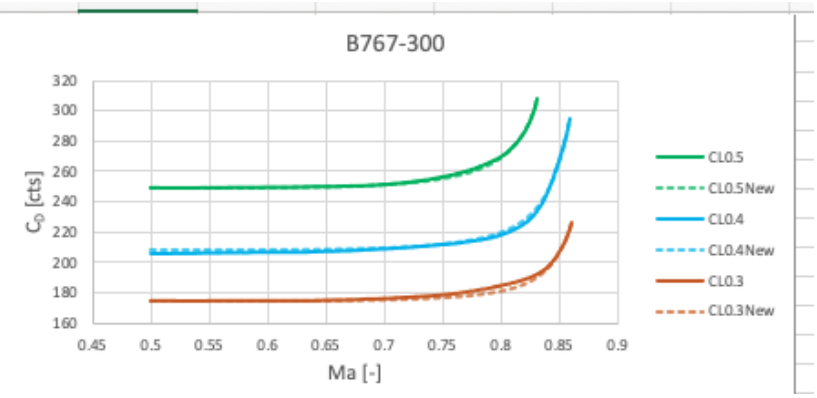

Figure 6.1 Parameters optimized by the Excel Solver for the B767-300

6.2 Optimizing with the Excel Solver

Several tools exist to work with and to analyze data. In this work, Microsoft Excel is used. The Excel Solver is used for the regression as it finds the best fit semi automatically. The screen window of the Excel Solver adjusted for the optimization of the B767-300 is presented in Figure 6.2.

To gain an optimization in general, the Excel solver needs the following inputs as displayed in Figure 6.2:

- "Set Objective": This is a single cell that obtains the purpose of the optimization.
- "To" answers the question if the objective cell should be minimal, maximal or a given value.
- "By Changing the Variable Cells": This can be a single cell or multiple cells. The value in these cells changes with the optimization.
- "Subject to the Constraints" gives the opportunity to set additional constraints. This is an optional input.
- "Make Unconstrained Variable Non-Negative" is eligible to restrict the domain of the variable cells. If suitable, this option saves time and yields a better optimization.
- "Select a Solving Method": Solving the mathematical problem is done either by the "GRG Nonlinear"-method for smooths nonlinear problems, the "LP Simplex"-method for linear problems or the "Evolutionary engine"-method for non-smooth problems.

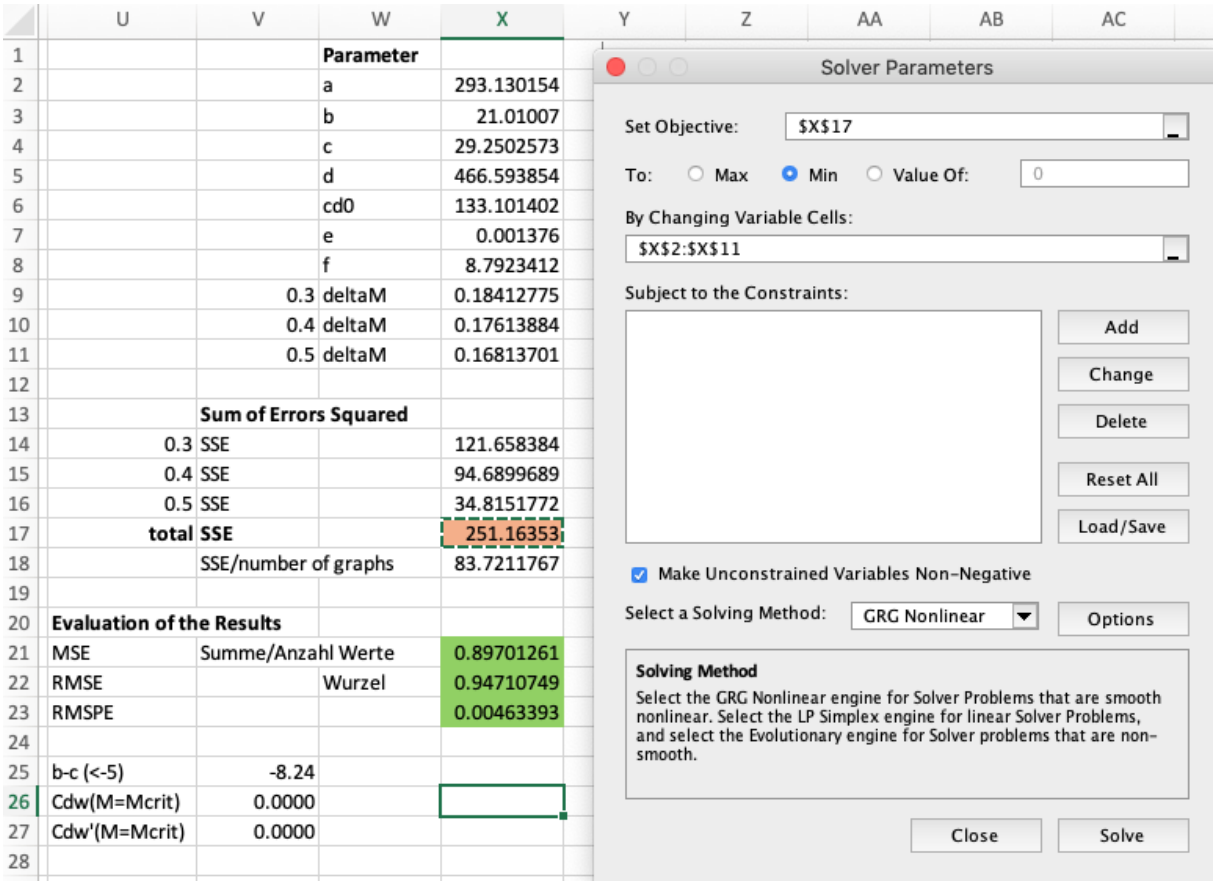

	U	V	W	X
1			**Parameter**	
2			a	293.130154
3			b	21.01007
4			c	29.2502573
5			d	466.593854
6			cd0	133.101402
7			e	0.001376
8			f	8.7923412
9		0.3	deltaM	0.18412775
10		0.4	deltaM	0.17613884
11		0.5	deltaM	0.16813701
12				
13		**Sum of Errors Squared**		
14	0.3	SSE		121.658384
15	0.4	SSE		94.6899689
16	0.5	SSE		34.8151772
17	**total**	**SSE**		251.16353
18		SSE/number of graphs		83.7211767
19				
20	**Evaluation of the Results**			
21	MSE	Summe/Anzahl Werte		0.89701261
22	RMSE		Wurzel	0.94710749
23	RMSPE			0.00463393
24				
25	b-c (<-5)	-8.24		
26	Cdw(M=Mcrit)	0.0000		
27	Cdw'(M=Mcrit)	0.0000		
28				

Figure 6.2 General settings of the Excel Solver

In terms of this work, the total sum of errors squared of the regression model becomes the objective cell as presented in Figure 6.2. This cell is to become minimal to gain the best fit. The variable cells are the parameters C_{D0}, *a, b, c, d, e* and *f* as well as ΔM for every lift coefficient. In general, there are no additional constraints set. If the optimization yields nothing but physically implausible results, additional constraints are inserted. As the definition of the parameters makes them positive, the tick for non-negative variable cells is selected. The GRG Nonlinear method is used for this work as its description fits the regression model.

If the mathematical problem is as complex as in this work, the outcome of the Excel Solver is very dependent on the initial values of the parameters as there might be many local extrema. In other words, changing the initial values of the parameters might change the solution of the Excel Solver. In practice, this means that several laps in the Excel Solver are necessary to find the best (achievable) fit of the regression.

6.3 Validation of the Regression

The result of an optimization has to be checked. First, this is possible by reviewing the parameters and the critical Mach numbers by plausibility. If for example the Excel Solver yields a promising regression line with a critical Mach number greater than 1 or below 0.3 this result is physically implausible. In like manner, the plausibility of the magnitude of the parameters is revisable. If the result is implausible, another run of the Excel Solver has to be done. This step is very important as the Excel Solver optimizes for a mathematical extremum only without considering any physics. This has been the major step in the validation.

In addition, a second approach is made for validation purposes. For this approach information about the aircraft's geometry is necessary. The definition of the parameter *d* in the generic equation is

$$d = \frac{1}{\pi A e_{geo}} \tag{6.6}$$

with

$$e_{geo} = e_{theo} \cdot k_{e,D0} \cdot k_{e,F} \tag{3.15}$$

based on the first method of the calculation the Oswald efficiency factor in Subchapter 3.2.3. Inserting (3.15) in (6.6) and rearranging it to $k_{e,D0}$ yields

$$k_{e,D0} = \frac{1}{\pi\ A\ e_{theo}\ k_{e,F}\ d}\ . \tag{6.7}$$

This equation only consists of parameters that are dependent on basic aircraft geometry and the optimized parameter *d*. If data on the aircraft's geometry is available $k_{e,D0}$ can be calculated and compared with general data presented in Table 3.2. According to Table 3.2 $k_{e,D0}$ = 0.873 was determined on average for passenger aircraft.

Similarly, the second method of the calculation of the Oswald efficiency factor in Subchapter 3.2.3 is also able to validate the results of an optimization. Based on (6.6) and

$$e = e_{geo} \cdot k_{e,M} \tag{3.16}$$

the parameter *d* is equal to

$$d = \frac{1}{\pi A e_{geo}} = \frac{k_{e,M}}{\pi A e}\ . \tag{6.8}$$

Inserting the definition of the Oswald efficiency factor of the second method

$$e = \frac{k_{e,M}}{Q + P\pi A} \tag{3.17}$$

with

$$Q = \frac{1}{e_{theo} \cdot k_{e,F}} \tag{3.18}$$

and

$$P = KC_{D0} \tag{3.19}$$

in (6.8) yields the definition of the parameter *d* as

$$d = \frac{k_{e,M}(Q + P\pi A)}{\pi A k_{e,M}} = \frac{Q + KC_{D0}\pi A}{\pi A} \quad . \tag{6.9}$$

Rearranging (6.9) to *K* leads to

$$K = \frac{d\pi A - Q}{C_{D0}\pi A} \quad . \tag{6.10}$$

Again, an aircraft's geometry is necessary to solve (6.10). In addition, the optimized zero lift drag coefficient C_{D0} and the optimized parameter *d* are needed. If the data is available, *K* can be calculated and compared to the generic value *K* = 0.38 as stated by Niţă (2012a).

The collection of aircraft parameters by Hirsch (2022) is mainly used to summarize the necessary parameters of the 16 aircraft. Further, parameters are taken from van der Zalm (2023a), van der Zalm (2023b), Beekmans (2018), Brady (1999), Jenkinson (2001a), Jenkinson (2001b), Jenkinson (2001c), Jenkinson (2001d) and Jenkinson (2001e).

Table 6.1 shows the necessary aircraft parameters for the 16 aircraft. The results of the calculation of $k_{e,D0}$ and *K* are stated in Table 6.2 exemplarily for the hyperbolic tangent approach. Table 6.2 shows that the resultant parameters are in general in the magnitude of the generic values stated above. Further, the results of the A320 stand out negatively. There are two possible explanations. a) It could be that the drag polar given by Obert (2009) for the A320 is not very accurate. This is possible, because drag polars are confidential and the source of the diagram is unknown. b) It could be that a better regression for this aircraft exists, which hasn't been found in the timeframe of this work. This is unlikely, because very many attempts have been made to find a more plausible fit, but no better fit was found. It is very nice to see the results of the B767 to stand out positively as they approximately equal the generic values. In Table 6.2 the values "with sweep" must be considered the final answer.

Table 6.1 Geometrical aircraft parameters

aircraft	aspect ratio A [-]	wing span b [m]	taper ratio λ [-]	fuselage width d_F [m]	sweep at 25% of chord φ_{25} [°]
DC-10-30	6.91	50.40	0.220	6.02	35.0
MD-11	7.91	51.77	0.239	6.02	35.0
B707-120	7.03	39.87	0.333	3.76	35.0
B727-200	6.86	32.92	0.309	3.76	32.0
B737-200	8.83	28.35	0.266	3.73	25.0
B737-300	9.16	28.88	0.250	3.76	26.0
B737-800	9.44	35.79	0.330	3.76	26.0
B747-100	6.96	59.64	0.284	6.50	37.5
B757-200	7.82	38.02	0.230	3.76	23.5
B767-300	7.99	47.57	0.210	5.03	30.5
B777-200	8.68	60.93	0.160	6.19	30.0
A300-B2	7.73	44.84	0.334	5.64	28.0
A320-200	9.39	35.80	0.250	3.95	23.5
A340-200	9.26	58.00	0.251	5.64	29.7
F28 Mk4000	7.96	25.07	0.250	3.30	16.0
F100	8.43	28.08	0.290	3.30	17.5

Table 6.2 Resulting parameters $k_{e,D0}$ and K for the hyperbolic tangent approach

aircraft	$k_{e,D0}$ [-]	$k_{e,D0}$ with sweep [-]	K [-]	K with sweep [-]
DC-10-30	0.9193	0.9151	0.2953	0.3107
MD-11	0.9661	0.9643	0.0907	0.0955
B707-120	0.9617	0.9711	0.1349	0.1018
B727-200	0.8984	0.9039	0.3096	0.2927
B737-200	0.9417	0.9406	0.1185	0.1204
B737-300	0.9154	0.9124	0.1589	0.1644
B737-800	0.9109	0.9029	0.1868	0.2035
B747-100	0.9841	0.9893	0.0535	0.0362
B757-200	0.9529	0.9470	0.1315	0.1480
B767-300	0.8950	0.8876	0.3681	0.3939
B777-200	0.8775	0.8598	0.4198	0.4801
A300-B2	0.7988	0.8051	0.6285	0.6089
A320-200	1.1908	1.1860	-0.2841	-0.2769
A340-200	0.9973	0.9956	0.0066	0.0108
F28 Mk4000	0.8890	0.8848	0.2649	0.2751
F100	0.9258	0.9251	0.1652	0.1667

6.4 Comparing the Outcome

The drag polar for each of the 16 aircraft is approximated by the generic equation with each of the 7 mathematical approaches for the wave drag optimized by several laps in the Excel solver. The outcome of this is presented in Table 6.3 and Table 6.4. Table 6.3 shows the mean values of the 16 aircraft's regressions per mathematical approach and Table 6.4 the median values. Presented are the variable parameters, the achievement of the additional conditions and the metrics to evaluate and compare the regressions. Cells highlighted in grey indicate that this approach doesn't use this parameter or that this condition is always fulfilled.

In Subchapter 5.2, the raise to power approach was expected to yield the best solution based on the number of parameters and the fulfilment of the additional conditions. Now the results show that the hyperbolic tangent yields the best fits in both mean and median outcome. The RSMPE makes it possible to compare the different approaches. The results of the parameters *d,* C_{D0}*, e* and *f* are of the same magnitude in all approaches, which is plausible as these parameters are wave drag approach independent parameters. Further, the difference in magnitude of the parameters *a, b,* and *c* for each mathematical approach stands out. The reason for this is the different definition and structure of the mathematical approaches. Moreover, are the additional conditions fulfilled, but for the tangent and hyperbolic sine difficult to achieve in average. The goodness of fit can be compared by the RSMPE. The green highlighted cells show that the hyperbolic tangent gains the best fit in average and in median. The red highlighted cells stand for the worst fit. This is the Lock approach in both cases. This is especially interesting as this approach is used for most current papers as stated in Chapter 2. The lack of knowledge of better approaches and the advantage of its simpleness by its lack of parameters might be the reason for this. Further especially interesting is that in the median values of RMSPE of the raise to power and the tangent are nearly equal to the hyperbolic tangent. This indicates that these approaches also yield a solid regression in most cases but aren't as flexible on the different aircraft's aerodynamics as the hyperbolic tangent.

Table 6.3 Mean outcome values of the regression

	hyperbolic tangent +1	Lock	Lock general	Raise To Power	tangent	hyperbolic sine	exponential
	mean	mean	mean	mean	mean	mean	mean
a [cts]	1101.02	0	23064.30	18433.92	8.771	1.209	4688.54
b [-]	14.632	0	1.174	1.288	2.943	14.057	23.664
c [-]	21.299	0	0	4.150	0	0	37.413
d [cts]	444.97	430.84	447.21	447.24	456.22	451.25	450.97
C_{D0} [cts]	168.51	169.22	168.85	168.83	166.19	167.44	167.63
e [-]	2.157E-02	4.397E-02	1.321E-03	2.290E-03	7.837E-03	1.921E-03	1.189E-03
f [-]	9.019	9.841	10.430	9.881	12.830	12.964	10.312
no jump	-6.67	-	-	-	-	-	-13.75
no kink	-6.67	-	-	-	2.169E-03	7.949E-04	-13.75
necessary condition	<-5	-	-	-	≈0	≈0	<-9
SSE per number of graphs [cts^2]	330.81	650.79	410.06	384.02	551.02	472.02	413.26
MSE [cts^2]	3.022	6.094	3.821	3.574	4.969	4.228	3.815
RMSE [cts]	1.637	2.329	1.848	1.788	1.931	1.891	1.832
RMSPE [-]	0.00684	0.00949	0.00773	0.00747	0.00793	0.00788	0.00764

Table 6.4 Median outcome values of the regression

	hyperbolic tangent +1	Lock	Lock general	Raise To Power	tangent	hyperbolic sine	exponential
	median	median	median	median	median	median	median
a [cts]	280.57	0	21889.58	18945.85	6.128	0.301	1320.51
b [-]	15.643	0	1.054	1.317	2.697	9.806	24.679
c [-]	21.089	0	0	3.991	0	0	33.783
d [cts]	443.87	442.50	443.90	439.41	464.43	450.55	449.63
C_{D0} [cts]	168.22	168.16	168.42	168.18	167.59	168.28	168.24
e [-]	1.347E-03	4.465E-04	2.322E-04	6.149E-04	2.089E-04	1.180E-04	3.522E-04
f [-]	8.115	10.232	11.001	10.522	12.478	13.236	10.773
no jump	-5.18	-	-	-	-	-	-9.00
no kink	-5.18	-	-	-	1.863E-03	5.470E-04	-9.00
necessary condition	<-5	-	-	-	≈0	≈0	<-9
SSE per number of graphs [cts^2]	257.65	615.32	325.24	269.07	353.61	363.428	365.51
MSE [cts^2]	2.799	5.625	3.553	2.810	3.049	3.642	4.263
RMSE [cts]	1.671	2.370	1.883	1.675	1.742	1.908	2.062
RMSPE [-]	0.00672	0.00941	0.00742	0.00682	0.00693	0.00720	0.00737

7 Generic Drag Polar of 16 Passenger Aircraft

This chapter unveils the drag polar of 16 passenger aircraft based on the best fit evaluated in Subchapter 6.4. The results of the other mathematical approaches are presented in Appendix B. For reasons of clarity, the generic equation is stated in Equation (6.4). Note that the wave drag is zero for $M<M_{crit}$.

$$C_D = C_{D0} + \frac{C_L^2 \cdot d}{-e\left(\frac{M}{M_{comp}} - 1\right)^f + 1} + a\left(1 + \tanh\left(b\frac{M}{M_{crit}} - c\right)\right) \tag{6.4}$$

Table 7.1 presents the resultant values of the parameters per aircraft. These values are generated by the Excel Solver. Especially the mean values of the parameters are further used as generic values for the calculation of a different aircraft as described in Chapter 8. Table 7.1 shows that the magnitude of the zero lift drag coefficient is of plausible magnitude. Further the values of *e* and *f* are in general in the range of magnitude as the generic value stated in Subchapter 3.2.4. The values of *b*, *c* and *d* for the 16 aircraft are each of similar scale. A few values in Table 7.1 stand out by being unusually large or small. As these aircraft have been optimized with the Excel Solver several times, the difference in magnitude is based on the variance in the drag polars and the aircraft's aerodynamics.

Table 7.1 Values of the parameters a to f for 16 aircraft

	a [cts]	b [-]	c [-]	d [cts]	C_{D0}[cts]	e [-]	f [-]
mean	1101.02	14.632	21.299	444.97	168.51	2.157E-02	9.019
median	280.57	15.643	21.089	443.87	168.22	1.347E-03	8.115
DC	209.33	21.027	41.634	526.23	143.83	2.005E-03	7.438
MD	276.53	17.892	22.950	437.03	163.59	8.655E-04	6.160
B707	58.52	21.807	26.808	485.70	137.69	1.710E-03	6.910
B727	250.28	13.395	19.228	537.53	176.41	1.100E-04	12.636
B737-200	51.06	28.168	34.749	404.58	199.09	1.185E-02	7.074
B737-300	596.92	7.902	12.902	401.87	213.97	2.386E-03	10.294
B737-800	1919.02	4.556	9.850	388.99	185.57	2.386E-03	21.607
B747	284.61	13.136	18.502	483.09	143.16	9.359E-05	6.210
B757	74.28	18.283	25.988	445.09	159.45	1.318E-03	9.133
B767	293.13	21.010	29.250	466.59	133.10	1.376E-03	8.792
B777	215.14	23.905	30.888	442.66	129.20	2.775E-04	9.870
A300	299.53	10.967	15.967	540.10	172.86	9.072E-05	14.092
A320	486.26	18.637	23.637	298.56	200.53	1.210E-01	1.632
A340	2811.52	3.496	8.496	359.35	146.79	4.009E-05	15.150
F28	9.408	7.810	12.810	475.38	199.10	1.654E-01	2.615
F100	9780.75	2.122	7.122	426.85	191.82	3.645E-02	4.693

The values in Table 7.2 show, that the additional conditions are approximately fulfilled and that the initial values of the wave drag are nearly zero. It can be noted in Table 7.2 that quite a few aircraft just fulfill the additional conditions. As this has been checked in the process of optimization this is the minimum condition that had to be fulfilled and is no coincidence. A comparison of the goodness of fit between the aircraft is done using the metrics in Table 7.3. The lower the score of each metric the better the regression.

Table 7.2 Additional conditions, initial value and initial climb rate for the wave drag for 16 aircraft

	no jump if b-c<≈-5 [-]	no kink if b-c<≈-5 [-]	C_{Dw} at M=M_{crit}[cts]	dC_{Dw}/dM at M=M_{crit} [cts]
mean	-6.67	-6.67	0.5209	1.0418
median	-5.18	-5.18	0.6558	1.3115
DC	-20.61	-20.61	0.0000	0.0000
MD	-5.06	-5.06	0.8075	1.6149
B707	-5.00	-5.00	0.9060	1.8120
B727	-5.83	-5.83	0.1717	0.3433
B737-200	-6.58	-6.58	0.0385	0.0770
B737-300	-5.00	-5.00	0.9080	1.8158
B737-800	-5.29	-5.29	0.5041	1.0081
B747	-5.37	-5.37	0.4369	0.8738
B757	-7.71	-7.71	0.0041	0.0081
B767	-8.24	-8.24	0.0014	0.0028
B777	-6.98	-6.98	0.0172	0.0344
A300	-5.00	-5.00	0.9080	1.8158
A320	-5.00	-5.00	0.9080	1.8158
A340	-5.00	-5.00	0.9080	1.8158
F28	-5.00	-5.00	0.9080	1.8158
F100	-5.00	-5.00	0.9080	1.8158

In the following, Figure 7.1 to Figure 7.16 display the drag polars of the 16 aircraft. Each diagram contains the original drag polar based on Chapter 4. This is represented by the solid lines. The dashed lines stand for the regression based on Equation (6.4).

In similarity to the results in Table 7.3, the diagrams illustrate that a regression based on Equation (6.4) yields a solid result in general. Further, the regression of the drag polars of the A340, B707 and B777 turned out worst. Due to their complicated character the regression of these three aircraft needed special attention with any mathematical approach.

Table 7.3 Quality of the regression model by statistical metrics for 16 aircraft

	SSE per number of graphs [cts²]	MSE [cts²]	RMSE [cts]	RMSPE [-]
mean	330.81	3.022	1.627	0.00684
median	257.65	2.799	1.671	0.00672
DC	271.43	2.513	1.585	0.00706
MD	76.47	0.762	0.873	0.00375
B707	856.48	6.691	2.587	0.01440
B727	234.18	3.603	1.898	0.00683
B737-200	53.46	0.595	0.704	0.00296
B737-300	96.69	1.047	1.023	0.00381
B737-800	286.10	2.248	1.499	0.00587
B747	535.10	4.694	2.167	0.00982
B757	243.88	3.087	1.757	0.00722
B767	83.72	0.897	0.947	0.00463
B777	629.14	5.200	2.280	0.01052
A300	470.60	4.614	2.148	0.00738
A320	278.74	3.086	1.757	0.00661
A340	939.81	7.066	2.658	0.01061
F28	154.00	1.456	1.207	0.00453
F100	83.11	0.887	0.942	0.00343

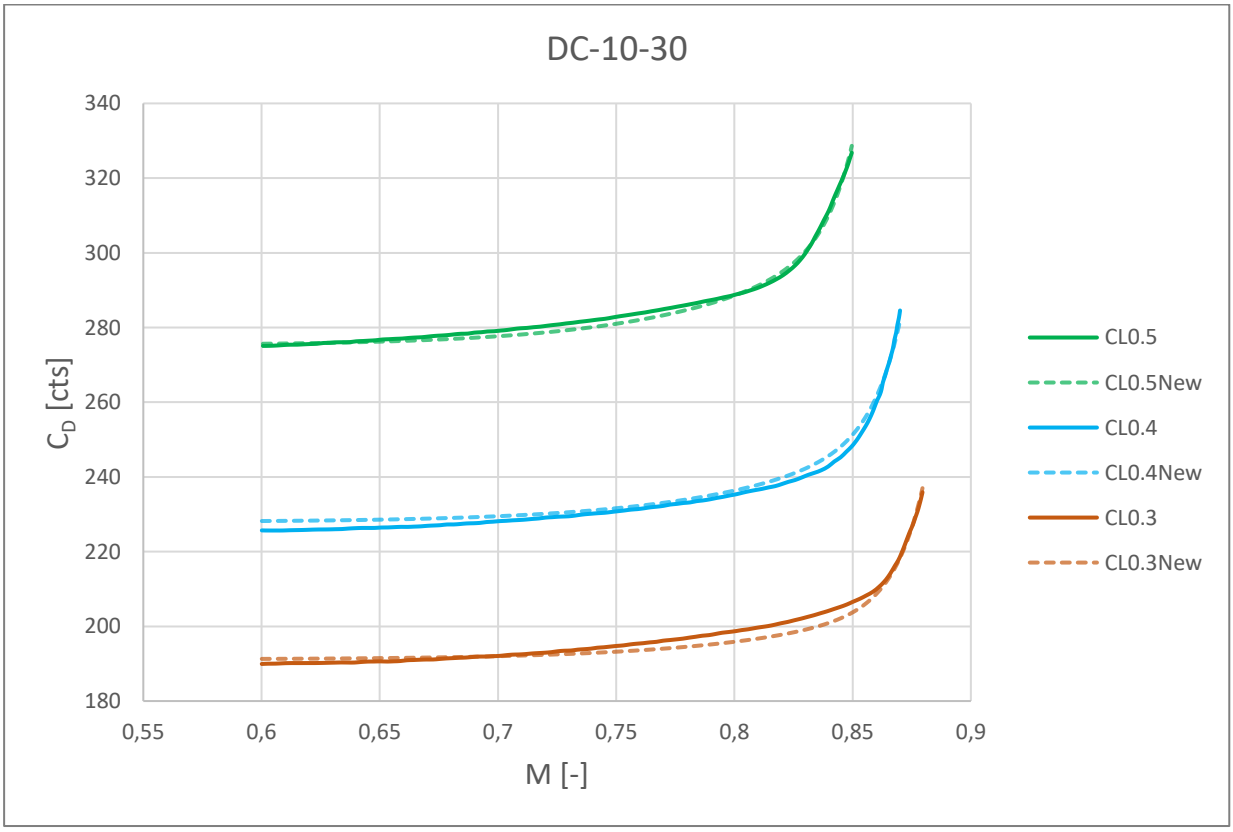

Figure 7.1 Original drag polar and its regression for DC-10-30

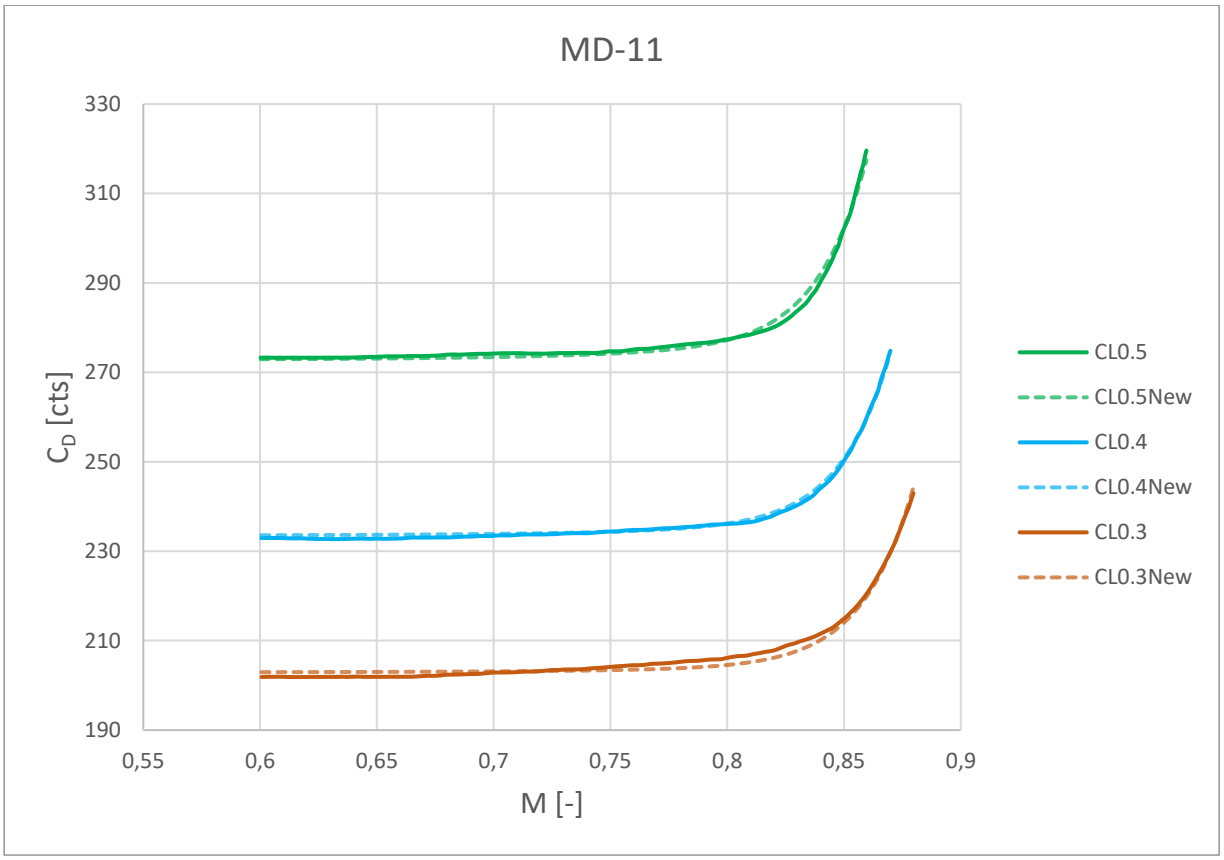

Figure 7.2 Original drag polar and its regression for MD-11

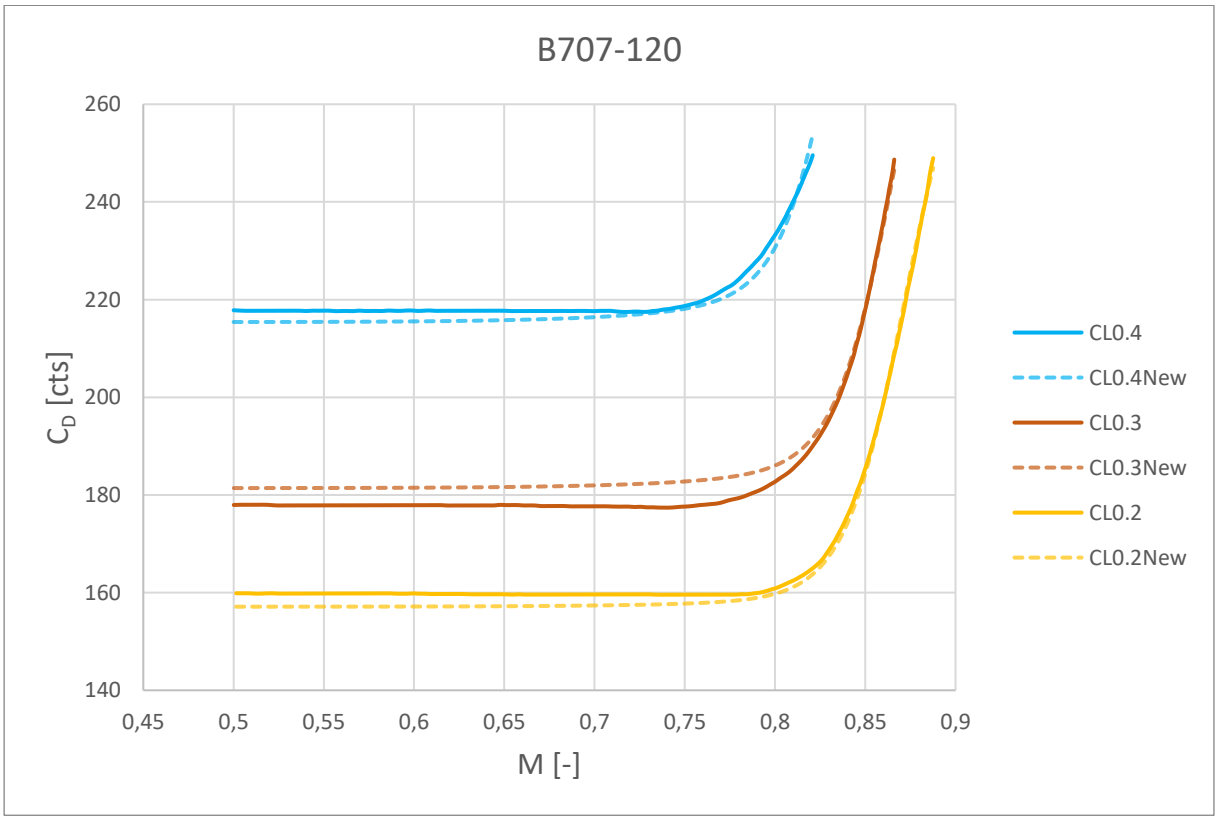

Figure 7.3 Original drag polar and its regression for B707-120

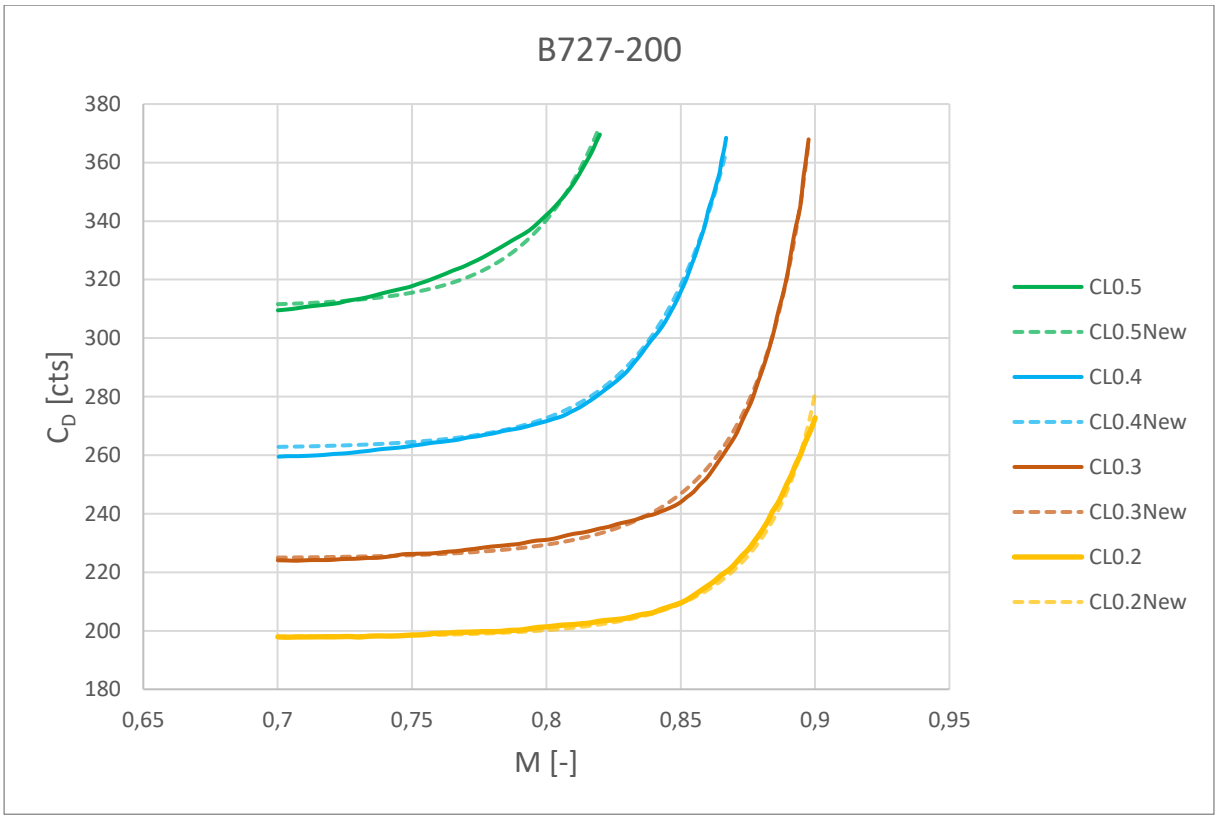

Figure 7.4 Original drag polar and its regression for B727-200

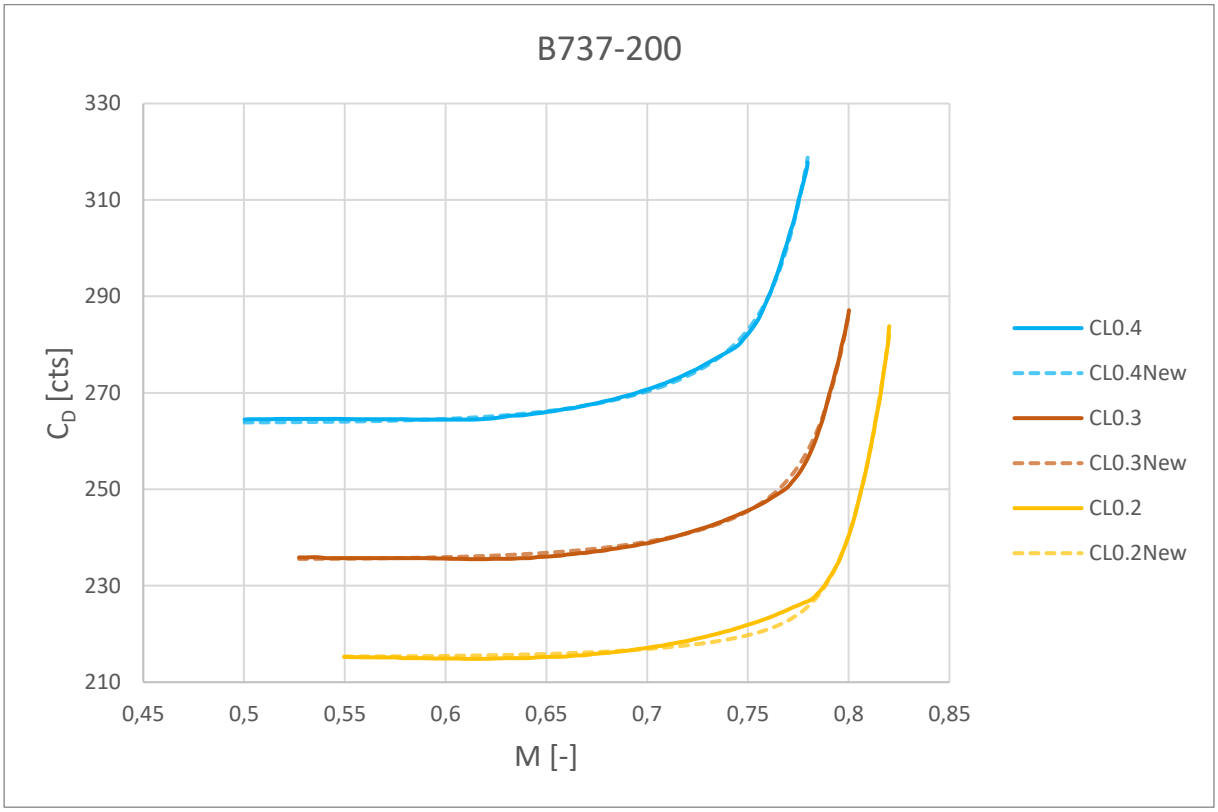

Figure 7.5 Original drag polar and its regression for B737-200

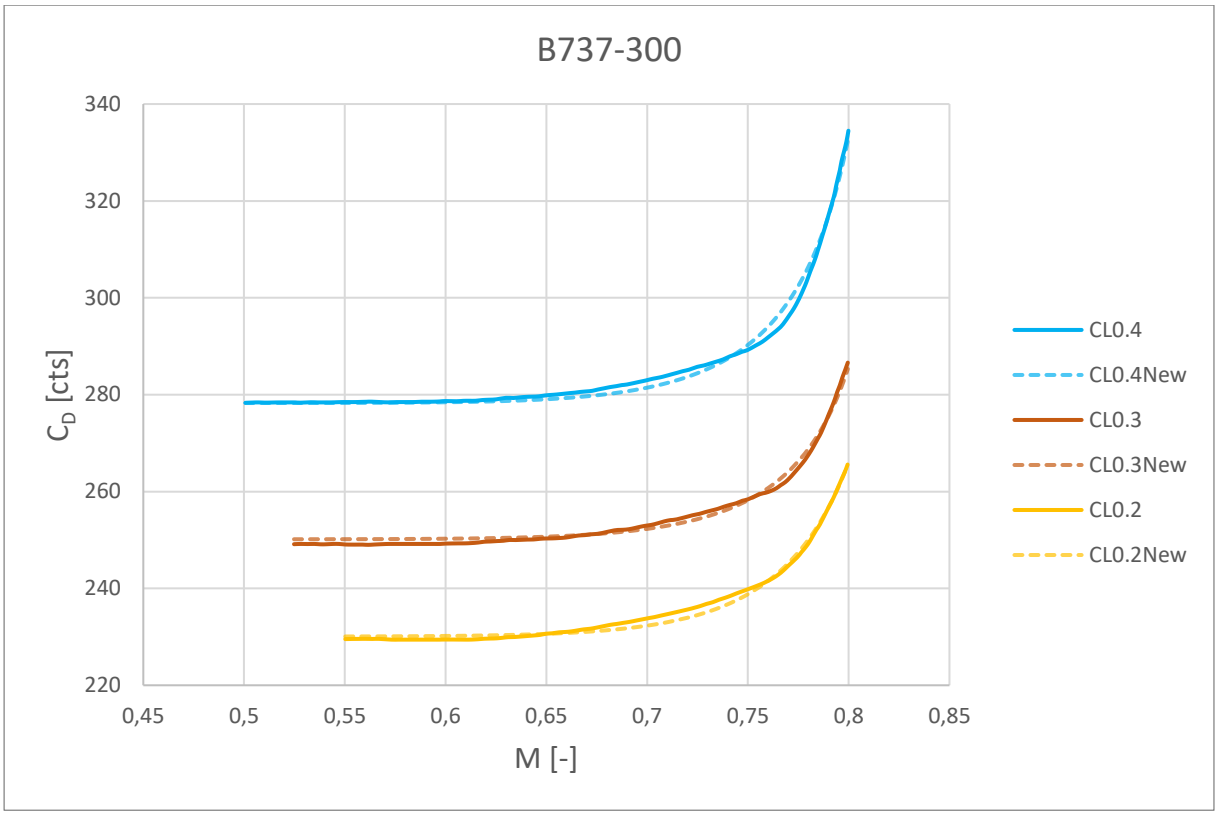

Figure 7.6 Original drag polar and its regression for B737-300

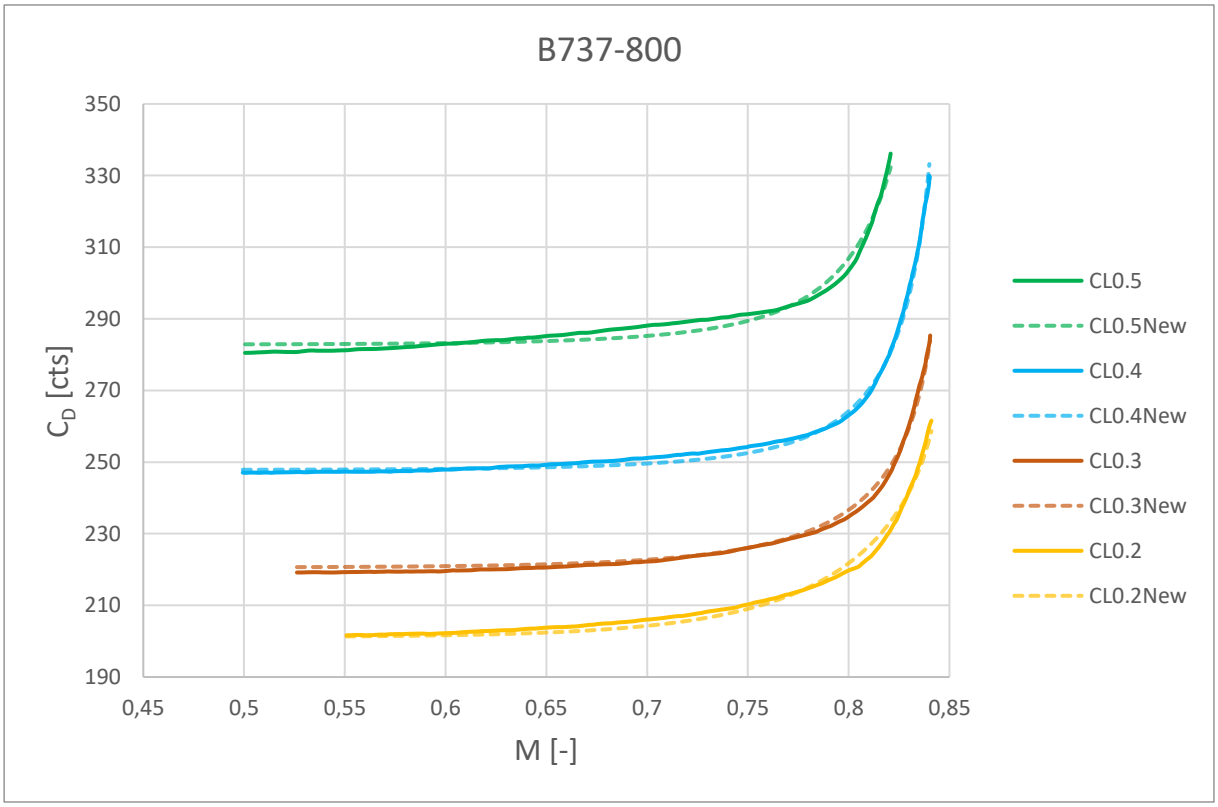

Figure 7.7 Original drag polar and its regression for B737-800

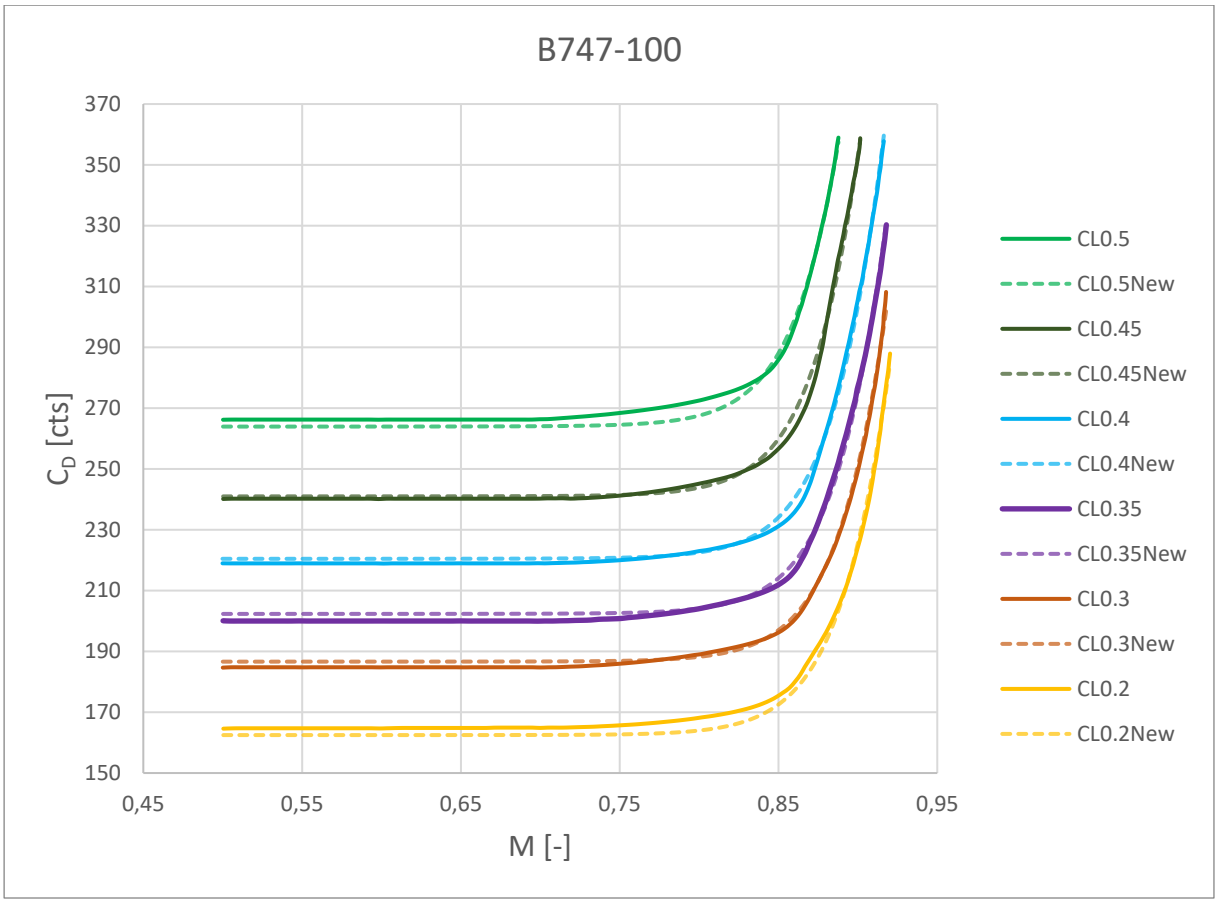

Figure 7.8 Original drag polar and its regression for B747-100

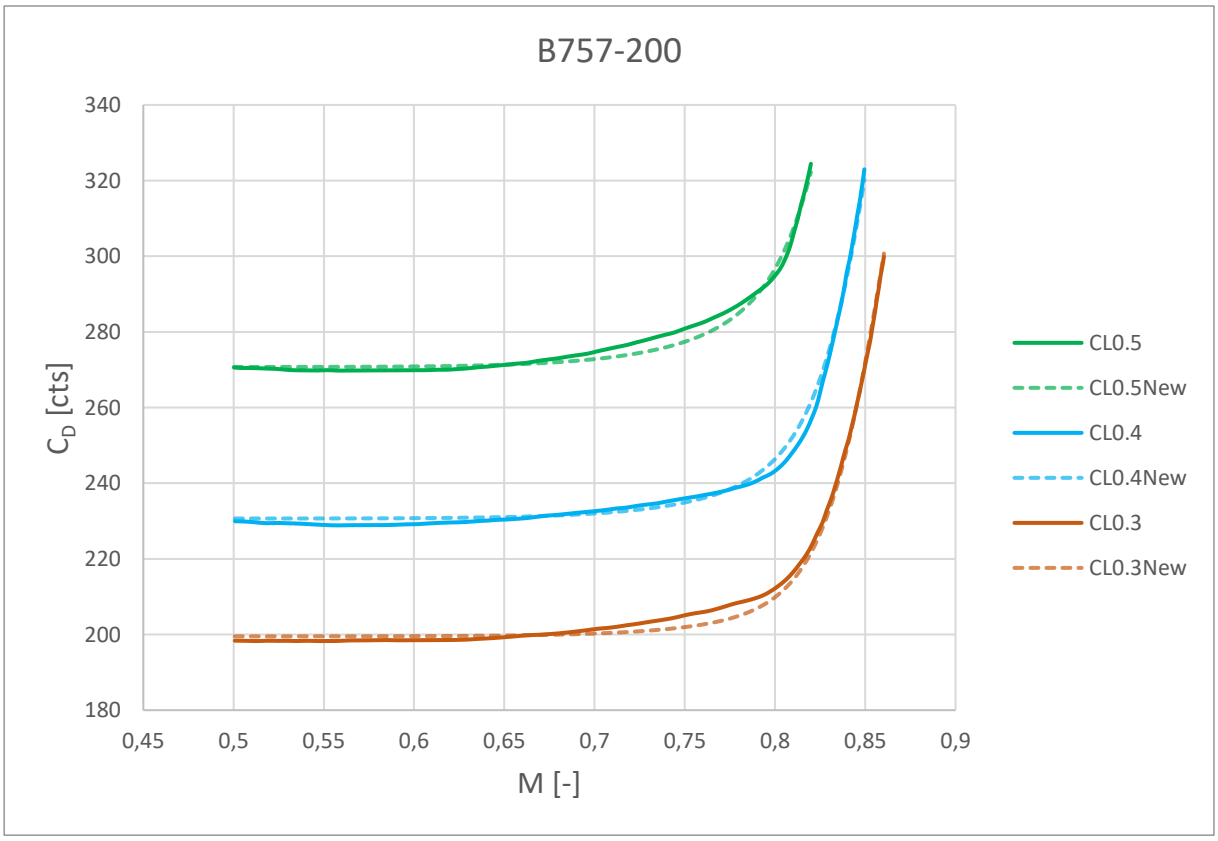

Figure 7.9 Original drag polar and its regression for B757-200

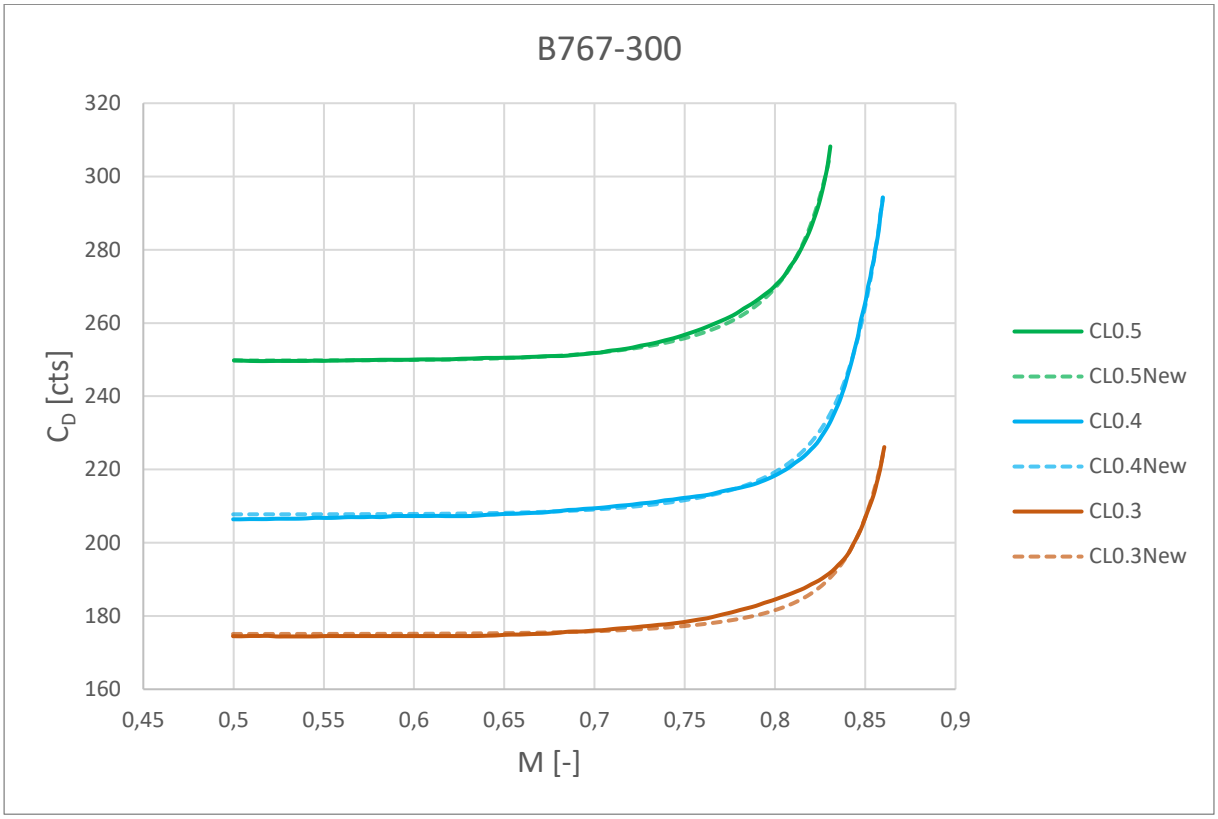

Figure 7.10 Original drag polar and its regression for B767-300

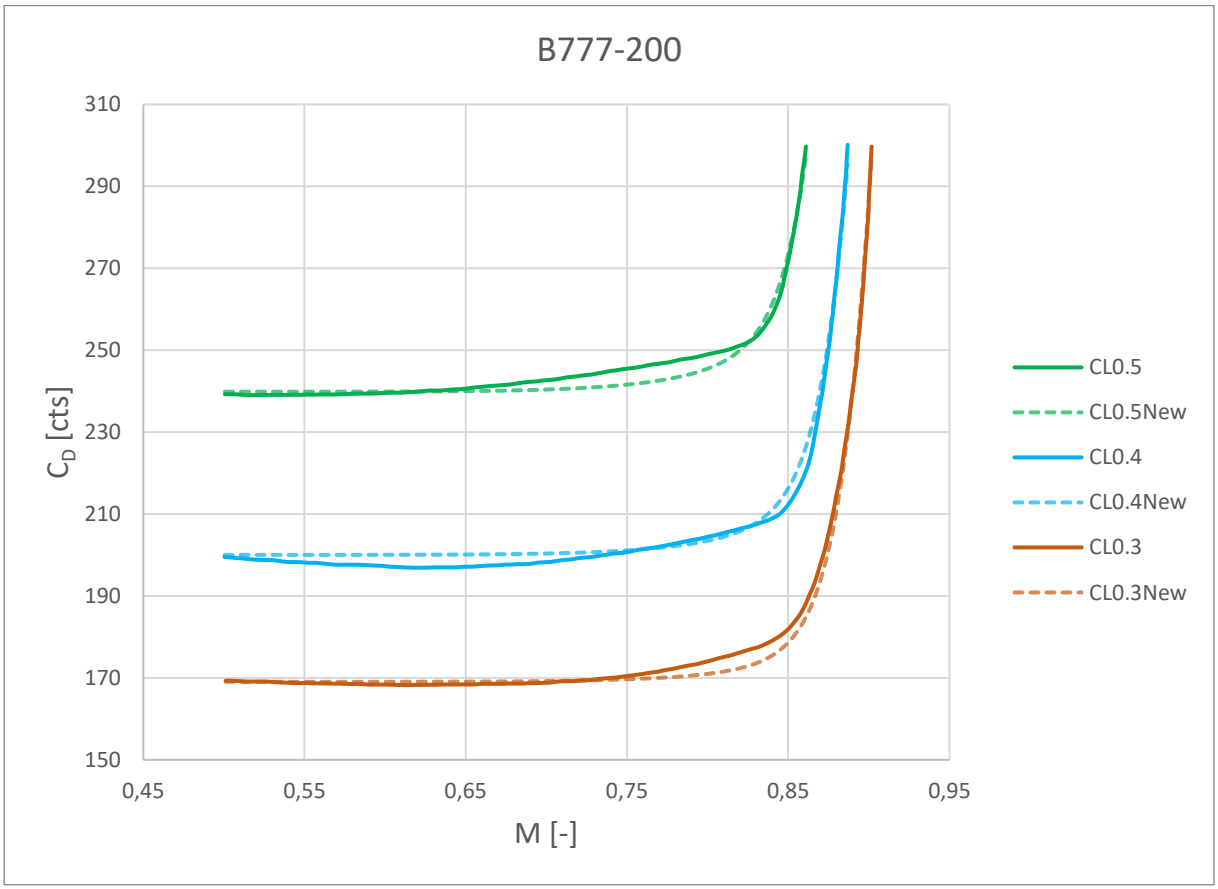

Figure 7.11 Original drag polar and its regression for B777-200

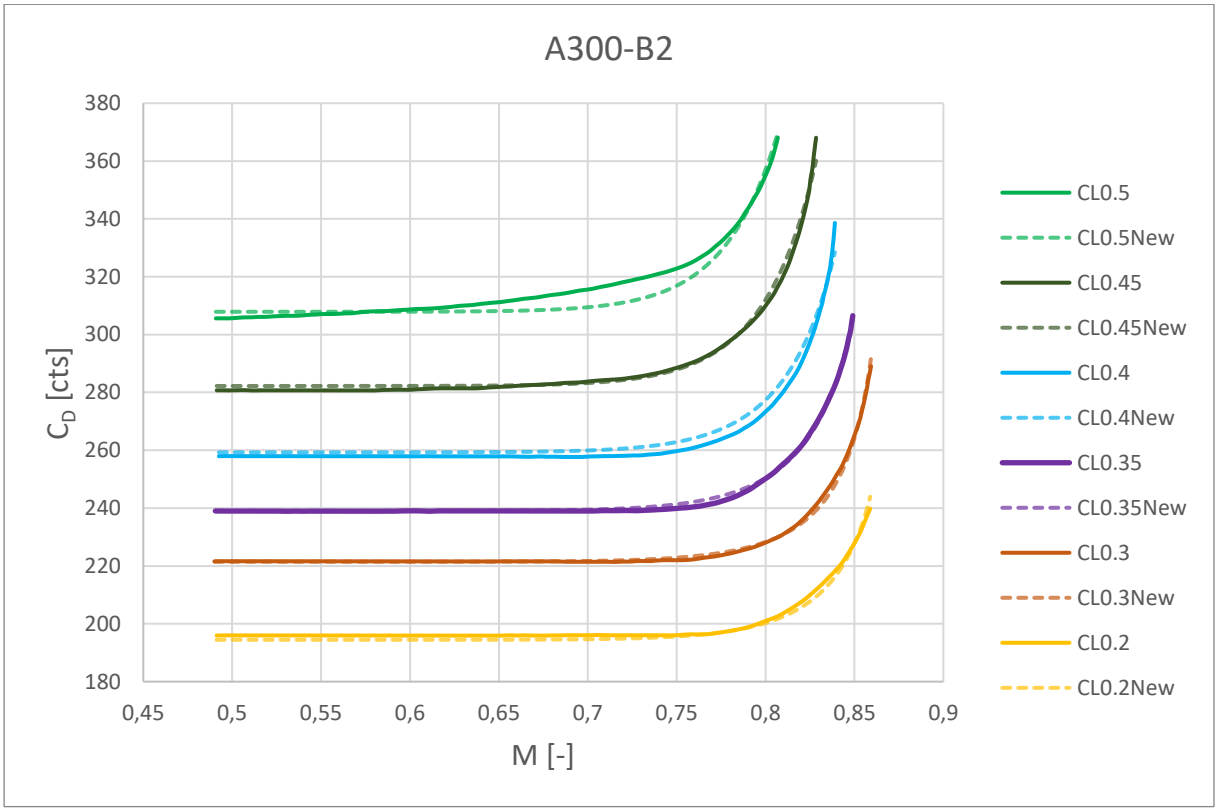

Figure 7.12 Original drag polar and its regression for A300-B2

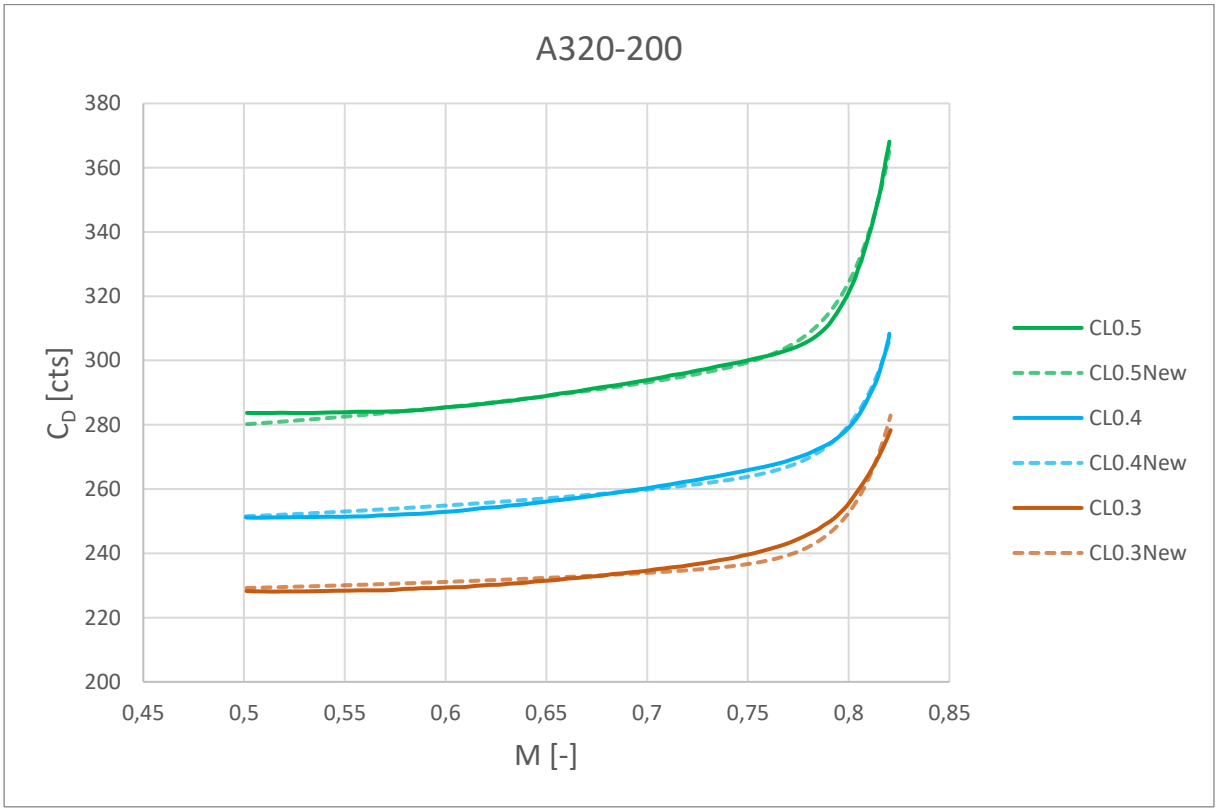

Figure 7.13 Original drag polar and its regression for A320-200

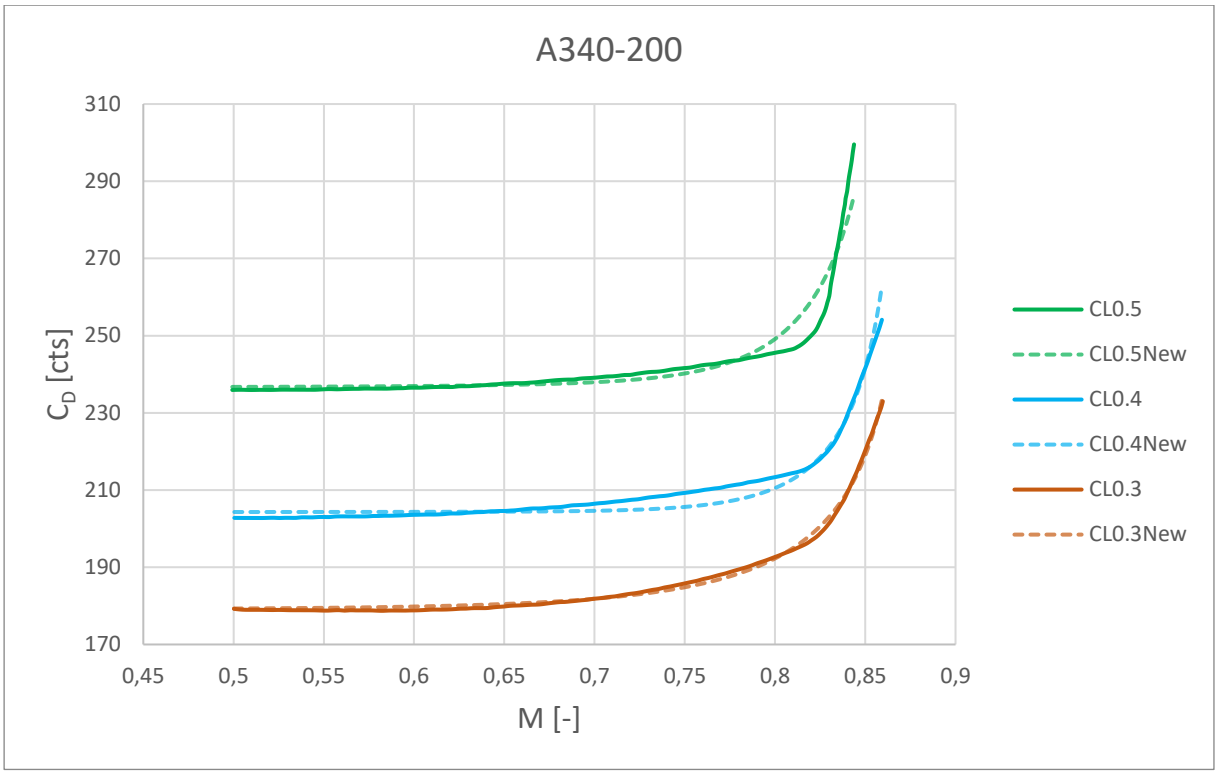

Figure 7.14 Original drag polar and its regression for A340-200

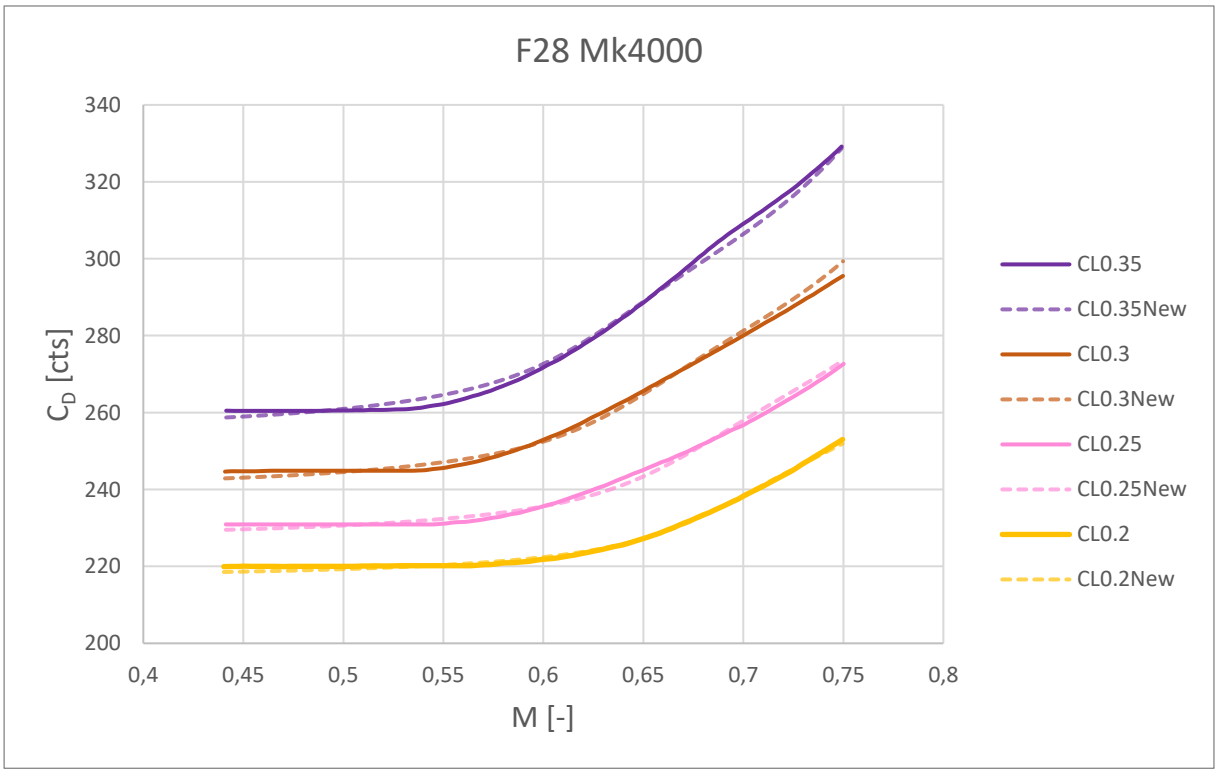

Figure 7.15 Original drag polar and its regression for Fokker28 Mk4000

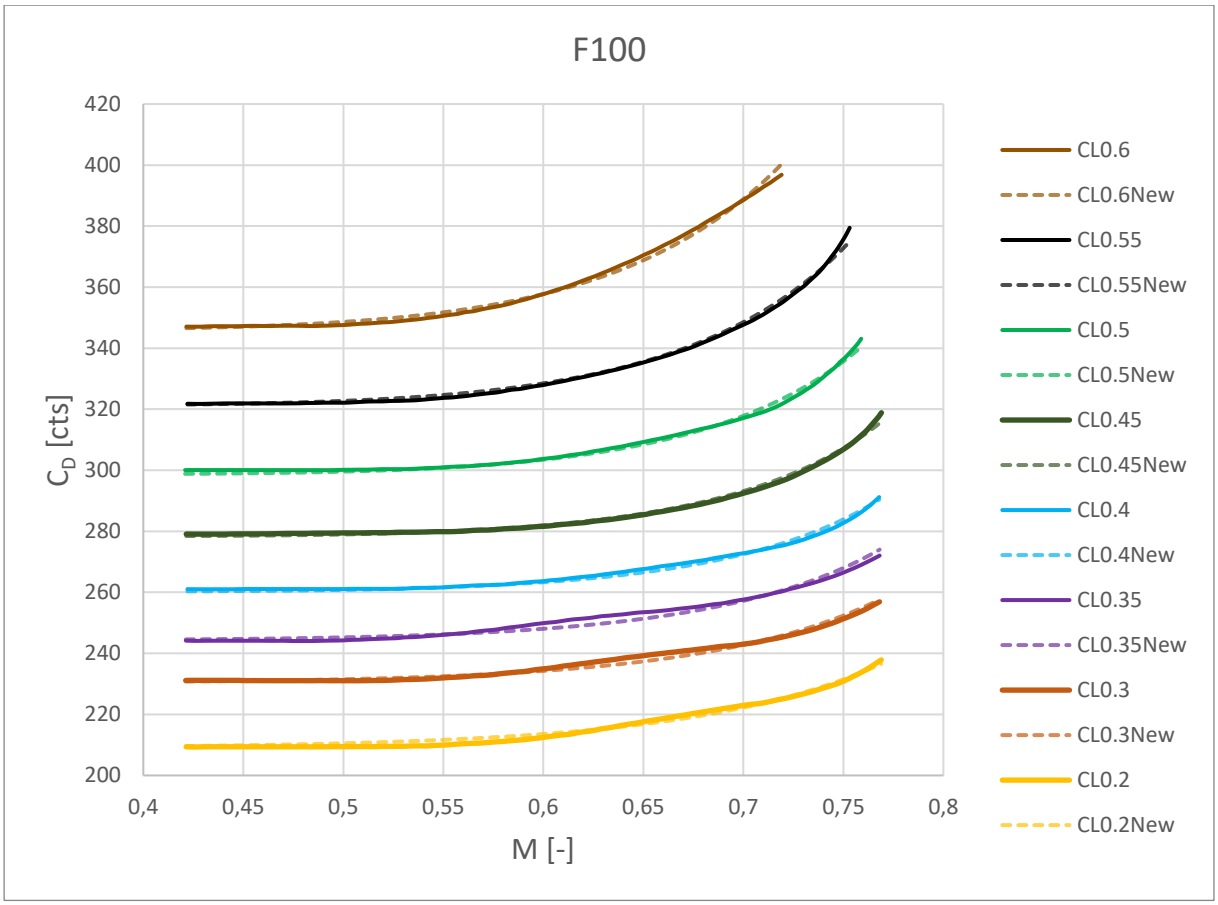

Figure 7.16 Original drag polar and its regression for Fokker100

8 Connecting the Parameters to the Geometry of the Aircraft

In this chapter an approach is made to generalize the generic equation and its parameters to enable an estimation of the drag polar also for new aircraft in preliminary design. The generic equation as used in this work is stated in (6.3). In (6.4) the wave drag coefficient is exemplarily presented as the approach with hyperbolic tangent. Note that the wave drag is zero for $M<M_{crit}$.

$$C_D = C_{D0} + \frac{C_L^2 \cdot d}{-e \cdot \left(\frac{M}{M_{comp}} - 1\right)^f + 1} + C_{Dw} \tag{6.3}$$

$$C_D = C_{D0} + \frac{C_L^2 \cdot d}{-e \cdot \left(\frac{M}{M_{comp}} - 1\right)^f + 1} + a\left(1 + \tanh\left(b\frac{M}{M_{crit}} - c\right)\right) \tag{6.4}$$

In general, this equation is valid for any aircraft at subsonic speeds. The aircraft dependent parameters *a, b, c, d, e* and *f* link it to the aircraft's individual geometry and aerodynamics. A guideline follows to estimate the necessary inputs of Equation (6.4).

Firstly, the aerodynamic inputs are discussed. The lift coefficient and the Mach number are the variables of this equation. The zero lift drag coefficient is kept a constant here. Subchapter 3.2.1 presents a method to estimate it and gives further literature. The compressible Mach number is usually about M_{comp}=0.3. If the critical Mach number is unknown, it is estimated by (3.20). In this, the drag divergence Mach number is estimated by an equation based on the aircraft's geometry for example the Korn Equation as stated in (3.29). Subchapter 3.2.5 also presents a nonlinear approach and states further literature. The delta in Mach number of (3.20) is still unknown. This is estimated on either being usually about $\Delta M = 0.08 \ldots 0.2$ as stated in Subchapter 3.2.4 or referencing to an akin aircraft of the 16 aircraft of this work in the Excel spreadsheets or using the calculated drag divergence Mach number and the generic values of *a, b* and *c* in (8.1). This equation is based on the approach of the hyperbolic tangent for the wave drag and therefore only valid for this approach with the combination of (3.29) and the Boeing definition of the drag divergence Mach number as stated in Subchapter 3.2.5. The approximate critical Mach number is also graphically readable if a drag polar in the form of drag coefficient over Mach number exists.

$$M_{crit} = M_{DD} - \Delta M \tag{3.20}$$

$$M_{DD} = \frac{K_A}{\cos \varphi_{25}} - \frac{\frac{t}{c}}{\cos^2 \varphi_{25}} - \frac{C_L}{10 \cos^3 \varphi_{25}} \tag{3.29}$$

$$\Delta M = M_{DD} - \frac{b \cdot M_{DD}}{\tanh^{-1}\left(\frac{0.0020}{a} - 1\right) + c} \tag{8.1}$$

Secondly, the aircraft dependent parameters *a, b, c, d, e* and *f* are discussed. The parameters *a, b* and *c* belong to the mathematical approach of the wave drag, here to the hyperbolic tangent. So far, these parameters are not linked to the aircraft's geometry. These parameters can be estimated by either referring to an akin aircraft using Table 7.1 (for the hyperbolic tangent; the parameters of the other mathematical approaches are presented in Appendix B) or using the mean and median values of Table 6.3 and Table 6.4. The same applies to the parameters *e* and *f*, but as described in Subchapter 3.2.3 Niţă (2012b) state their generic values to be *e*=0.00152 and *f*=10.82. The parameter *d* is defined in (6.6) as stated in Subchapter 6.3. The geometrical Oswald efficiency factor and the aspect ratio are only dependent on the geometry of the aircraft, so that *d* is calculatable. The definition and calculation of geometrical Oswald efficiency factor is presented in Subchapter 3.2.3.

$$d = \frac{1}{\pi A e_{geo}} \tag{6.6}$$

Summing up this information a general guideline to use Equation (6.4) is:

- select the compressible Mach number
- define the approach for the wave drag
- select values for the parameters *a, b* and *c* of this approach
- calculate the drag divergence Mach number with aircraft's geometry
- estimate the delta in Mach number
- calculate the critical Mach number
- calculate the zero lift drag coefficient
- calculate the parameter *d*
- select values for the parameters *e* and *f*
- calculate the drag coefficient

With this information an approximate estimation of the drag coefficient and the drag polar is therefore possible also for new aircraft in preliminary design.

9 Summary and Conclusions

In this work, a literature study on the topic is conducted, stating the fundamentals of aerodynamic drag and the state of the art. In the literature different approaches to define the wave drag are already made. Furthermore, the work of Obert (2009) presents the drag polars for 16 aircraft. These diagrams are digitalized by the WebPlotDigitizer resulting in the existence of data points for these drag polars. A generic equation modelling the drag polar is established based on the theory, additional conditions and mathematical approaches describing wave drag. These approaches are also grounded on theory. The generic equation with the mathematical approaches is then analyzed and reviewed with the data of the 16 aircraft and reveals reliable results. As a final step, the parameters in the generic equation are linked to an aircraft's geometry. This enables the estimation of the drag coefficient for new aircraft.

As usual, difficulties emerge at some point during a project. The first difficulty of this work has been the hunt for a general equation for the drag polar in the form of the drag coefficient over the Mach number, as to start with it wasn't obvious that the equation is valid for the form of the drag polar with the drag coefficient over the Mach number as well as the standard form with the lift coefficient over the drag coefficient. Then the main part of this work, the creation of the Excel spreadsheets, started. These had to be adapted several times as the final methods of the calculation and the approaches for the wave drag were formed while working on the spreadsheets. Working with the Excel Solver worked in general and led to a solid result. But also optimizing the parameters with the Excel Solver didn't come on its own as the outcome often wasn't physically plausible or sufficiently good. The sheer scale of loops in the Excel Solver timed by 16 aircraft and by 7 mathematical approaches has been very time-consuming.

To conclude, the aim of this project was mainly to digitalize available data of drag polars and to use it for the generation of an equation for the drag polar with special interest in the wave drag. This aim has been sufficiently achieved as presented in Chapter 7. Furthermore, a second aim was to link the generic equation to the geometry of an aircraft to yield a universally valid estimation for the drag coefficient. As no correlation between the parameters of the wave drag approach and the aircraft's geometry exists yet, this aim has been realized as far as possible as Chapter 8 shows. Nevertheless, the goal of a universally valid estimation of the drag coefficient is achieved by using generic values.

10 Recommendations

This project achieves a fair bit as stated in Chapter 9. Still there is always more to consider and analyze in future. So, the parameters of the wave drag approaches aren't linked to geometry yet. Of course, the parameters vary with each mathematical approach and there is superior correlation. But picking the best one or two approaches and trying to link them to geometry might reveal new correlations. Furthermore, the estimation of the delta in Mach number between the critical Mach number and the drag divergence Mach number is currently vague. This might improve by further investigations.

Further recommendation refers to the use of the associated Excel spreadsheets, possible future adaption to different aircraft and approaches and the Excel Solver. The optimization of a successful regression is not done at the touch of a button. A good regression takes time to try various initial values, check results on plausibility, check on the physical or aerodynamic plausibility and to seek the lowest sum of squared errors. Especially when expanding this work, this is of importance. Finally, the upper limit of applicability needs to be considered. The estimation of the drag coefficient is not to be extrapolated far beyond the limits of the original aircraft's data.

List of References

AGARD, 1980. *Multilingual Aeronautical Dictionary*. Neuilly, France: Advisory Group for Aerospace Research and Development (AGARD/NATO).
Available from: http://mad.profscholz.de/
Archived at: https://bit.ly/AGARD-1980

BARTON, David I., HALL, Cesare A., OLDFIELD, Matthew K., 2023. Design of a Hydrogen Aircraft for Zero Persistent Contrails. In: *Aerospace*, vol. 10, no. 8 art. 688.
Available from: https://doi.org/10.3390/aerospace10080688

BEEKMANS, Rob, VAN DRUNEN, Mark, 2018. *Fokker 28 General*.
Available from: http://www.fokker-aircraft.info/f28general.htm
Archived at: https://perma.cc/AU7H-SBTM

BENSEL, Arthur, 2018. *Characteristics of the Specific Fuel Consumption for Jet Engines*. Project. Hamburg University of Applied Sciences.
Available from: https://doi.org/10.15488/4316
Available from: https://nbn-resolving.org/urn:nbn:de:gbv:18302-aero2018-08-31.016

BERTIN, John J., CUMMINGS, Russel M., 2009. *Aerodynamics for Engineers*. 5th Edition, Upper Saddle River, NJ, USA: Pearson Prentice Hall.
Available from: https://bit.ly/3FwKskD
Open Access at: https://bit.ly/4biycQP
Archived at: https://perma.cc/9PLN-E5MU

BRADY, Chris, 1999. *The 737 Information Site: Detailed Technical Data*. Kingsley, UK. Tech Pilot Services.
Available from: http://www.b737.org.uk/techspecsdetailed.htm
Archived at: https://perma.cc/TC7H-MHGA

CAMBRIGDE UNIVERSITY PRESS, 2025a. Aircraft. In: *Cambridge Dictionary*.
Available from: https://dictionary.cambridge.org/dictionary/english/aircraft

CAMBRIGDE UNIVERSITY PRESS, 2025b. Equation. In: *Cambridge Dictionary.*
Available from: https://dictionary.cambridge.org/dictionary/english/equation

CAMBRIGDE UNIVERSITY PRESS, 2025c. Generic. In: *Cambridge Dictionary*.
Available from: https://dictionary.cambridge.org/dictionary/english/generic

CAMBRIGDE UNIVERSITY PRESS, 2025d. Identify. In: *Cambridge Dictionary.*
Available from: https://dictionary.cambridge.org/dictionary/english/identify

CAMBRIGDE UNIVERSITY PRESS, 2025e. Passenger. In: *Cambridge Dictionary.*
Available from: https://dictionary.cambridge.org/dictionary/english/passenger

CAMBRIGDE UNIVERSITY PRESS, 2025f. Unveil. In: *Cambridge Dictionary.*
Available from: https://dictionary.cambridge.org/dictionary/english/unveil?q=unveiling

DUBS, F., 1975. *Hochgeschwindigkeits-Aerodynamik*: *Vorgänge und Probleme in kompressibler Strömung*. Basel, Switzerland: Birkhäuser Verlag.
Available from: https://doi.org/10.1007/978-3-0348-5924-0 (Closed Access)

FILIPPONE, Antonio, 2008. Comprehensive Analysis of Transport Aircraft Flight Performance. In: *Progress in Aerospace Sciences*, vol. 44, pp. 192-236.
Available from: https://doi.org/10.1016/j.paerosci.2007.10.005 (Closed Access)
Open Access at: https://www.researchgate.net/publication/239374135
Archived at: https://perma.cc/44JX-LZAV

GUDMUNDSSON, Snorri, 2022. Aircraft Drag Analysis. In: *General Aviation Aircraft Design*: *Applied Methods and Procedures*. 2nd Edition, Oxford, UK: Butterworth-Heinemann.
Available from: https://doi.org/10.1016/C2018-0-03861-X
Chapter 16 Aircraft Drag Analysis, 16.3 Estimating the Drag of a Complete Aircraft (click “Show more”)
Open Access at: https://www.sciencedirect.com/topics/engineering/drag-divergence
Archived at: https://perma.cc/6N93-3DRQ

HIRSCH, Sebastian, 2022. *The 50 Most Important Parameters of the 60 Most Used Passenger Aircraft.* Project. Hamburg University of Applied Sciences.
Available from: https://nbn-resolving.org/urn:nbn:de:gbv:18302-aero2022-10-01.013
Archived at: https://perma.cc/M27Y-SUML
Available from: https://purl.org/aero/AircraftDatabase/html
Archived at: https://perma.cc/Q46D-ADZW

HOERNER, Sighard F., 1965. *Fluid Dynamic Drag: Practical Information on Aerodynamic Drag and Hydrodynamic Resistance*. Bakersfield, CA, USA: Hoerner Fluid Dynamics.
Available from: https://n2t.net/ark:/13960/t57f0bk2j
Archived at: https://perma.cc/R6CB-3FH2

HORN, Andreas, 2022. *Beyond Vmo/Mmo: A Closer Look at High-Speed Certification Rules*.
Available from: https://bit.ly/4ikxQLS
Archived at: https://perma.cc/6J5M-PYVJ

JENKINSON, Lloyd, SIMPKIN, Paul, RHODES, Darren, 2001a. *Civil Jet Aircraft Design*. Data A: Aircraft Data File, Table 1: Airbus Aircraft. Oxford, UK: Butterworth-Heinemann.
Available from: https://bit.ly/41gNfG5
Archived at: https://perma.cc/K3JM-AHBV

JENKINSON, Lloyd, SIMPKIN, Paul, RHODES, Darren, 2001b. *Civil Jet Aircraft Design.* Data A: Aircraft Data File, Table 2: Boeing Aircraft. Oxford, UK: Butterworth-Heinemann.
Available from: https://bit.ly/4kmWrBi
Archived at: https://perma.cc/32EH-VCLU

JENKINSON, Lloyd, SIMPKIN, Paul, RHODES, Darren, 2001c. *Civil Jet Aircraft Design*. Data A: Aircraft Data File, Table 3: Boeing Aircraft. Oxford, UK: Butterworth-Heinemann.
Available from: https://bit.ly/4ik0zQC
Archived at: https://perma.cc/A3XB-WMUR

JENKINSON, Lloyd, SIMPKIN, Paul, RHODES, Darren, 2001d. *Civil Jet Aircraft Design*. Data A: Aircraft Data File, Table 6: Douglas, Boeing (Douglas Products Division) & Lockheed Aircraft. Oxford, UK: Butterworth-Heinemann.
Available from: https://bit.ly/41cKOEc
Archived at: https://perma.cc/CKZ5-JKQZ

JENKINSON, Lloyd, SIMPKIN, Paul, RHODES, Darren, 2001e. *Civil Jet Aircraft Design*. Data A: Aircraft Data File, *Table 8:* Miscellaneous Manufacturers. Oxford, UK: Butterworth-Heinemann.
Available from: https://bit.ly/4hWIzfH
Archived at: https://perma.cc/8JG8-92BR

LOCK, C. N. H., 1951. *The Ideal Drag Due to a Shock Wave Parts I and II*. Technical Report 2512, Aeronautical Research Council.
Available from: https://reports.aerade.cranfield.ac.uk/handle/1826.2/3677
Archived at: https://perma.cc/S3ZR-3RTS

MALONE, Brett, MASON, William H., 1995. Multidisciplinary Optimization in Aircraft Design Using Analytic Technology Models. In: *Journal of Aircraft*, vol. 32 no. 2, pp. 431-438.
Available from: https://doi.org/10.2514/3.46734 (Closed Access)
Open Access at: https://archive.aoe.vt.edu/mason/Mason_f/MRRpubs95.html
Archived at: https://perma.cc/YJK6-8CVJ

MASON, William H., 2019. Configuration Aerodynamics. Lecture Notes AOE 4124. Blacksburg, VA, USA: Virginia Polytechnic Institute and State University.
Archived at: https://bit.ly/41NMe8M

NIŢĂ, Mihaela, SCHOLZ, Dieter, 2012a: Estimating the Oswald Factor from Basic Aircraft Geometrical Parameters. In: *Publikationen zum DLRK 2012* (Deutscher Luft- und Raumfahrtkongress, Berlin, 10. - 12. September 2012). Bonn, Germany: Deutsche Gesellschaft für Luft- und Raumfahrt (DGLR).
Available from: https://nbn-resolving.org/urn:nbn:de:101:1-201212176728

NIŢĂ, Mihaela, SCHOLZ, Dieter, 2012b. *Estimating the Oswald Factor from Basic Aircraft Geometrical Parameters*. Presentation. (Deutscher Luft- und Raumfahrtkongress, Berlin, 10. – 12. September 2012.)
Available from: https://bit.ly/4km58fm
Archived at: https://perma.cc/TM6M-SEWP

OBERT, Ed, 2009. *Aerodynamic Design of Transport Aircraft*. Delft, Netherlands: IOS Press.
Available from: https://ebooks.iospress.nl/book/aerodynamic-design-of-transport-aircraft
Archived at: https://perma.cc/TZQ2-W3L9

POLL, D.I.A, SCHUMANN, U., 2024. On the Conditions for Absolute Minimum Fuel Burn for Turbofan Powered, Civil Transport Aircraft and a Simple Model for Wave Drag. In: *The Aeronautical Journal*. Cranfield, UK: Cambridge University Press.
Available from: https://doi.org/10.1017/aer.2024.10
Archived at: https://perma.cc/VBF8-EMFY

POOLE, Daniel J., ALLEN, Christian B., RENDALL, T., 2017. Objective Function and Constraints for Robust Transonic Aerofoil Optimization. In: *58th AIAA/ASCE/AHS/ASC Structures, Structural Dynamics, and Materials Conference*. Grapevine, TX, USA: AIAA.
Available from: https://doi.org/10.2514/6.2017-0360
Archived at: https://perma.cc/V96K-SJXX

RAYMER, Daniel P., 1992. *Aircraft Design: A Conceptual Approach.* 2nd Edition, Washington, DC, USA: American Institute of Aeronautics and Astronautics.
Available from: https://doi.org/10.2514/4.107290
Open Access at: https://bit.ly/3NVO0xT
Archived at: https://perma.cc/BXX6-ZQAM

ROHATGI, Ankit, 2024. *WebPlotDigitizer: Extract Data from Charts*. Version 5.1.
Available from: https://automeris.io/
Archived at: http://bit.ly/2yZBee4 (Software Version 4.1)

ROSKAM, Jan, LAN, Chuan-Tau Edward, 1997. *Airplane Aerodynamics and Performance*. Lawrence, KS, USA: Roskam Aviation and Engineering Corporation.
Available from: https://bit.ly/Roskam1997
Open Access at: https://bit.ly/4kyTa1P
Archived at: https://perma.cc/5EV8-W227

SAGI, Ori, 2024. *Model Performance Metrics for Regression Models*. Tel Aviv, Israel: Pecan AI.
Available at: https://bit.ly/4klDJKs
Archived at: https://perma.cc/65E7-G8P4

SEGOVIA GARCIA, Roberto, 2013. *Turboprop Aircraft Design Optimization – Tool Development*. Master Thesis: University of Applied Sciences Hamburg.
Available from: https://bit.ly/3uxLIMr
Archived at: https://perma.cc/L3R7-GPNJ

SCHOLZ, Dieter, CIORNEI, Simona, 2005. Mach Number, Relative Thickness, Sweep and Lift Coefficient of the Wing – An Empirical Investigation of Parameters and Equations. In: BRANDT, Peter (Ed.). *Jahrbuch 2005* (Deutscher Luft- und Raumfahrtkongress Friedrichshafen, 26. - 29. September 2005). Bonn, Germany: Deutsche Gesellschaft für Luft- und Raumfahrt (DGLR).
Available from: https://bit.ly/3Xouj78
Archived at: https://perma.cc/6DPL-A64Z

SCHOLZ, Dieter, 2015. *Aircraft Design*. Lecture Notes. Hamburg University of Applied Sciences.
Available from: http://lecturenotes.aircraftdesign.org/
Archived at: https://bit.ly/3F7YA3U

SCHOLZ, Dieter, 2017. *Drag Estimation.* Hamburg University of Applied Sciences.
Available from: https://bit.ly/3Fa9Uw5
Archived at: https://perma.cc/HU3L-EEXX

SHEVELL, Richard S., 1989. *Fundamentals of Flight*. 2nd Edition, Englewood Cliffs, NJ, USA: Prentice Hall.
Available from: https://www.amazon.com/dp/0133390608

SUN, Junzi, 2019. *Open Aircraft Performance Modelling: Based on an Analysis of Aircraft Surveillance Data*. Dissertation. Delft University of Technology
Available from: https://doi.org/10.4233/uuid:af94d535-1853-4a6c-8b3f-77c98a52346a
Archived at: https://perma.cc/PS3P-UJFT

VAN DER ZALM, B., 2023a. *Wide-Body Airliner Airbus A300B2-200*.
Available from: https://www.aircraftinvestigation.info/airplanes/A300B2-200.html
Archived at: https://perma.cc/C3DF-RQLJ

VAN DER ZALM, B., 2023b. *Boeing 707-120*.
Available from: https://www.aircraftinvestigation.info/airplanes/707-120.html
Archived at: https://perma.cc/P8G6-UG8Y

WIKIPEDIA, 2023. *Residual Sum of Squares*.
Available from: https://en.wikipedia.org/wiki/Residual_sum_of_squares
Archived at: https://perma.cc/SXX8-2YYJ

WIKIPEDIA, 2025a. *Drag Curve*.
Available from: https://en.wikipedia.org/wiki/Drag_curve
Archived at: https://perma.cc/Y4JJ-RZGU

WIKIPEDIA, 2025b. *Mean Squared Error.*
Available from: https://en.wikipedia.org/wiki/Mean_squared_error
Archived at: https://perma.cc/ZY56-5GWD

WISLICENUS, Jan, DAIDZIC, Nihad E., 2022. Estimation of Transport-Category Jet Airplane Maximum Range and Airspeed in the Presence of Transonic Wave Drag. In: *Aerospace*, vol. 9, no. 4 art. 192.
Available from: https://doi.org/10.3390/aerospace9040192

All online resources have been accessed on 2025-03-06 or later.

Appendix A – Additional Conditions Continued

This Appendix presents the analysis of the additional conditions for the tangent, hyperbolic sine, hyperbolic tangent and the exponential function as stated in Chapter 5.2.

First, the tangent approach is treated. The first condition applied on the tangent is stated in (A.1). Solving this equation yields (A.3). This means that this condition is fulfilled if the parameters *b* and *c* are equal. (A.3) is inserted in (A.1) yields (3.23).

$$C_{Dw}(M = M_{crit}) = a \tan\left(b \frac{M_{crit}}{M_{crit}} - c\right) = a \tan(b - c) \stackrel{!}{=} 0 \tag{A.1}$$

$$0 = \tan(b - c) = b - c \tag{A.2}$$

$$c = b \tag{A.3}$$

$$C_{Dw} = a \tan\left(b \frac{M}{M_{crit}} - b\right) \tag{3.23}$$

The second condition is analyzed based on (3.23) and showed in (A.4). Because *a* and *b* can't be zero while having wave drag, this condition is never fulfilled exactly. In practice, this is fulfilled if (A.5) is true. To reach this, either *a* or *b* needs to be small.

$$\frac{d}{dM} C_{Dw}(M = M_{crit}) \stackrel{!}{=} 0 = \frac{a \frac{b}{M_{crit}}}{\cos^2\left(b \frac{M_{crit}}{M_{crit}} - b\right)} = \frac{a \frac{b}{M_{crit}}}{\cos^2(0)} = a \frac{b}{M_{crit}} \neq 0 \tag{A.4}$$

$$a \cdot b \approx 0 \tag{A.5}$$

Next, the hyperbolic sine is analyzed. The first condition is shown in (A.6). The second condition is presented in (A.9). As the hyperbolic sine behaves like the tangent the results are the same.

$$C_{Dw}(M = M_{crit}) = a \sinh\left(b \frac{M_{crit}}{M_{crit}} - c\right) = a \sinh(b - c) \stackrel{!}{=} 0 \tag{A.6}$$

$$0 = \sinh(b - c) = b - c \tag{A.7}$$

$$c = b \tag{A.8}$$

$$C_{Dw} = a \sinh\left(b\frac{M}{M_{crit}} - b\right) \tag{5.11}$$

$$\frac{d}{dM}C_{Dw}(M = M_{crit}) = a\frac{b}{M_{crit}}\cosh\left(b\frac{M_{crit}}{M_{crit}} - b\right) = a\frac{b}{M_{crit}}\cosh(0) \neq 0 \tag{A.9}$$

$$a \cdot b \approx 0 \tag{A.10}$$

Then the hyperbolic tangent is analyzed. (A.11) shows the first condition. Solving this equation yields (A.14). In theory, this fulfills the condition exactly, but it isn't reached in practice.

$$C_{Dw}(M = M_{crit}) = a\left(1 + \tanh\left(b\frac{M_{crit}}{M_{crit}} - c\right)\right) = a\,(1 + \tanh(b - c)) \stackrel{!}{=} 0 \tag{A.11}$$

$$0 = 1 + \tanh(b - c) \tag{A.12}$$

$$-1 = \tanh(b - c) \tag{A.13}$$

$$b - c = -\infty \tag{A.14}$$

Adding 0.0001=1cts to the zero in (A.12) and then solving the equation yields (A.15). This delta defines the accuracy. The first condition is fulfilled approximately if (A.16) is true as (A.17) shows.

$$\tanh^{-1}(-1 + 0.0001) = -4{,}9517 = (b - c)_{max} \tag{A.15}$$

$$b - c \leq -4{,}9517 \approx -5 \tag{A.16}$$

$$1 + \tanh(-5) = 0.000091 \approx 0 \tag{A.17}$$

The review of the second condition is presented in (A.18). (A.20) shows the result to fulfill the condition exactly, but the positive infinity is no option, because of the restriction in (A.14).

$$\frac{d}{dM}C_{Dw}(M = M_{crit}) = a\frac{b}{M_{crit}}\operatorname{sech}^2\left(b\frac{M_{crit}}{M_{crit}} - c\right) \stackrel{!}{=} 0 \tag{A.18}$$

$$0 = \operatorname{sech}^2(b - c) \tag{A.19}$$

$$b - c = \pm\infty \tag{A.20}$$

In like manners, the condition can be fulfilled approximately if (A.22) is true as (A.23) shows.

$$\operatorname{sech}^{-1}\left(\sqrt{0+0.0001}\right) = 5.2983 \tag{A.21}$$

$$b - c \leq -5.2983 \approx -5 \tag{A.22}$$

$$\operatorname{sech}^{2}(-5) = 0.00018 \approx 0 \tag{A.23}$$

Finally, the exponential function is checked. (A.24) shows the first condition. (A.26) shows that this condition is again exactly fulfillable in theory.

$$C_{Dw}(M = M_{crit}) = ae^{b\cdot\frac{M_{crit}}{M_{crit}}-c} = ae^{b-c} \stackrel{!}{=} 0 \tag{A.24}$$

$$0 = e^{b-c} \tag{A.25}$$

$$\ln(0) = b - c = -\infty \tag{A.26}$$

In practice the condition is fulfilled if (A.28) is true as (A.29) shows.

$$\ln(0+0.0001) = -9.2103 = (b-c)_{min} \tag{A.27}$$

$$b - c \leq -9.2103 \approx -9 \tag{A.28}$$

$$e^{-9} = 0.00012 \approx 0 \tag{A.29}$$

The second condition is presented in (A.30). (A.32) shows that this condition is exactly fulfillable in theory, too.

$$\frac{d}{dM}C_{Dw}(M = M_{crit}) = a\frac{b}{M_{crit}}e^{b\frac{M_{crit}}{M_{crit}}-c} = a\frac{b}{M_{crit}}e^{b-c} \stackrel{!}{=} 0 \tag{A.30}$$

$$0 = e^{b-c} \tag{A.31}$$

$$\ln(0) = b - c = -\infty \tag{A.32}$$

In practice the condition is fulfilled if (A.34) is true as (A.35) shows.

$$\ln(0+0.0001) = -9.2103 = (b-c)_{min} \tag{A.33}$$

$$b - c \leq -9.2103 \approx -9 \tag{A.34}$$

$$e^{-9} = 0.00012 \approx 0 \tag{A.35}$$

Table A.1 summarizes these findings neatly. Interesting is the fact that the tangent and the hyperbolic sine fulfill the first condition easily but struggle to fulfill the second condition. In contrast to this the hyperbolic sine and the exponential approach don't fulfill any condition exactly but fulfill both conditions easily approximate.

Table A.1 Overview of the fulfillment of the additional conditions

	condition 1		condition 2	
	fulfilment possible exactly	fulfilment possible approximately	fulfilment possible exactly	fulfilment possible approximately
tangent	yes	-	no	if $a \cdot b \approx 0$
hyperbolic sine	yes	-	no	if $a \cdot b \approx 0$
hyperbolic tangent	at -∞	if $b - c \leq -5$	at -∞	if $b - c \leq -9$
exponential function	at -∞	if $b - c \leq -5$	at -∞	if $b - c \leq -9$

Appendix B – Remaining Results and Parameters

In this appendix, the results for the remaining mathematical approaches are presented as stated in Chapter 7. Table B.1 shows the results of the optimization with the Lock approach for the wave drag. Stated are the used parameters and the metrics to validate the regression per aircraft. The mean and median values are also given. Table B.1 shows that the values of the zero lift drag coefficient are of plausible magnitude and that the values of the parameters *e* and *f* are overall in the scale of the generic value stated in Subchapter 3.2.4. Only the F28 and the F100 look different. There is a notable difference in the mean and median value of *e*. Their cruise Mach number is lower than that of other aircraft. Accordingly, their drag polars look differently.

Table B.1 Parameters of Lock

	d [cts]	C_{D0} [cts]	e [-]	f [-]	SSE / nr. of graphs [cts^2]	MSE [cts^2]	RMSE [cts]	RMSPE [-]
mean	430.84	169.22	4.397E-02	9.841	650.79	6.094	2.329	0.00949
median	442.50	168.16	4.465E-04	10.232	615.32	5.625	2.370	0.00941
DC	531.59	143.38	5.611E-04	9.666	567.14	5.251	2.292	0.00951
MD	438.80	163.50	2.499E-04	7.712	186.73	1.861	1.364	0.00541
B707	489.85	137.53	1.000E-05	10.997	879.90	6.874	2.622	0.01453
B727	538.31	177.20	3.486E-05	14.244	328.98	5.061	2.250	0.00818
B737-200	408.75	199.03	5.113E-03	9.077	99.90	0.925	0.962	0.00382
B737-300	392.06	215.13	7.324E-03	7.235	206.43	2.236	1.495	0.00577
B737-800	372.78	189.27	3.318E-04	12.614	645.43	5.072	2.252	0.00969
B747	481.68	143.28	2.581E-05	13.638	683.79	5.998	2.449	0.01067
B757	446.21	159.20	6.913E-04	10.797	310.34	3.928	1.982	0.00791
B767	468.00	133.09	2.860E-04	12.068	159.05	1.704	1.305	0.00596
B777	448.55	128.09	1.275E-05	15.671	1080.55	8.930	2.988	0.01293
A300	540.96	172.82	5.881E-04	8.627	666.79	6.537	2.557	0.00861
A320	338.70	200.59	3.713E-03	8.718	700.66	7.756	2.785	0.01007
A340	343.50	150.46	1.466E-04	12.944	1129.95	8.495	2.915	0.01308
F28	238.39	200.84	6.112E-01	0.441	2181.78	20.631	4.542	0.01638
F100	415.34	194.03	7.312E-02	3.007	585.22	6.242	2.498	0.00930

Table B.2 shows the results of the optimization for the general Lock approach for the wave drag. Stated are the used parameters and the metrics to validate the regression per aircraft and their mean and median values.

Table B.2 Parameters of Lock general

	a [cts]	b [-]	d [cts]	C_{D0} [cts]	e [-]	f [-]	SSE / nr. of graphs [cts^2]	MSE [cts^2]	RMSE [cts]	RMSPE [-]
mean	23064	1.1743	447.21	168.85	1.321E-03	10.43	410.06	3.821	1.848	0.00773
median	21890	1.0544	443.90	168.42	2.322E-04	11.00	325.24	3.553	1.883	0.00742
DC	11797	3.4630	517.80	144.02	6.390E-03	5.564	244.74	2.266	1.505	0.00673
MD	34674	1.7410	435.54	163.87	2.805E-04	9.732	91.70	0.914	0.956	0.00420
B707	21986	1.3516	489.38	137.73	1.000E-05	11.19	863.91	6.749	2.598	0.01434
B727	25596	1.1420	533.43	176.80	1.839E-04	11.95	317.16	4.879	2.209	0.00776
B737-200	38484	1.5750	408.19	199.14	6.138E-03	8.641	65.18	0.604	0.777	0.00325
B737-300	16159	0.4948	408.18	213.54	1.355E-03	11.40	84.77	0.918	0.958	0.00365
B737-800	10928	0.5145	388.90	186.58	1.103E-04	14.55	415.58	3.266	1.807	0.00724
B747	29291	1.5424	477.73	143.72	1.608E-04	10.81	646.09	5.667	2.381	0.01096
B757	20309	1.5420	445.33	159.50	7.975E-04	10.26	303.42	3.841	1.960	0.00793
B767	44151	0.2529	464.83	133.61	1.811E-04	12.82	154.53	1.656	1.287	0.00590
B777	33468	2.4720	442.48	129.22	1.387E-04	11.64	649.60	5.369	2.317	0.01073
A300	20636	0.9669	540.57	172.98	6.198E-05	14.61	521.65	5.114	2.261	0.00760
A320	26855	0.3263	349.98	198.81	1.682E-03	10.23	616.57	6.825	2.613	0.00938
A340	21793	0.8606	347.96	149.69	6.823E-05	14.17	1097.05	8.249	2.872	0.01250
F28	5471	0.2122	478.36	198.80	9.355E-04	2.975	333.31	3.152	1.775	0.00673
F100	7429	0.3315	426.67	193.54	2.643E-03	6.326	155.68	1.661	1.289	0.00484

Table B.3 shows the results of the optimization for the raise to power approach for the wave drag. Stated are the used parameters and the metrics to validate the regression per aircraft and their mean and median values.

Table B.3 Parameters of Raise To Power

	a [cts]	b [-]	c [-]	d [cts]	C_{D0} [cts]	e [-]	f [-]	SSE / nr. of graphs [cts^2]	MSE [cts^2]	RMSE [cts]	RMSPE [-]
mean	18434	1.288	4.150	447.24	168.83	2.290E-03	9.881	384.02	3.574	1.788	0.00747
median	18946	1.317	3.991	439.41	168.18	6.149E-04	10.522	269.07	2.810	1.675	0.00682
DC	13585	3.223	4.081	516.58	144.03	7.532E-03	5.266	240.07	2.223	1.491	0.00669
MD	25733	1.962	4.385	435.60	163.83	3.572E-04	9.216	90.95	0.906	0.952	0.00417
B707	16316	1.330	3.349	489.72	137.77	9.369E-06	7.642	854.63	6.677	2.584	0.01427
B727	31426	1.457	4.350	539.52	176.73	1.871E-04	11.877	298.06	4.586	2.141	0.00778
B737-200	21381	1.304	5.884	413.15	199.17	1.805E-03	10.916	138.86	1.286	1.134	0.00459
B737-300	20494	0.773	3.720	391.53	214.53	7.711E-03	7.893	220.52	2.388	1.545	0.00553
B737-800	14117	0.492	6.443	388.18	186.64	1.246E-04	14.346	385.42	3.029	1.740	0.00695
B747	28659	1.521	3.901	478.54	143.87	1.516E-04	10.592	604.54	5.303	2.303	0.01063
B757	22008	1.659	3.625	434.95	159.82	1.399E-02	4.531	204.66	2.591	1.610	0.00666
B767	23532	0.942	4.123	468.32	133.20	2.000E-04	12.642	157.75	1.690	1.300	0.00603
B777	31914	2.313	3.862	443.22	129.34	4.325E-05	13.549	689.85	5.701	2.388	0.01109
A300	12605	2.142	5.673	542.32	172.53	8.726E-04	9.708	530.66	5.203	2.281	0.00813
A320	17398	0.309	5.095	352.55	198.27	1.492E-03	10.451	611.92	6.774	2.603	0.00933
A340	14789	0.202	2.657	359.76	147.13	5.390E-05	14.674	942.33	7.085	2.662	0.01065
F28	744.3	0.494	1.621	478.92	201.32	9.152E-04	3.939	91.06	0.861	0.928	0.00344
F100	244.0	0.486	3.632	423.04	193.16	1.195E-03	10.837	83.04	0.886	0.941	0.00353

Table B.4 shows the results of the optimization with the tangent approach for the wave drag. Stated are the used parameters and the metrics to validate the regression per aircraft and their mean and median values. Further the additional condition is checked.

Table B.4 Parameters of Tangent

	a [cts]	b [-]	d [cts]	C_{D0} [cts]	e [-]	f [-]	a*b [cts]	SSE / nr. of graphs [cts^2]	MSE [cts^2]	RMSE [cts]	RMSPE [-]
mean	8.771	2.943	456.22	166.19	7.837E-03	12.830	21.69	551.01	4.969	1.931	0.00793
median	6.128	2.697	464.43	167.71	2.089E-04	12.478	18.63	353.61	3.049	1.742	0.00693
DC	6.224	1.705	521.57	144.43	4.187E-05	14.151	10.61	376.66	3.488	1.868	0.00768
MD	6.582	1.439	448.96	161.41	3.705E-06	17.940	9.404	85.94	0.857	0.926	0.00335
B707	3.684	0.239	537.04	129.65	1.714E-03	9.138	0.881	1923.7	15.03	3.877	0.02067
B727	3.528	6.898	520.44	175.36	1.292E-03	9.252	24.34	375.03	5.770	2.402	0.00876
B737-200	5.375	5.792	417.13	197.98	2.366E-04	14.452	31.13	92.16	0.853	0.924	0.00357
B737-300	6.329	4.222	413.36	212.33	1.946E-05	19.364	26.72	22.36	0.242	0.492	0.00179
B737-800	6.033	3.333	394.46	185.27	1.133E-04	14.494	20.11	332.18	2.610	1.616	0.00617
B747	7.246	2.760	498.01	138.67	3.658E-04	10.425	20.00	2203.4	19.33	4.396	0.01816
B757	3.690	1.834	461.52	155.44	7.304E-04	10.965	6.768	389.93	4.936	2.222	0.00846
B767	0.761	2.634	467.34	133.09	1.812E-04	12.814	2.005	109.98	1.178	1.086	0.00513
B777	9.220	0.448	480.49	120.46	7.188E-05	13.307	4.126	1429.4	11.81	3.437	0.01418
A300	3.791	6.545	544.69	171.78	2.992E-04	12.142	24.81	578.91	5.676	2.382	0.00869
A320	9.768	2.768	354.77	195.33	1.349E-07	26.841	27.04	80.76	0.894	0.946	0.00347
A340	4.962	3.479	342.41	148.82	1.000E-07	10.288	17.26	556.69	4.186	2.046	0.00881
F28	54.54	2.089	469.89	200.53	1.125E-01	2.387	113.9	103.77	0.981	0.991	0.00373
F100	8.608	0.916	427.44	188.52	7.797E-03	7.319	7.887	155.46	1.658	1.288	0.00433

Table B.5 shows the results of the optimization with the hyperbolic sine approach for the wave drag. Stated are the used parameters and the metrics to validate the regression per aircraft and their mean and median values. Further the additional condition is checked.

Table B.5 Parameters of Hyperbolic Sine

	a [cts]	b [-]	d [cts]	C_{D0} [cts]	e [-]	f [-]	a*b [cts]	SSE / nr. of graphs [cts^2]	MSE [cts^2]	RMSE [cts]	RMSPE [-]
mean	1.2089	14.057	451.25	167.44	1.921E-03	12.964	7.949	472.0	4.228	1.891	0.00788
median	0.3014	9.806	450.55	168.28	1.180E-04	13.236	5.470	363.4	3.642	1.908	0.00720
DC	2.7446	2.321	516.58	145.02	5.538E-05	13.735	6.369	373.3	3.457	1.859	0.00763
MD	0.0115	9.000	437.99	163.64	4.440E-06	17.713	0.103	156.6	1.561	1.249	0.00511
B707	0.0029	8.726	494.28	135.54	2.306E-03	8.684	0.025	2151	16.81	4.100	0.02177
B727	0.0546	38.757	536.22	175.93	9.657E-04	9.093	2.116	248.8	3.827	1.956	0.00702
B737-200	0.3600	20.426	414.18	198.90	2.833E-04	14.239	7.353	133.4	1.235	1.111	0.00441
B737-300	1.0748	10.612	413.14	212.39	1.762E-06	23.903	11.41	32.63	0.353	0.594	0.00220
B737-800	0.4737	11.675	388.88	186.41	1.325E-04	14.236	5.530	354.5	2.786	1.669	0.00660
B747	1.5062	26.599	482.62	143.30	1.384E-07	11.423	40.06	605.5	5.312	2.305	0.01005
B757	0.1965	7.799	454.95	156.98	7.462E-04	10.938	1.533	372.4	4.713	2.171	0.00828
B767	0.0136	10.853	464.96	133.62	1.780E-04	12.852	0.147	147.3	1.578	1.256	0.00584
B777	0.1567	41.201	446.15	129.00	3.998E-05	11.890	6.458	693.3	5.730	2.394	0.01110
A300	0.1848	22.355	540.02	172.93	7.954E-05	14.310	4.130	467.7	4.586	2.141	0.00737
A320	8.2347	3.178	363.51	193.13	1.228E-05	18.953	26.17	208.7	2.310	1.520	0.00574
A340	0.7902	6.846	366.20	145.75	1.034E-04	13.620	5.410	978.9	7.360	2.713	0.01066
F28	3.2948	3.035	476.22	195.19	2.088E-02	3.854	10.00	544.6	5.150	2.269	0.00882
F100	0.2428	1.526	424.15	191.23	4.943E-03	7.982	0.370	82.99	0.885	0.941	0.00342

Table B.6 shows the results of the optimization with the exponential approach for the wave drag. Stated are the used parameters and the metrics to validate the regression per aircraft and their mean and median values. Further the additional condition is checked.

Table B.6 Parameters of Exponential function

	a [cts]	b [-]	c [-]	d [cts]	C_{D0} [cts]	e [-]	f [-]	initial C_{Dw} [cts]	SSE / nr. of graphs [cts^2]	MSE [cts^2]	RMSE [cts]	RMSPE [-]
mean	4688	23.59	37.34	450.97	167.63	1.189E-03	10.312	1.080	413.25	3.815	1.832	0.00764
median	1320	24.68	33.78	449.63	168.24	3.522E-04	10.773	1.234	365.51	4.263	2.062	0.00737
DC	891.4	24.88	94.21	528.71	143.74	1.151E-03	8.449	8E-31	295.39	2.735	1.654	0.00732
MD	955.4	36.69	45.69	438.94	163.58	3.975E-05	11.530	1.234	80.45	0.802	0.895	0.00392
B707	1420	24.48	33.48	486.96	137.40	1.000E-05	10.792	1.234	1074.1	8.391	2.897	0.01573
B727	756.9	37.02	46.02	537.95	175.87	4.557E-04	10.478	1.234	250.59	3.855	1.963	0.00708
B737-200	36102	46.15	55.15	408.79	199.02	6.033E-03	8.478	1.234	69.90	0.647	0.804	0.00331
B737-300	1674	10.07	19.07	415.32	212.36	1.261E-03	11.527	1.234	63.93	0.692	0.832	0.00308
B737-800	1220	11.38	20.38	388.78	186.36	1.336E-04	14.221	1.234	354.98	2.790	1.670	0.00662
B747	1540	25.09	34.09	483.75	142.94	1.733E-06	10.753	1.234	589.85	5.174	2.275	0.00997
B757	1589	7.720	16.72	455.66	156.79	6.799E-04	11.088	1.234	376.04	4.760	2.182	0.00831
B767	959.0	55.85	80.51	469.71	132.90	2.487E-04	12.299	2E-11	150.74	1.615	1.271	0.00594
B777	889.9	42.51	51.51	443.60	128.95	5.800E-04	8.032	1.234	622.97	5.148	2.269	0.01041
A300	359.6	21.02	30.02	539.70	172.91	8.140E-05	14.275	1.234	476.39	4.671	2.161	0.00741
A320	2430	4.253	13.25	371.92	193.99	8.464E-04	11.409	1.234	529.85	5.866	2.422	0.00856
A340	1103	25.10	34.10	346.32	149.95	2.289E-04	7.240	1.234	1064.2	8.001	2.829	0.01246
F28	16165	3.047	12.05	475.03	194.20	1.023E-04	7.056	1.234	529.33	5.007	2.238	0.00867
F100	6958	3.344	12.34	424.39	191.17	7.174E-03	7.371	1.234	83.38	0.889	0.943	0.00344